2006

Modeling the effects of endocrine disrupting chemicals on Atlantic croaker: understanding biomarkers and predicting population responses

Cheryl Anne Murphy
Louisiana State University and Agricultural and Mechanical College

MODELING THE EFFECTS OF ENDOCRINE DISRUPTING CHEMICALS ON ATLANTIC CROAKER: UNDERSTANDING BIOMARKERS AND PREDICTING POPULATION RESPONSES

A Dissertation

Submitted to the Graduate Faculty of the
Louisiana State University and
Agricultural and Mechanical College
in partial fulfillment of the
requirements for the degree of
Doctor of Philosophy

in

Department of Oceanography and Coastal Sciences

by
Cheryl Anne Murphy
B.Sc., Dalhousie University, 1993
M.Sc., University of Alberta, 1998
May, 2006

ACKNOWLEDGEMENTS

When I first attempted to write this section of my dissertation, I was overwhelmed by the number of people who have played a role in the completion of this degree. Many individuals have either played a direct or indirect role in shaping this degree by providing empirical data, guidance and support (financial, mental and emotional).

First, and foremost, I must thank my advisor, Dr. Kenneth Rose. With a tremendous amount of patience, he provided excellent training to a biologist who arrived at LSU with very little experience in modeling. I am forever grateful to Kenny because he opened up the world of modeling to me as a way of approaching scientific problems; I will always be inspired by his intelligence and creative solutions.

This research has been supported by a grant from the US Environmental Protection Agency's Science to Achieve Results (STAR) Program through funding from US EPA agreement (R 827399) and from the STAR and Estuarine and Great Lakes (EaGLe) program through funding to CEER-GOM, US EPA Agreement (R 829458). Through these grants I worked in collaboration with a number of people. First, I thank Dr. Peter Thomas at the University of Texas Marine Science Institute. Peter was essential to this project and provided important input for the physiologically-based model; I admire his contagious enthusiastic and optimistic approach to science. Several people in Peter Thomas's lab also contributed valuable empirical data: Dr. Saydur Rahman, Dr. Izhar Khan, James Kummer and Larisa Ford. I greatly benefited by working with Dr. Lee Fuiman, also at the University of Texas Marine Science Institute. His work on larval fish behavior was critical to the development of the larval IBM. Also, Dr. Maria Alvarez and Dr. Ian McCarthy, while they were at University of Texas, provided

much empirical data for modeling. Dr. Sandra Diamond, at Texas Tech University in Lubbock, was essential for the development of the matrix models. Finally, I benefited from many discussions with the scientists in the CEER-GOM EPA group.

I thank my committee members, Dr. Jaye Cable, Dr. Kevin Carman, Dr. Barry Moser and Dr. Allen Rutherford for guidance and practical insight; I enjoyed interacting with each committee member. I was also fortunate to benefit from discussions with Dr. Jim Cowan and his lab group, as well as Dr. Rick Shaw, Dr. Mark Benfield, Dr. Malinda Sutor and Dr. Grover Waldrop. Also, I extend a big thank-you to the people of the Department of Oceanography and Coastal Fisheries Institute for all the interesting conversations and support. I thank the Department of Oceanography and Coastal Sciences for awarding me with a graduate student enhancement scholarship.

I must thank my academic "siblings", we have been through lots…Shaye Sable, Susanne Hoeppner and Aaron Adamack have all provided immeasurable support throughout my tenure as a doctoral student. In addition to the people I have already mentioned, I also thank other friends I met through the department and in Louisiana: Sean Keenan, Dr. Pam MacRae, Emily Hyfield, Guerry Holm, Angela Schrift, Andy Fischer, Scott Baker, Anneliese Westphal, Dr. Cara Miller, Mark Mcrae, Dr. Lori Benson, and Dr. Jim Parham.

I also have core support group who have encouraged me and provided great advice along the way: Dr. Norm Stacey, Dr. Leah Hanson, Dr. Jean Joss, Dr. Lynda Corkum, Dr. Mike Fitzsimons, Kim Christopher and Mike Norton. I also thank Dr. Brian Shuter and Dr. Peter Abrams at the University of Toronto for giving me flexibility in my job to allow for the completion of my PhD.

I thank my parents, Peter and Janet, and my sisters, Kelly and Erin, for their love and their continued support of my life decisions. I also extend a very special thank-you to the people of Louisiana for the time I spent in their wondrous state; I wish you a speedy recovery from Hurricanes Katrina and Rita.

TABLE OF CONTENTS

ABSTRACT

A number of environmental stressors have been shown to interfere with reproductive and behavioral processes of fish by interfering with endocrine function. Most biomarkers of endocrine disturbance tend to be static measurements from dynamic systems making them difficult to evaluate within the context of an individual, or subtle effects that do not relate well to endpoints of ecological significance. I present an approach that uses a series of models, based on Atlantic croaker, to extrapolate laboratory results to indicators of individual and population health. First, I created a physiologically based model that simulates vitellogenesis in a female fish. The model simulates the major biochemical reactions from the secretion of gonadotropin to the production of vitellogenin. I simulated the effects of three environmental stressors that affect vitellogenin production differently. Model simulations demonstrated that it is possible to relate contaminant-induced changes in biomarkers to vitellogenin production and fecundity. A field application of the vitellogenesis model showed potential utility in interpreting field-measured biomarkers and to infer potential population hazards. Uncertainty analyses identified parameters that contributed most to variability of predictions. Second, I used a statistical model linked to an individual-based model to convert changes in behavior of ocean larvae exposed to two different contaminants to population relevant endpoints. Each contaminant imposed different effects and the effects were largely driven by impaired foraging abilities. Finally, I developed a matrix population model that realistically simulated two distinct populations of Atlantic croaker: Gulf of Mexico and Mid-Atlantic Bight. Simulations incorporated contaminant induced changes that were predicted by the other models, and compared population dynamics for

100 years under baseline conditions and under two separate contaminant scenarios. Predictions generated from the matrix model suggested that contaminant exposures at higher levels than observed in field measurements have the potential to impact populations, and that contaminant residency time within fish and the number of individuals exposed, interact with site-specific factors and life history traits, to determine population effects. The bottom-up approach employed here suggests that it is possible to scale laboratory effects to the population and provides a framework from which to base future model development and testing.

CHAPTER 1. GENERAL INTRODUCTION

1.1. Introduction

Endocrine disruption is a phenomenon that has been documented in numerous species of aquatic, avian, and terrestrial wildlife (Colborn et al., 1993). The definition of an endocrine disruptor was officially described by the WHO (2002) as "an exogenous chemical substance or mixture that alters the structure or function(s) of the endocrine systems and causes adverse effects at the level of the organism, its progeny, populations, or subpopulations of organisms...". Although endocrine disruption can be a natural event (e.g., plant phytoestrogens), the influx of man-made chemicals into the environment since the beginning of the Industrial Revolution has produced many unexplained detrimental effects on wildlife populations (Colborn et al., 1993).

Endocrine disruption as a cause of population decline has been difficult to ascertain because much of the adverse effects of endocrine disruptors on animals are relatively subtle (sublethal or small in magnitude). Since endocrine disruptors were first recognized, numerous biomarkers have been measured that demonstrate abnormalities of endocrine function in wildlife exposed to industrial and domestic wastes (e.g., vitellogenin production in male fish -- Folmar et al.,1996; Kime et al., 1999). These biomarkers appear to correlate with decreased fertility (Kime, 1998; Rolland, 2000), but to date, there are few studies that directly link an adverse effect of endocrine disruptors to a population level response (Mills and Chichester, 2005). Here I apply a series of linked statistical and computer simulation models to predict how endocrine-disruptor effects observed in laboratory-based toxicity studies translate to population level responses of Atlantic croaker (*Micropogonias undulatus*).

Prior attempts to link endocrine-disruptor exposure to population responses have focused on circumstantial evidence. Previous studies have demonstrated that populations exposed to endocrine disruptors showed endocrine abnormalities not observed in unexposed populations. For example, alligators from the pesticide-contaminated Lake Apopka, Florida showed abnormal hormone concentrations and significantly reduced phallus size in comparison to populations of alligators from uncontaminated lakes (Pickford et al., 2000). The decline of the alligator population in Lake Apopka was attributed to a 1980 pesticide spill (Woodward et al., 1993), but cause and effect could not be proven. To date, there are several studies demonstrating endocrine disruption in aquatic organisms from contaminated ecosystems (Mills and Chichester, 2005), and a very few extreme cases where population declines could be attributed to endocrine disruptors (e.g., Lake trout in Lake Ontario in 1950's due to dioxin --Ankley and Geisy, 1998). Few studies have been able to quantitatively predict how subtle and sublethal effects of endocrine disruptors will affect wildlife population dynamics.

Aquatic organisms are of particular concern because they are continually immersed in contaminants from sewage discharge, pulp and paper mill effluents, and other sources of endocrine disruptors, and may be sentinels for environmental degradation (Goodbred et al., 1997). In fish, many endocrine-disruption events have been observed including: altered steroid levels; reduced gonad growth and gamete production; inhibited gamete maturation; decreased fertilization success; and decreased larval survival and growth (Kime, 1998; Faulk et al., 1999; Rolland., 2000; Mills and Chichester, 2005; Sumpter, 2005).

For this study, I created a series of linked statistical and computer models that simulate how endocrine disruptors affect two ecologically different croaker populations [Mid Atlantic Bight (MAB) and Gulf of Mexico (GOM)]. The endocrine disruptors examined in the various analyses include: polychlorinated biphenyls (PCBs), cadmium, methyl mercury (MeHg), and hypoxia. Atlantic croaker is a good species to model the effects of endocrine disruptors on population dynamics because their reproduction, survival, and growth have been well-studied, extensive long-term field monitoring data are available, and much of the available information has been synthesized (Diamond et al., 1999, 2000, in prep). In addition, Atlantic croaker larval development and behavior has been studied extensively in the laboratory (Faulk et al., 1999; McCarthy et al., 2003; Alvarez, 2005), and the Atlantic croaker has been used as a model species in toxicological and reproductive studies (Thomas, 1994; Khan and Thomas, 2000). Accordingly, models can be developed that are heavily based on and well grounded in empirical information.

1.2. Modeling Overview

The overall modeling framework is outlined in Fig.1.1. The physiologically-based model (Model I) modeled the major biochemical processes involved in vitellogenesis within a single adult female fish, and examined how exposure as indicated by specific biomarkers (box A) results in changes in fecundity (box B). In general, predicted fecundity values from the physiological model could be used as input into the matrix population model (Model IV). In my specific analyses, reductions in fecundity were also available from measurements so the predicted fecundity from the physiological

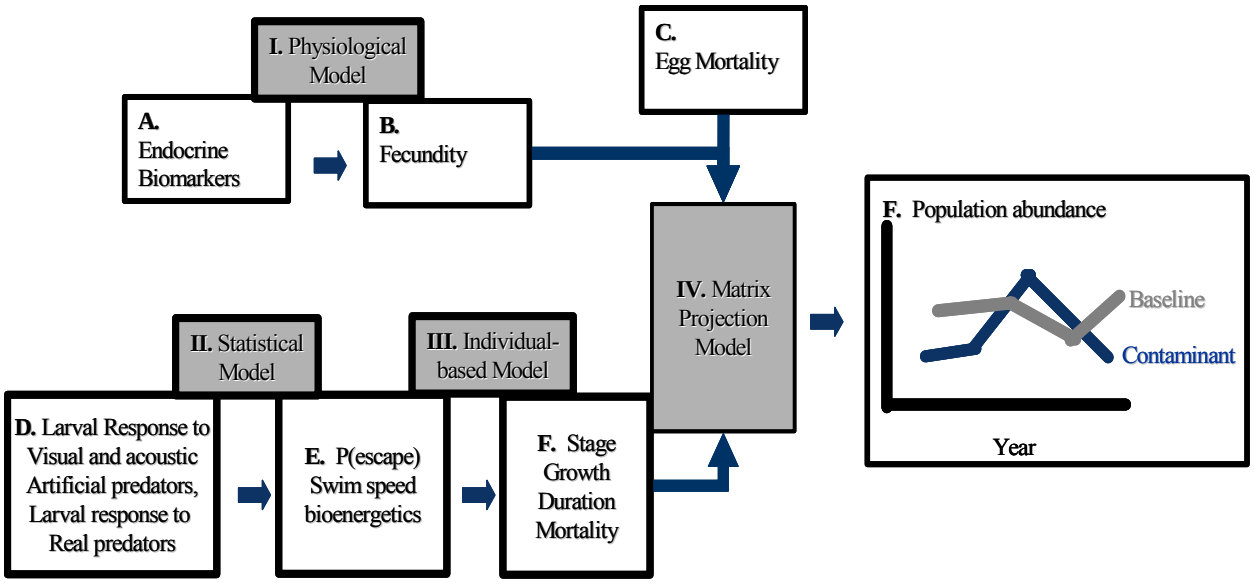

Figure 1.1. Flowchart showing how toxicological endpoints measured in the laboratory can be scaled to population responses using a series of linked statistical and computer simulation models.

model was not used as input to the matrix model. Measured effects of contaminants on egg mortality were also available from laboratory studies, and these were also directly imposed in the matrix model (box C). The second model (Model II) was a statistical model that converts subtle changes in larval performance (e.g., swimming speed, responses to acoustic and visual stimuli) that were measured in the laboratory by colleagues (McCarthy et al., 2003; Alvarez, 2005) using video-taping of control and contaminant-exposed larvae (box D) into the probability of escaping an attack from a real predator (box E). The third model (Model III) was an individual-based model (IBM) that used the changes in probability of escape due to contaminant exposure from Model II, plus changes in swim speeds, and predicted changes in larval growth and mortality rates, which determine larval stage duration and survival (box F). Predicted changes in larval stage duration and survival (box F) were used to change the appropriate parameters of the

matrix projection model (Model IV). The matrix model then simulated long-term population dynamics with baseline and contaminant-exposed parameter values. Models I through III converted biomarkers of endocrine disruption to population-relevant metrics, such as changes in fecundity and larval stage duration and survival. The last model (Model IV) was a matrix population projection model that simulated the long term population dynamics; matrix projection models are commonly used to simulate the population dynamics of fish (Saila et al., 1991; Rose et al., 1996). Matrix models require stage or age-specific fecundity, survival, and growth, and are appropriate for the types of data commonly reported for fish populations and fisheries.

1.3. Dissertation Overview

The development of the physiologically-based model (Model I in Fig. 1.1) is the focus of Chapter 2. The model simulated vitellogenesis in a mature, female, sciaenid fish. The model used ordinary differential equations to simulate the major biochemical reactions over a six-month period from the secretion of gonadotropin into the blood through the production of vitellogenin. Cumulative vitellogenin production can be related to fecundity, a population relevant endpoint. The effects of two endocrine disrupting chemicals (PCBs and cadmium) on cumulative vitellogenin production were simulated, and the results were compared to available laboratory studies. PCBs and cadmium affect the hypothalamus-pituitary-gonadal-liver axis of fish in different ways.

In Chapter 3, the physiologically-based vitellogenesis model that was developed in Chapter 2, is applied to simulate the effects of hypoxia and was analyzed using Monte Carlo uncertainty analysis. Model dynamics were evaluated using the results of laboratory studies that explored the effects of low concentrations of dissolved oxygen

(DO) on reproduction, and included measurement of suite of endocrine-related biomarkers (e.g., estradiol). The model was then applied to the same biomarkers measured in field-caught fish sampled at normoxic and hypoxic locations in Penasacola Bay, Florida. Monte Carlo uncertainty analysis was applied under increasing variability in model parameters and under normoxic and hypoxic conditions. The results of the uncertainty analysis were used to identify sensitive model parameters to target future laboratory experiments.

Chapter 4 is focused on the development of Models II and III (Fig. 1.1) that link behavior of larval fish to the ecologically relevant endpoints of stage duration and survival. Two models were used: statistical and individual-based. The statistical model converted changes in swimming speed and sensory responses to artificial stimuli resembling predator attacks to the probability of escaping an attack from a real fish predator. The individual-based model then converted the probability of escaping a predator, combined with swimming speed, to larval stage duration and survival. The statistical and IBM models were used with laboratory experiments on Atlantic croaker exposed to PCBs and to MeHg to predict contaminant-related changes to parameters of the matrix projection model.

In Chapter 5, I expanded existing lifetables of Atlantic croaker populations (Diamond et al., 1999) into stochastic, density-dependent matrix projection models for the MAB and the GOM populations of Atlantic croaker. The matrix model developed is an extension of the classic formulation, and simulated two nursery areas for each population, represented the first year of life as life stages, used multiple time steps to accommodate different stage durations, and included stochastic and density-dependent

mortality effects. The matrix model was used to simulate croaker population dynamics for 100 years under baseline, PCB exposure, and MeHg exposure using the contaminant induced changes predicted from Model III in Chapter 4, along with other laboratory results. Population responses were compared between contaminants and between the MAB and GOM populations, which differ in their vital rates and exploitation history.

The final chapter is a summary of my major results and some thoughts about my modeling methodology viewed in a broader context. I discuss how the use of linked models can be used for better understanding and for forecasting fish population responses to multiple stressors. I also discuss how the use of linked models for extrapolating from behavioral effects measured on individuals in seconds to long-term population dynamics over 100 years is an example of the importance of scaling (Levin, 1992) in ecological studies.

1.4. References

Alvarez, M. C. 2005. Significance of environmentally realistic levels of selected contaminants to ecological performance of fish larvae: effects of atrazine, malathion, and methylmercury. PhD Dissertation. University of Texas, Austin, Texas.

Ankley, G. T. and Giesy, J. P. 1998. Endocrine disruptors in wildlife: a weight of evidence perspective. *In*: Kendall, R., Dickerson, R., and Giesy, J. et al. (editors), Principles and Processes for Evaluating Endocrine Disruption in Wildlife. SETAC Press, Pensacola, FL, USA. pp 349-367.

Colborn, T., Saalvom, F.S. and Soto, A.M. 1993. Developmental effects of endocrine disrupting chemicals in wildlife and humans. *Environ. Health Perspect.* 101:378-384

Diamond, S. L., Cowell, L.G. and Crowder, L.B. 2000. Population effects of shrimp trawl bycatch on Atlantic croaker. *Can J Fish Aquat Sci*. 57:2010-2021.

Diamond, S. L., Crowder, L. B., and Cowell. L. G. 1999. Catch and bycatch: the qualitative effects of fisheries on population vital rates of Atlantic croaker. *Trans. Am. Fish. Soc.* 128: 1085-1105.

Diamond, S.L., Murphy, C. A. and Rose, K. A. (in prep). Simulating the effects of global warming on Atlantic croaker population dynamics in the Mid-Atlantic region: pushing the limits on what we know. To be submitted to *Global Change Biology*.

Faulk, C. K. Fuiman, L. A., Thomas, P. 1999. Parental exposure to *ortho, para*-dichlorodiphenyltrichloroethane impairs survival skills of Atlantic croaker (*Micropogonias undulatus*) larvae. *Environ. Toxicol. Chem.* 18: 254-262.

Folmar, L.C., Denslow, N. D., Rao, V., Chow, M., Crain, D. A., Enblom, J., Marcino, J. Guillette, L. J. Jr. 1996. Vitellogenin induction and reduced serum testosterone concentrations in feral male carp (*Cyprinus carpio*) captured near a major metropolitan sewage treatment plant. *Environ. Health Perspect.* 104:1096-1101.

Goodbred, S. L., Gilliom, R. J., Gross, T. S., Denslow, N. P., Bryant, W. L., and Schoeb, T. R.1997. Reconnaissance of 17**$**-estradiol, 11-ketotestosterone, vitellogenin, and gonad histopathology in common carp of United States streams: Potential for contaminant-induced endocrine disruption. U.S. Geological Survey, Open-file Report, Sacremento, California.

Khan, I.A. and Thomas, P. 2000. Lead and Arochlor 1254 disrupt reproductive neuroendocrine function in Atlantic croaker. *Mar. Environ. Res.* 50: 119-123.

Kime, D. E., Nash, J. P., and Scott, A. P. 1998. Vitellogenesis as a biomarker of reproductive disruption by xenobiotics. *Aquaculture* 177: 345-352.

Kime, D. E. 1998. *Endocrine disruption in Fish*. Kluwer Academic Publishers. Norwell.

Levin, S. A. 1992. The problem of pattern and scale in ecology. Ecology 73: 1943-1967.

McCarthy, I. D., Fuiman, L. A. and Alvarez, M.C. 2003. Aroclor 1254 affects growth and survival skills of Atlantic croaker *Micropogonias undulatus* larvae. *Mar. Ecol. Prog. Ser*. 252:295-301.

Mills, L. J., and Chichester. C. 2005. Review of evidence: are endocrine-disrupting chemicals in the aquatic environment impacting fish populations? *Sci. Tot. Environ*. 343:1-34.

Pickford, D. B., Guillette Jr., L. J., Crain, D. A., Rooney, A. A. and Woodward, A. R. 2000. Plasma dihydrotestosterone concentrations and phallus size in juvenile American alligators (*A. mississippiensis*) from contaminated and reference populations. *J. Herpet.* 34:233-239.

Rolland, R. M. 2000. Ecoepidemiology of the effects of pollution on reproduction and survival of early life stages in teleosts. *Fish Fish*. 1: 41-72.

Rose, K. A., Tyler, J. A., Chambers, R. C., MacPhee, G., and Danila, D. J. 1996. Simulating winter flounder population dynamics using coupled individual-based young-of-the-year and age-structured adult models. *Can. J. Fish. Aquat. Sci.* 53: 1071-1091.

Saila, S., Martin, B., Ferson, S., Ginzburg, L., and Millstein, J. 1991. Demographic modeling of selected fish species with RAMAS. Final Report, Research Project 2553, EPRI EN-7178 EPRI, Palo Alto, CA. 123p.

Sumpter, J. P. 2005. Endocrine disrupters in the aquatic environment: an overview. *Acta. hydrochim. hydrobiol.* 33:9-16.

Thomas, P. 1994. Hormonal control of final oocyte maturation in sciaenid fishes. *In* Perspectives in Comparative Endocrinology. K.G. Davey, R.E. Peter, and S.S. Tobe (eds.), pp. 619-625. *Perspectives in Comparative Endocrinology*. National Research Council of Canada, Ottawa.

WHO. Global Assessment of the State-of-the-Science of Endocrine Disruptors. 2002. In Damstra, T, Barlow S, Bergman A, Kavlock R, van der Kraak G, eds. International Programme On Chemical Safety.

Woodward, A.R., Jennings, M.L., Percival, H. F., Moore, C. T. 1993. Low clutch viability of American alligators on Lake Apopka. *Fl. Sci.* 56:52-63.

CHAPTER 2. MODELING VITELLOGENESIS IN FEMALE FISH EXPOSED TO ENVIRONMENTAL STRESSORS: PREDICTING THE EFFECTS OF ENDOCRINE DISTURBANCE DUE TO EXPOSURE TO A PCB MIXTURE AND CADMIUM[1]

2.1. Introduction

There is now extensive evidence of reproductive and developmental abnormalities in fish and wildlife populations exposed to a wide variety of chemicals in the environment (Colborn et al., 1993; Kime, 2001; WHO, 2002). The aquatic environment is a sink for endocrine disrupting chemicals (EDCs) and other organic chemicals; therefore it is not surprising that there exist many examples of endocrine disruption in fish (Kime, 2001) Fish immersed in the aquatic environment bioaccumulate lipophilic chemicals via ingestion from food items and via absorption of contaminants through their gills and scales. Among the many examples of endocrine disruptors that affect fish are man-made chemicals such as PCBs that affect the neuroendocrine system (Khan and Thomas, 2001), and excessive concentrations of trace elements such as cadmium that can interfere with gonadotropin regulation and steroidogenesis (Thomas and Khan, 1995).

Fish play an integral role in the aquatic ecosystem food web, and any effects that change the population structure of fish may also alter community and food web dynamics. Because fish can biomagnify contaminants, fish are potentially useful sentinels of aquatic environmental degradation (Davis, 1995). Fish carrying high loads of EDCs in their body tissue potentially suffer impaired health and can deliver high concentrations of EDCs to their consumers (i.e., apex predator species and humans). However, in many situations, the overall reproductive significance of the observed

[1] Reprinted from Reproductive Toxicology 19. pp.395-409. Copyright (2005), with permission from Elsevier. Note: Minor editorial changes were made in the published paper to conform to dissertation formatting requirements.

endocrine changes after exposure to EDCs remains unclear, and the potential ecological relevance is unknown.

Disturbances of reproductive function in field-caught female fish have been inferred from changes in endocrine and reproductive function biomarkers, such as altered sex steroid hormone, atypical gonadotropin and vitellogenin concentrations in circulation, and abnormal gonadal and oocyte growth. For example, fish exposed to bleached kraft pulp mill effluent showed changes in the induction of the hepatic mixed function oxygenase enzyme system (MFO), reduced circulating levels of reproductive steroid hormones, reduced gonad growth, younger age to sexual maturation, and slower development of secondary sex characteristics. Examination of multiple biomarkers provides information on the exposure and reproductive health of the exposed fish (Munkittrick, et al., 1991; McMaster et al., 1996).

Plasma concentrations of hormones taken at specified stages during the reproductive cycle can be a good indication of disruption of the reproductive process (Donaldson, 1990). However, such biomarkers can be confounded by naturally occurring fluctuations in the reproductive cycle, and care must be taken when considering the timing of biomarker measurements (McMaster et al., 2001). Biomarkers are snapshots in time from a dynamic system. There is a need for models that can relate biomarker measurements to the entire reproductive cycle, and that can extrapolate biomarkers to ecologically relevant endpoints such as the production of eggs.

In this paper, I use a physiological model to simulate how two nonestrogenic EDCs that act via different mechanisms could affect vitellogenesis in fish. Vitellogenesis results in the production of the yolk precursor protein vitellogenin. Vitellogenesis is

sensitive to disruption by EDCs and of ecological relevance because vitellogenin production is directly related to the reproductive output (fecundity and egg quality) of individual fish (Tyler and Sumpter, 1996). My goal was to develop a modeling tool that quantitatively links relevant biomarkers of endocrine disruption in adult female fish to cumulative vitellogenin production over the reproductive season. I then used the model to simulate the effects of vitellogenin production of exposure to a PCB mixture and cadmium. I base my computer model on two fish species from the family Sciaenidae: spotted seatrout (*Cynoscion nebulosus*) and Atlantic croaker (*Micropogonias undulatus*). Spotted seatrout and Atlantic croaker are well-established estuarine teleost model organisms used to study reproductive endocrinology and endocrine toxicity. Simulations illustrate how the model can be used to estimate the reproductive significance of endocrine biomarker measurements in field-caught fish. I am early in the process of model development, and my model should be considered as preliminary. Continued corroboration and testing, and targeted laboratory and field measurements, are planned to refine and improve the realism of the model.

2.2. Model Description and Simulations

2.2.1. Model Overview

The model is a system of eight ordinary differential equations that simulate vitellogenesis in an individual mature female fish (Table 2.1; Fig. 2.1). The model is driven by the hourly introduction of gonadotropin (GtH) and the resultant biochemical reactions are simulated for 6 months, resulting in a prediction of the cumulative production of vitellogenin. There is an equation for the rate of change of each of the eight state variables: free testosterone (T), unbound or free steroid binding protein (SBP),

steroid binding protein bound to testosterone (SBP-T), steroid binding protein bound to estradiol (SBP-E2), free estradiol (E2), unbound or free estrogen receptor (ER), estrogen receptor bound to E2 or activated ER (ER-E2), and vitellogenin (Vtg).

There are also three additional differential equations that keep track of the output variables of total testosterone (free testosterone plus testosterone bound to steroid binding proteins), total estradiol (free estradiol plus estradiol bound to steroid binding proteins) and total estrogen receptor (free estrogen receptor plus estrogen receptor bound to estradiol). These output differential equations use the same processes as the state variables, but enable bookkeeping of the portion of the bound complexes that are the state variable of interest (e.g., how much testosterone is in the testosterone bound with the steroid binding protein state variable). Laboratory and field measurements are frequently reported as total concentrations, rather than the concentrations of the free and bound forms.

All of the state variable differential equations follow a standard format of expressing the rate of change of a state variable as equal to its synthesis rate minus degradation rate plus inactivation rate minus activation rate. All state variables and output variables are expressed as mass (pg or mg) per milliliter of blood (plasma), except for variables involving the estrogen receptor. The free estrogen receptor state variable (equation 2.7) is reported in nM units. However, field measurements are reported in pico moles per gram of liver (pmol/g liver) (Smith and Thomas, 1991). I report the total estrogen receptor concentration output variable (equation 2.14) in pico moles per gram of liver (pmol/g liver) to allow comparison to field measurements. Based on laboratory

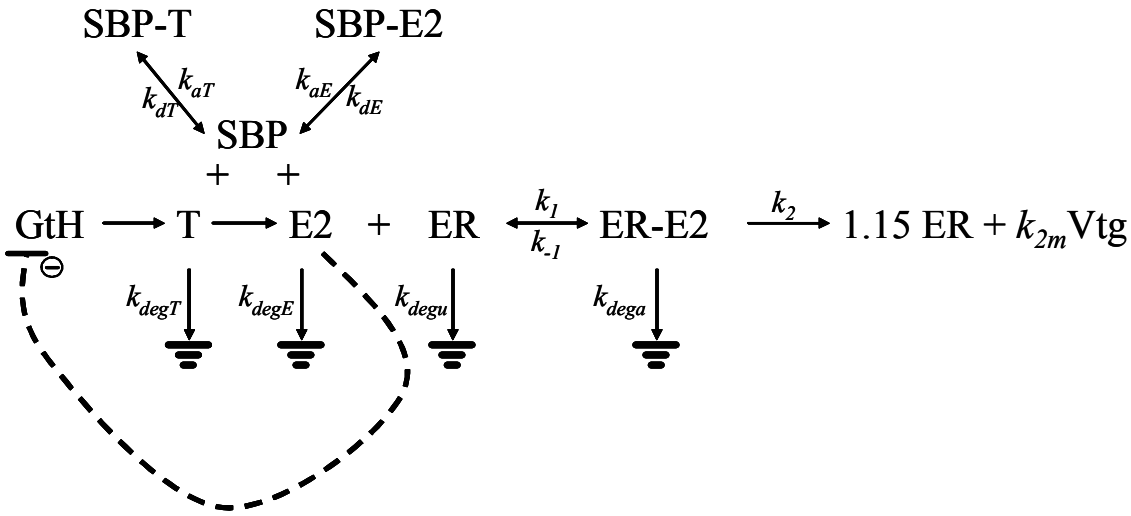

Figure 2.1. Schematic representation of the major biochemical reactions represented in the model of vitellogenesis in an individual female fish. Gonadotropin (GtH) stimulates the production of testosterone (T), which provides a substrate for the production of estradiol (E2). T and E2 bind and unbind to steroid binding proteins (SBP) at rates of association (k_{aT}, k_{aE}) and rates of dissociation (k_{dT}, k_{dE}). Unbound steroids (free) are susceptible to degradation at specified rates (k_{degT}, k_{degE}). Free E2 binds to the estrogen receptor (ER) at a rate of k_1, forming an activated ER complex (E2-ER) and disassociates at rate of k_{-1}. High levels of E2 inhibit the production of GtH. The activated ER initiates a cascade of reactions that results in the production of more ER and (k_{2m} times) vitellogenin (Vtg) at a rate of k_2. Un-activated ER is susceptible to degradation at a rate of k_{degu}, whereas activated ER (E2-ER) degrades at a much faster rate (k_{dega}). A double arrow refers to a reversible reaction, a single arrow refers to an irreversible reaction, and the dotted line refers to inhibition

Table 2.1. System of ordinary differential equations that define the model of vitellogenesis in an individual mature female fish. Equation (2.1) is the equation for the single driving variable of gondadotropin concentration in the blood. Equations (2.2) – (2.9) correspond to each of the eight state variables in the model. Equations (2.10) and (2.11) are the Hill functions that appear in equations (2.2) and (2.6), respectively. Equations (2.12)-(2.14) correspond to three output variables that use the same reactions as the state variables but allow for the reporting of total concentrations of testosterone, estradiol, and estrogen receptor.

Driving variable:

2.1. $$GtH = \frac{0.5(1 - 1.0\cos\frac{2\pi(t - 6.0)}{24.0})}{1.0 + \frac{[E2]}{10}}$$

State variables:

2.2. $$\frac{dT}{dt} = synT(GtH) - k_{\deg T}[T] + k_{dT}[SBP - T] - synE2(T) - k_{aT}[T][SBP]$$

2.3. $$\frac{dSBP}{dt} = k_{dT}[SBP - T] + k_{dE}[SBP - E2] - k_{aT}[T][SPB] - k_{aE}[E2][SPB]$$

2.4. $$\frac{dSBP - T}{dt} = k_{aT}[T][SBP] - k_{dT}[SBP - T]$$

2.5. $$\frac{dSBP - E2}{dt} = k_{aE}[E2][SBP] - k_{dE}[SBP - E2]$$

2.6. $$\frac{dE2}{dt} = synE2(T) - k_{\deg E}[E2] + k_{-1}[ER - E2] + k_{dE}[SBP - E2] - k_1[E2][ER] - k_{aE}[E2][SBP]$$

2.7. $$\frac{dER}{dt} = 1.15 \bullet k_2[ER - E2] - k_{\deg u}[ER] + k_{-1}[ER - E2] - k_1[E2][ER]$$

2.8. $$\frac{dER - E2}{dt} = k_1[E2][ER] - k_{\deg a}[ER - E2] - k_{-1}[ER - E2] - k_2[ER - E2]$$

2.9. $$\frac{dVtg}{dt} = k_{2m} \cdot k_2[ER - E2]$$

(Table continued)

Where:

$$2.10.\ synT(GtH) = \frac{V_{1_T}(GtH^{h_T})}{K_{m_T}^{h_T} + GtH^{h_T}}$$

$$2.11.\ synE2(T) = \frac{V_{1_E}(T^{h_E})}{K_{m_E}^{h_E} + T^{h_E}}$$

Output variables:

$$2.12.\ \frac{dTotal\ T}{dt} = synT(GtH) - k_{\deg T}[T] - synE2(T)$$

$$2.13.\ \frac{dTotal\ E2}{dt} = synE2(T) - k_{\deg E}[E2] + k_{-1}[ER - E2] - k_1[E2][ER]$$

$$2.14.\ \frac{dTotal\ ER}{dt} = (0.15 \bullet k_2[ER - E2] - k_{\deg u}[ER] - k_{\deg a}[ER - E2]) \bullet 4.0\ L/g$$

experiment protocol and dilutions, I multiplied nM units by 4.0 L/g to obtain the units of pmol/g liver (Smith and Thomas, 1990).

The vitellogenic processes represented in the model are based on a very simplified view of the many biochemical reactions involved (Fig. 2.1). The model simulates the major reactions from the introduction of gonadotropin into the blood through the production of vitellogenin. Gonadotropin (GtH), which is produced in the pituitary, is released into the bloodstream where GtH travels to the ovary and stimulates thecal cells to produce testosterone. Free or unbound testosterone (T) is then converted to free estradiol (E2) in the neighboring ovarian granulosa cells (Nagahama, 1994). Free testosterone and free estradiol rapidly associate with steroid binding proteins located in the plasma and form the SBP-T and SBP-E2 complexes. Once bound, testosterone and estradiol are protected from metabolic degradation; steroids in the free form (T and E2) are subjected to degradation. Free estradiol diffuses through tissues and acts at the pituitary and liver. In the pituitary, high levels of free estradiol inhibit the release of gonadotropin (dotted line in Fig. 2.1). In the liver, free estradiol associates with the estrogen receptor (ER) to form the estradiol-estrogen receptor complex (ER-E2). Small amounts of estradiol disassociate from the estrogen receptor and are re-introduced into the bloodstream. Activated estrogen receptor (ER-E2) is degraded. Activation of the estrogen receptor causes alterations in the rates of transcription of estrogen responsive genes leading to the synthesis of more estrogen receptor and vitellogenin (ER and k_{2m}Vtg).

I wanted a model prediction that could be interpreted as related to the total fecundity of an individual fish. Therefore, the model accumulates vitellogenin

production over the simulation. In reality, vitellogenin concentration in the plasma varies over time, depending on both its production and its loss due to being taken up in rapidly growing oocytes. Vitellogenin is a yolk-precursor protein, and is an essential building block for oocytes and critical to the production of healthy eggs (Specker and Sullivan, 1994).

2.2.2. Model Processes and Parameter Estimation

Below I describe each of the major processes represented in the model, including the rationale for their formulations and the sources used to estimate model parameters. As much as possible, I use information from spotted seatrout and Atlantic croaker. Seatrout and croaker are both sciaenids, and have been well studied in a series of laboratory and field experiments (Thomas, 1988, 1989; Smith and Thomas, 1990, 1991; Laidley and Thomas, 1994, 1997; Thomas and Khan, 1995; Khan and Thomas, 2001). Seatrout and croaker are both important estuarine species and croaker is widely distributed along most of the Atlantic coast extending up to Cape Cod (Diamond et al., 1999, 2000). In some instances, I used information from other species of fish. All equation numbers in the text refer to the equations listed in Table 2.1.

2.2.2.1. Gonadotropin

I used data on luteinizing hormone (LH) secretion as representative of gonadotropin in model simulations. Ovarian function in vertebrates, including oocyte and ovarian growth, is primarily regulated by gonadotropins secreted by the pituitary gland in response to neuroendocrine signals from the brain. As in most tetrapod vertebrates, the pituitary in teleosts produces two gonadotropins: follicle stimulating hormone (FSH) and LH (Suzuki et al., 1988). Growth of the oocyte and ovarian follicle

in tetrapods is primarily regulated by an increase in FSH secretion, whereas the physiological role of FSH (formerly GTH I) in regulating oocyte and ovarian follicle growth remains to be demonstrated in most teleost species. Salmonids are the only group of fishes for which a sensitive FSH radioimmunoassay has been developed. In salmonids, the secretion of FSH coincides with the period of gonadal growth, whereas LH secretion increases towards the end of the reproductive cycle roughly coinciding with oocyte maturation and spawning (Swanson, 1991). However, LH secretion in Atlantic croaker and several other teleosts shows diurnal changes and is under precise neuroendocrine control by transmitters, peptides, and steroids during ovarian growth (Copeland and Thomas, 1989; Khan and Thomas, 1999). Moreover, stressor-induced alterations in gonadal growth in Atlantic croaker have been associated with changes in LH secretion (Khan and Thomas, 2000, 2001). LH has similar steroidogenic potency to that of FSH at the gonadal growth stage of the reproductive cycle (Patino et al., 2001). Although FSH has been identified in Atlantic croaker, no quantitative information is currently available on FSH secretion (Copeland and Thomas, 1993). Taken together, these findings suggest a potential role for LH during ovarian and oocyte growth in Atlantic croaker. Therefore, data on LH secretion was used as representative of gonadotropin secretion, with the realization that I may need to revisit this issue as more data become available.

I represented LH concentrations in the plasma with a diurnal cycle based on observations on Atlantic croaker. During the period of gonadal recrudescence (which lasts about 8 weeks), LH plasma levels in croaker exhibit a diurnal pattern gradually reaching maximum values of about 1.0 ng/mL at dusk, and minimum values below detection by dawn (P. Thomas, unpublished data). I created a sinusoidal function to

mimic the diurnal pattern of plasma gonadotropin concentration (numerator of equation 2.1; Fig. 2.2). The amount of gonadotropin produced by the sinusoidal function reflects the net plasma concentration of gonadotropin, and thereby accounts for degradation and removal. Gonadotropin was introduced for the first 8 weeks of the simulation, corresponding to the period of gonadal recrudescence, and then set to zero for the remainder of the simulation.

I also include a negative feedback by which steroids inhibit the introduction of the gonadotropin driving variable (denominator of equation 2.1). Steroids such as testosterone and estradiol have been shown to have a negative feedback effect on FSH production in salmonids (Breton et al., 1997; Dickey and Swanson, 1998; Saligaut et al., 1998). In Atlantic croaker, testosterone and estradiol stimulate LH production during early gonadal recrudescence, but inhibit the production of LH after gonad maturation (Khan et al., 1999). Quantitative information is not available on the details of these positive and negative feedbacks. I did not model the estrogen receptor in the brain, but I incorporated the negative feedback mechanism into my model by reducing the plasma concentration of gonadotropin when free estradiol concentrations got very high. For example, a free estradiol concentration of 25 pg/mL incorporated into the denominator of equation (2.1) would decrease the plasma gonadotropin concentration by 0.3%, and a higher concentration of 1000 pg/mL would decrease the plasma gonadotropin concentration by 9%.

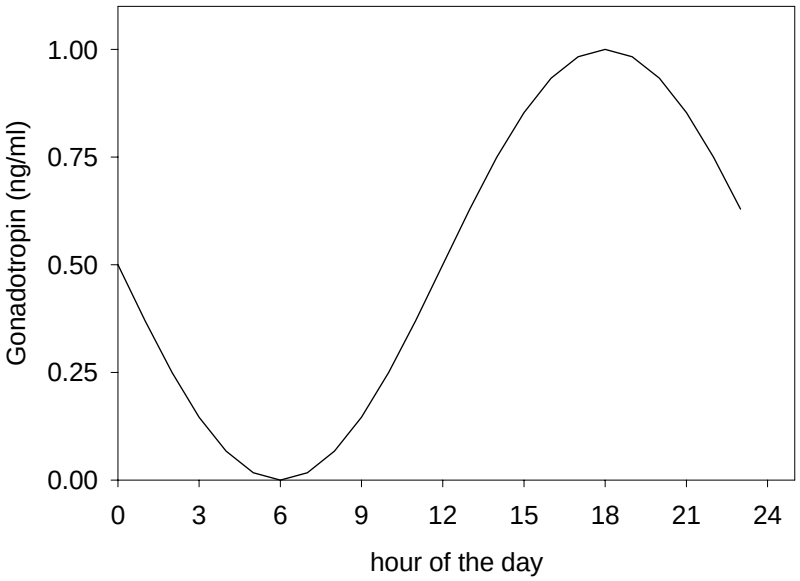

Figure 2.2. Hourly concentrations of the gonadotropin driving variable showing the diurnal cycling assumed for the first eight weeks of the baseline simulation

2.2.2.2. Steroidogenesis

I opted for an aggregate approach to represent the many reactions involved in the stimulation of testosterone production by gonadotropin, and the subsequent use of testosterone for the production of estradiol. Many of the reactions involved have not been clearly defined. I therefore adopted the approach used by Schlosser and Selgrade (2001) who aggregated many biochemical reactions into a few processes to model the synthesis of LH in humans and then used the model to predict the effects of EDCs on the human menstrual cycle. In my model, I grouped all of the reactions occurring between the release of gonadotropin and the production of testosterone into a general synthesis function (equation 2.10), and I also grouped all of the reactions occurring between the release of testosterone and the production of estradiol into a second synthesis function (equation 2.11). The basic form of both of these synthesis functions was a Hill equation, which exhibits a sigmoid relationship between substrate and product (Segel, 1975).

I estimated the parameter values of the Hill function that related gonadotropin concentration to testosterone production (equation 2.10) from a study of steroidogenesis in goldfish (van der Kraak et al., 1992). In this study, the rate of testosterone production was obtained from pre-ovulatory follicles of goldfish incubated in increasing concentrations of carp gonadotropin. I derived the parameter values of the Hill function for the conversion of gonadotropin to testosterone by maintaining the shape of the relationship observed in the experiment with goldfish. The maximum testosterone production rate was chosen so that the assumed gonadotropin driving variable stimulated a maximum concentration of testosterone of about 1200 pg/mL within the first month of the baseline simulation. Smith and Thomas (1991) reported a maximum total

testosterone concentration of 1200 pg/mL in April in field-caught spotted seatrout. I tried a variety of values of V_1, K_m and h_t in equation (2.10) until I obtained set of values (Table 2.2) that produced a similarly shaped relationship between gonadotropin concentration and testosterone production rate as observed in the goldfish experiment but with concentrations pertinent to our baseline simulation (Fig. 2.3A).

To estimate the parameters for the second Hill function that related estradiol production to testosterone concentration, I maintained a sigmoidal shape to the function while constraining the function to occur within our simulated ranges of free testosterone concentration and free estradiol production. I used the range of free testosterone concentrations that occurred under baseline conditions in my model (0-100 pg/mL) because only 1-10% of the total testosterone is available as a ligand; much of testosterone and estradiol are bound to steroid binding proteins (Petra et al., 1985). I assumed that testosterone is rapidly converted estradiol so that 23% is converted within 0.01 hours; this assumption was based on a study by van der Kraak et al. (1992) that reported estradiol production at high gonadotropin concentrations was approximately 23% of what would be the expected testosterone production from the same gonadotropin concentration. The value I assigned to V_{1E} (Table 2.2) was based on the assumption that at maximum concentrations of free testosterone (e.g., 100 pg/mL) estradiol production in one timestep of the model (0.0001 hours) would be 0.23% of the maximum free testosterone concentration (i.e. 0.23 pg/mL/0.0001 hr). I arbitrarily determined parameter values (K_m and h_E, Table 2.2) to maintain a sigmoid relationship between testosterone concentration and estradiol production (Fig. 2.3B).

Table 2.2. Definitions, relevant equation numbers, units, and baseline values of the parameters of the model of vitellogenesis in an individual female fish.

Name	Definition	Equation	Units	Value
V_{IT}	Maximum rate of free testosterone production	2.10	pg/mL/h	80.0
V_{IE}	Maximum rate of free estradiol production	2.11	pg/mL/h	2300.0
K_{mT}	Half-saturation of free testosterone production	2.10	ng/mL	0.3
K_{mE}	Half-saturation of free estradiol production	2.11	pg/mL	52.0
h_T	Hill coefficient for free testosterone	2.10		1.8
h_E	Hill coefficient for free estradiol	2.11		3.5
k_{2m}	Multiplier for rate constant k_2	2.9		10.0
k_1	Association rate of free estradiol with estrogen receptor	2.6-2.8, 2.13	$1/10^8$ M/h	7.43
k_{-1}	Dissociation rate of free estradiol with estrogen receptor	2.6-2.8, 2.13	1/h	0.81
k_2	Rate of production of vitellogenin and estrogen receptor	2.7-2.9, 2.14	1/h	0.3465
k_{aT}	Association rate of free testosterone with steroid binding protein	2.2-2.4	$1/10^9$ M/h	5.6687
k_{dT}	Dissociation rate of free testosterone with steroid binding protein	2.2-2.4	1/h	27.72
k_{aE}	Association rate of free estradiol with steroid binding protein	2.4-2.6	$1/10^9$ M/h	5.6687
k_{dE}	Dissociation rate of free estradiol with steroid binding protein	2.4-2.6	1/h	17.74
k_{degT}	Degradation rate of free testosterone	2.2, 2.12	1/h	1.386
k_{degE}	Degradation rate of free estradiol	2.6, 2.13	1/h	1.386
k_{degu}	Degradation rate of free estrogen receptor	2.7, 2.14	1/h	0.00058
k_{dega}	Degradation rate of activated estrogen receptor	2.8, 2.14	1/h	0.012
	Initial conditions for state variables that are different than 0:			
T	Free testosterone	2.2	pg/mL	10.0
SBP	Free steroid binding protein	2.3	nM	400.0
E2	Free estradiol	2.6	pg/mL	10.0
ER	Free estrogen receptor	2.7	nM	0.125

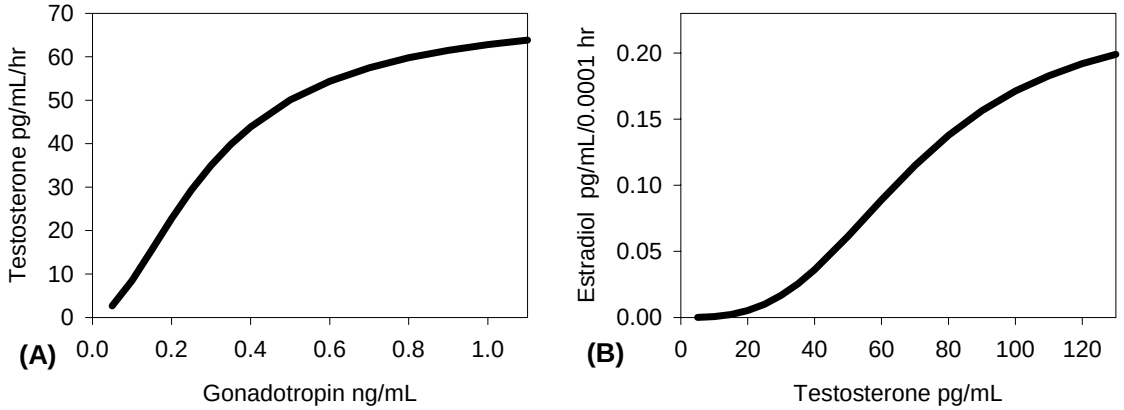

Figure 2.3. Derived Hill functions for the production of free testosterone from gonadotropin and for the production of free estradiol from testosterone. A) simulated relationship between testosterone production and gonadotropin concentration, B) simulated relationship between estradiol production and testosterone concentration..

2.2.2.3. Steroid Binding Proteins

Although steroid binding proteins have multiple functions, I only simulated their binding with free testosterone and free estradiol that resulted in steroids being protected from degradation. The main functions of steroid binding proteins appear to be to protect bound steroids from degradation, to regulate steroid uptake into the target tissue, and to participate directly in signal transduction (Pardridge, 1981; Petra et al., 1985; Rosner, 1990). However, because of limited information on the regulation and signal transduction functions, I only focused on the protection function of steroid binding proteins.

The kinetics of binding of estradiol and testosterone to the steroid binding proteins were represented with first order dissociation reactions and second order

association reactions (equations 2.3-2.5). I used equilibrium dissociation constants (K_d) reported by Laidley and Thomas (1994) to estimate the model rate constants for the association and dissociation between testosterone and steroid binding proteins (k_{aT} and k_{dT}; Table 2.3), and between estradiol and steroid binding proteins (k_{aE}, and $k_{dE;}$ Table 2.3). K_d is the ratio of the dissociation rate to the association rate, $K_d = k_{dissociation} / k_{association}$. The reported K_d of free testosterone with steroid binding proteins was 4.89 nM, whereas estradiol had a greater affinity to steroid binding proteins with a reported K_d of 3.13 nM (Laidley and Thomas, 1994).

To separate the reported K_d values for estradiol with steroid binding proteins and for testosterone with steroid binding proteins into constituent association and dissociation rate constants, I first determined their dissociation rates. Laidley and Thomas (1994) reported that radioactive testosterone had rapid association (half life or $t_{1/2} < 30$ sec) and rapid dissociation ($t_{1/2}$ of about 90 sec) with steroid binding proteins. I assumed k_{dT} was a first order rate constant, and then I solved for k_{dT} using the general relationship between the half-life ($t_{1/2}$) and the first-order rate constant (k): $t_{1/2} = 0.693/k$ (McQuarrie and Rock, 1987). Then to determine the testosterone association rate constant with steroid binding proteins (k_{aT}), I divided k_{dT} by K_d. The association and dissociation rate constants of estradiol with steroid binding proteins was calculated assuming the association rate constant was the same as the association rate constant estimated for testosterone ($k_{aE} = k_{aT)}$ and from the reported K_d for estradiol binding with steroid binding proteins reported by Laidley and Thomas (1994).

I represented the dynamics of steroid binding proteins without synthesis or degradation reactions so that the total steroid binding protein concentration remained

constant throughout the simulation. I fixed the total steroid binding protein concentration because, although the concentration of steroid binding protein increases with ovary maturation, their binding affinity to steroids decreases, suggesting a compensatory effect (Laidley and Thomas, 1997). The initial concentration of total steroid binding protein was set to 400 nM, which corresponded to the mean value reported by Laidley and Thomas (1997). The percent of the total steroid binding protein found in the free form versus bound to testosterone and to estradiol varied over time in the simulations.

Free testosterone (equation 2.2) and free estradiol (equation 2.6) are affected by synthesis (equations 2.10 and 2.11), interactions with steroid binding proteins (k_{aT}, k_{dT}, k_{aE}, k_{aE}), and undergo first order degradation (k_{degT}, k_{degE}). All of the biochemical reactions, except degradation, have been described. I assumed that the degradation rates for both steroids (k_{degT}, k_{degE}; Table 2.2) were 1.386 /hour. This degradation rate was calculated based upon the assumption that $t_{1/2}$ was 30 min, a value reported for the degradation rate of estradiol in salmonids (Zohar, 1982).

2.2.3.4. Estrogen Receptor and Vitellogenin

I represented the binding of free estradiol to the estrogen receptor with first and second order kinetics. Free estradiol associates with the estrogen receptor using a second order rate constant (k_1) and dissociates from the estrogen receptor with a first order rate constant (k_{-1}) (equations 2.6-2.8). The rate constants k_1 and k_{-1} (Table 2.2) were derived from values for K_d of 1.09 nM and k_{-1} of 0.0135/min reported for estradiol association and dissociation with estrogen receptor in spotted seatrout (Smith and Thomas, 1990). I calculated k_1 from the reported values of k_{-1} and K_d and then multiplied both k_{-1} and k_1 by 60 to create hourly rates (Table 2.2).

I calculated different degradation rates for the free and bound estrogen receptors. In mammals, degradation of free estrogen receptor depends on the presence of estradiol. In the absence of estradiol, degradation rates of estrogen receptor are relatively slow (Reid et al., 2002). Smith and Thomas (1990) reported a $t_{1/2}$ of 45 hours or a rate of 0.0002/min for spotted seatrout. I used the degradation rate constant for the activated estrogen receptor (k_{dega}, Table 2.2) reported by Smith and Thomas (1990), and calibrated the free estrogen receptor degradation rate (k_{degu}, Table 2.2) so that the maximum estrogen receptor concentration peaked at 5.25 pmol/g liver (Smith and Thomas, 1991)

I assumed that one activated estrogen receptor resulted in the production of both vitellogenin (equation 2.9) and more estrogen receptor (first term of equation 2.7). I adopted a modeling approach used to model autocatalytic enzymatic reactions (e.g. Manjabacas et al., 2002). In this modeling approach, only one rate parameter (k_2) is required for the conversion of activated estrogen receptor to vitellogenin and more estrogen receptor. Although the exact length of time required to produce estrogen receptor protein is unknown, I estimated k_2 based on transcription rates for vitellogenin mRNA in rainbow trout where estrogen receptor mRNA transcription units reach 50% of maximum values by 2 hours (Flouriot et al., 1996). In order for the estrogen receptor to produce more of itself, the coefficient for the estrogen receptor must equal or exceed one. The magnitude of the coefficient affects the concentration of total estradiol; larger values lead to increased production of estrogen receptor that, in turn, results in a steeper decline in total estradiol concentration. I set the coefficient for the estrogen receptor to 1.15 (Fig. 2.1) in order to slow the decline in total estradiol concentration in the baseline simulation. Although production of estrogen receptor proceeds more rapidly than vitellogenin

production, much more vitellogenin is produced than estrogen receptor (Flouriot et al., 1996); but the exact quantities are unknown. Therefore I assigned a value of 10 to the multiplier of vitellogenin (i.e., $k_{2m} = 10$) to initially get appropriate predictions of final cumulative concentrations of vitellogenin. The value of k_{2m} was not adjusted further during calibration.

2.2.3. Model Simulations

Three model simulations were performed that illustrate the utility of the model for understanding the effects of endocrine disruptors on vitellogenesis in fish. The first simulation was for baseline, or unstressed, conditions. I used the results of long-term field measurements to calibrate the model (adjusted values of V_{1T}, k_{degu}, and the coefficient of estrogen production as described below) until model predictions roughly mimicked the dynamics observed in field-caught fish. The two remaining simulations involved simulating the effects of a PCB mixture (Aroclor 1254) and cadmium. These stressors differ on how they affect vitellogenin production. For each of these stressors, I compared predicted dynamics of selected state and output variables between baseline and stressed simulations, and also compared model-predicted changes in cumulative vitellogenin production to changes in the gonadosomatic index (GSI) measured in laboratory experiments. GSI is based on percent of gonadal weight divided by body weight, and is a commonly used measure of reproductive functioning in fish (Barton et al., 2002).

All model simulations were for 6 months duration covering the period roughly from April 1 through October 1, which is the spawning season of spotted seatrout in the northern Gulf of Mexico (Brown-Peterson, 2003). The system of differential equations was solved using a 4^{th} order Runge-Kutta method with a numerical time step of 0.0001

hours; values of each of the eight state variables and three output variables were outputted every hour for the 6 months. The model was coded in Fortran90. A small numerical time step was used because some of the reactions were very rapid.

2.2.3.1. Calibration and Baseline Conditions

I calibrated the model for baseline conditions based on the values of total testosterone, total estradiol, and total estrogen receptor measured monthly over two years in field-caught spotted sea trout (Smith and Thomas, 1991). I compared model predictions to the values measured between April and October because this was when total testosterone, total estradiol, and total estrogen receptor were near or at their maximum concentrations. I also show the dynamics of free testosterone and free estradiol to illustrate model dynamics. The baseline model simulation used the standard diurnal introduction of gonadotropin (Fig. 2.2) for the first 8 weeks of the simulation.

Calibration focused on three model parameters: the synthesis rate of testosterone (V_{1T} in equation 2.10), the degradation rate of free estrogen receptor (k_{degu} in equation 2.7) and the coefficient for the production of estrogen receptor (1.15 in Fig. 2.1 and in equation 2.7). Values of all model parameters were originally derived from the literature. I adjusted V_{1T}, k_{degu}, and the coefficient of estrogen production in repeated model simulations until predicted maximum values of total testosterone, total estradiol, and total estrogen receptor were similar in magnitude and occurred in approximately the same month as observed in the field measurements. All other parameters were maintained at the values originally derived from the literature.

2.2.3.2. Effects of PCBs

I simulated the effects of the PCB mixture (Aroclor 1254) exposure using the results of laboratory experiments performed on Atlantic croaker (Thomas, 1988, 1989; Khan and Thomas, 2001). Aroclor 1254 affects fish hypothalamic-pituitary-gonadal-liver axis at multiple sites (Thomas, 1990). However, in this analysis I only focused on the PCB effect on gonadotropin releasing hormone functioning and luteinizing hormone (LH) secretion; in Atlantic croaker, Aroclor 1254 inhibits tryptophan hydroxylase activity (Khan and Thomas, 2001). In a laboratory experiment (Khan and Thomas, 2001), adult croaker were acclimated for one month and then were exposed to Aroclor 1254 (2 μg/g body weight per day) for 15 days during early gonadal recrudescence. Plasma levels of LH measured after the 15 days of exposure were 38% of the values of the control fish.

Two earlier studies that examined the effects of PCBs on Atlantic croaker documented reduced GSI and testosterone, and somewhat opposite effects on estradiol concentrations. Female Atlantic croaker exposed to Aroclor 1254 (5 μg/g body weight per day) for 17 days during early gonadal recrudescence had GSI values and total estradiol levels that were roughly 50% lower than in control fish (Thomas, 1989). In another experiment, female Atlantic croaker were also exposed to Aroclor 1254 (3.5 μg/g body weight per day), but for a longer 30-day exposure (Thomas, 1988). GSI levels were 34% and total testosterone concentrations that were 50% of control values, but plasma estradiol concentrations were 25% higher than in control fish (Thomas, 1988). The contrasting PCB effects on total estradiol levels can be explained, in part, by the different durations (17 and 30 days) of the two experiments. Under PCB exposure, estradiol could initially be reduced due to reduced gonadotropin release, and then increase later in the

season due to PCBs affecting a different mechanism of the HPLG axis other than gonadotropin release.

To simulate the effects of PCBs, I multiplied the plasma gonadotropin driving variable concentrations by 0.38. I compared predicted model dynamics under PCB exposure to baseline results. I compared predicted changes in testosterone, estradiol and cumulative vitellogenin production to the roughly 50% reductions in testosterone, estradiol and GSI observed in the lab experiments.

2.2.3.3. Effects of Cadmium

Cadmium appears to disrupt vitellogenesis in fish at multiple steps. Cadmium acts on both the pituitary and the gonad to alter gonadotropin secretion and steroidogenic activity (Thomas, 1989; Thomas and Khan, 1995). Female croaker acclimated for 30 days and then exposed to cadmium *in vivo* (1 mg/L) for 40 days showed 295% higher GtH concentrations and 211% higher total estradiol concentrations as compared to control fish (Thomas, 1989). Ovarian fragments of spotted seatrout were incubated in various concentrations of cadmium *in vitro* (Thomas and Khan, 1995). Incubation in cadmium *in vitro*, at a range of cadmium exposures (range from 0.01 to 5.0 ppm) that should encompass the exposure level imposed in the *in vivo* Thomas (1989) study on croaker, resulted in a doubling of testosterone production after 9 hours, and a doubling of estradiol production after 18 hours.

To simulate the endocrine disrupting effects of cadmium, I increased the plasma concentration of gonadotropin and the rate of testosterone synthesis (conversion of gonadotropin to testosterone). The gonadotropin concentration was increased by multiplying the hourly baseline values (Fig. 2.2) by 2.95, as observed in the *in vivo*

experiment (Thomas, 1989). The testosterone synthesis rate was increased by multiplying equation (2.10) by 2.0 (Table 2.1), as observed in the *in vitro* ovarian fragment incubation experiment (Thomas and Khan, 1995). I assumed that a doubling of the testosterone synthesis rate would roughly translate into a doubling of estradiol production that was also observed in the *in vivo* (Thomas, 1989) and *in vitro* ovarian fragment (Thomas and Khan, 1995) experiments. I compared model predictions under baseline and cadmium exposure, and compared predicted cadmium effects on cumulative vitellogenin production to changes in GSI reported by Thomas (1989).

2.3. Results

2.3.1. Calibration and Baseline Conditions

The calibrated baseline simulation predicted magnitudes and timing of peak concentrations of total estrogen receptor, total testosterone, and total estradiol that roughly mimicked those measured in spotted seatrout by Smith and Thomas (1991). Model-predicted cumulative vitellogenin production under baseline conditions was 161.0 mg/mL (Fig. 2.4A; Table 2.3). Measured estrogen receptor concentration peaked at about 2 pmol/g liver in September during the first year of measurements and had a higher and longer duration peak (5.25 pmol/g liver for May through September) during the second year of measurements. In the baseline simulation, predicted total estrogen receptor concentration, while increasing throughout the period of gonadotropin introduction in the simulation, approached a maximum concentration of 5.2 pmol/g liver by the middle of the simulation that was similar magnitude to the field measured concentrations (Fig. 2.4B). Measured total testosterone reached a maximum concentration of about 1200 pg/mL sometime between April and June, and then declined

slowly to about 300 pg/mL by October to November. Predicted total testosterone peaked in the baseline simulation at 1290 pg/mL within the first month of simulation (April), remained elevated during the period of gonadotopin release and then declined rapidly to

Table 2.3. Predicted cumulative vitellogenin production of an individual female fish during 6-month simulations under baseline conditions, and under exposure to PCBs and cadmium.

Simulation	Cumulative Vitellogenin Produced (mg/mL)	Percent of Baseline
Baseline	161.0	100 %
PCB	29.1	18 %
Cadmium	970.2	603 %

zero, contrasting field measurements that measured minimum concentrations of 300 pg/mL (Fig. 2.4C). Finally, over the two years of observations, total estradiol attained a maximum concentration of about 1750 pg/mL sometime during May and July. Predicted total estradiol concentration in the baseline simulation peaked at 1800 pg/mL during April (Fig. 2.4D).

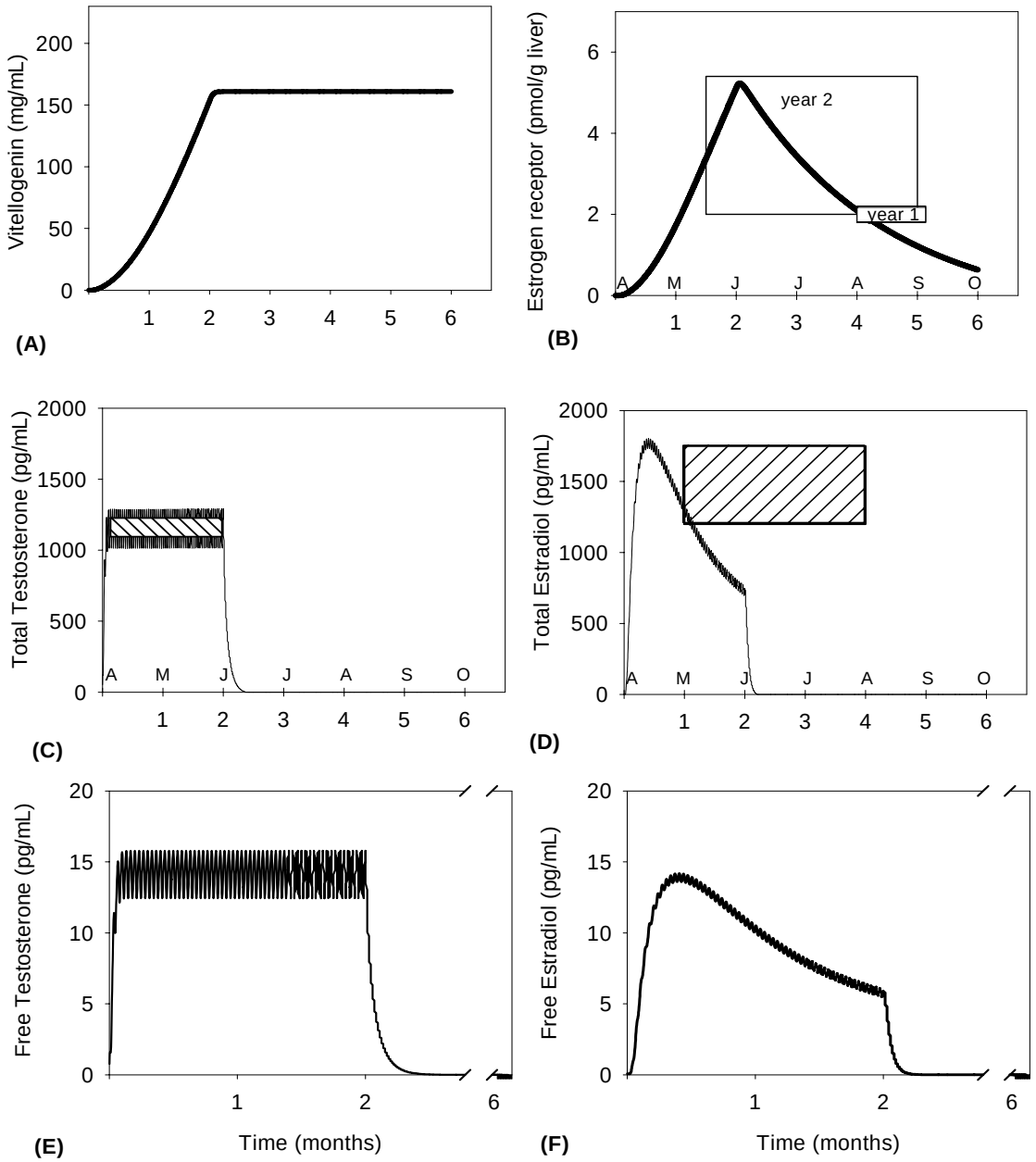

Figure 2.4. Baseline simulation predictions of (A) cumulative vitellogenin production, (B) estrogen receptor concentration, (C) total testosterone concentration, (D) total estradiol concentration, (E) free testosterone concentration, and (F) free estradiol concentration. Boxes represent ranges of field-measured maximum concentrations. The small box in (B) represents the range of peak concentrations of total estrogen receptor observed in first year of field measurements, and the large box represents the range of peak concentrations of total estrogen receptor observed in the second year of field measurements. The hatched box in (C) represents the peak reported concentrations of total testosterone, and the hatched box in (D) represents the range in reported peak total estradiol concentrations.

Although detailed measurements concerning concentrations of the free forms of testosterone and estradiol are not available, model predictions of very low concentrations of these were consistent with general observations. Petra et al. (1985) reported that in mammals only a small percentage (about 1%) of free steroids are available as a ligand at any given time; much of available steroid is bound to SBP. Maximum predicted free testosterone concentration in the baseline simulation was 15.8 pg/mL (Fig. 2.4E), which was about 1.2% of the total testosterone concentration. Similarly, predicted concentrations of free estradiol reached a maximum of 14.2 pg/mL (Fig. 2.4F), which was about 0.8% of the maximum total estradiol concentration.

The temporal dynamics of the free forms of testosterone and estradiol were consistent with the model structure and assumed parameter values. Rapid fluctuations in free estradiol (Fig. 2.4F) and testosterone (Fig. 2.4E) were due to hourly variation in gonadotropin concentration over the diurnal cycle, values of parameter (k_{aT}, k_{dT}, k_{aE} and k_{dE}) that resulted in rapid association and dissociation of the free forms with steroid binding proteins, the rapid degradation rates of free testosterone and estradiol (k_{degu} and k_{dega}), and the fast reaction rates of testosterone and estradiol as substrates in subsequent reactions. The initial rapid rise of free estradiol concentrations during the first month of the simulation (Fig. 2.4F) was due to the rapid synthesis of estradiol from the rapid increase in concentration of free testosterone.

2.3.2. Effects of PCBs

Predicted reduction in cumulative vitellogenin production due to PCB exposure was higher compared to the observed reductions in GSI documented in the laboratory experiments (Fig. 2.5A). Predicted cumulative vitellogenin production was 18% of

baseline (Table 2.3), compared to the 34% to 50% reductions in GSI reported by Thomas (1988, 1989).

Predicted estrogen receptor concentration was reduced under PCB exposure (Fig. 2.5B). Predicted total estrogen receptor showed similar dynamics under PCB exposure and baseline conditions of gradually rising concentrations during gonadotropin introduction, with maximum concentrations under PCB exposure being 13% of baseline reached by the middle of the simulation.

Predicted changes in total testosterone and estradiol concentrations were either consistent or equivocal when compared to the experimental results. PCBs were predicted to cause a 26% decrease in maximum total testosterone concentrations (Fig. 2.5C), which is roughly comparable to the 50% reduction in peak total testosterone concentrations reported by Thomas (1989). Predicted response to PCBs reflected a 62% decrease in total estradiol concentrations (Fig. 2.5D). This reduction in total estradiol is consistent with the interpretation of an initial reduction in estradiol in the shorter duration experiment (1989) but is inconsistent with the increase in estradiol observed in the longer duration experiment (Thomas, 1988). The discrepancy between the two experimental results may be related to differences in their durations or perhaps to other differences in experimental design or protocol.

Predicted responses in other state variables to PCB exposure were reduced free testosterone (Fig. 2.5E) and reduced free estradiol (Fig. 2.5F) concentrations. Free estradiol and free testosterone under PCB exposure both showed reductions in their peak concentrations compared to baseline conditions, with free testosterone and free estradiol

reaching peak concentration that were 75% and 38% of the baseline peak concentration respectively.

2.3.3. Effects of Cadmium

Cadmium exposure caused large increases in vitellogenin production in both the model simulation and in the laboratory experiment. Predicted cumulative vitellogenin production was 603% higher than under baseline conditions (Table 2.2, Fig. 2.6A). Thomas (1989) reported that cadmium exposed fish had GSIs that were 931% higher than control values (GSI of 1.16% in control versus 10.8% in cadmium exposed).

The imposition of higher rates of gonadotropin introduction and testosterone synthesis assumed under cadmium exposure resulted in increased total estrogen receptor concentrations, total testosterone, and total estradiol concentrations. Total estrogen receptor concentrations behaved similarly under cadmium exposure and baseline conditions, but attained maximum concentrations 6.2 times higher under cadmium exposure than under baseline conditions (Fig. 2.6B). Predicted total testosterone concentrations under cadmium exposure increased similar to baseline conditions, but attained a slightly higher maximum concentration at 1.4 times baseline (Fig. 2.6C). Predicted total estradiol concentrations under cadmium exposure rose more rapidly and maintained maximum concentrations at 3.2 times that of baseline conditions (Fig. 2.6D).

Free testosterone and free estradiol concentrations also reached higher peak concentrations under cadmium exposure than under baseline conditions. Free testosterone concentrations under cadmium exposure peaked at a concentration 1.4 times that of baseline conditions (Fig. 2.6E). Free estradiol levels were more sensitive to

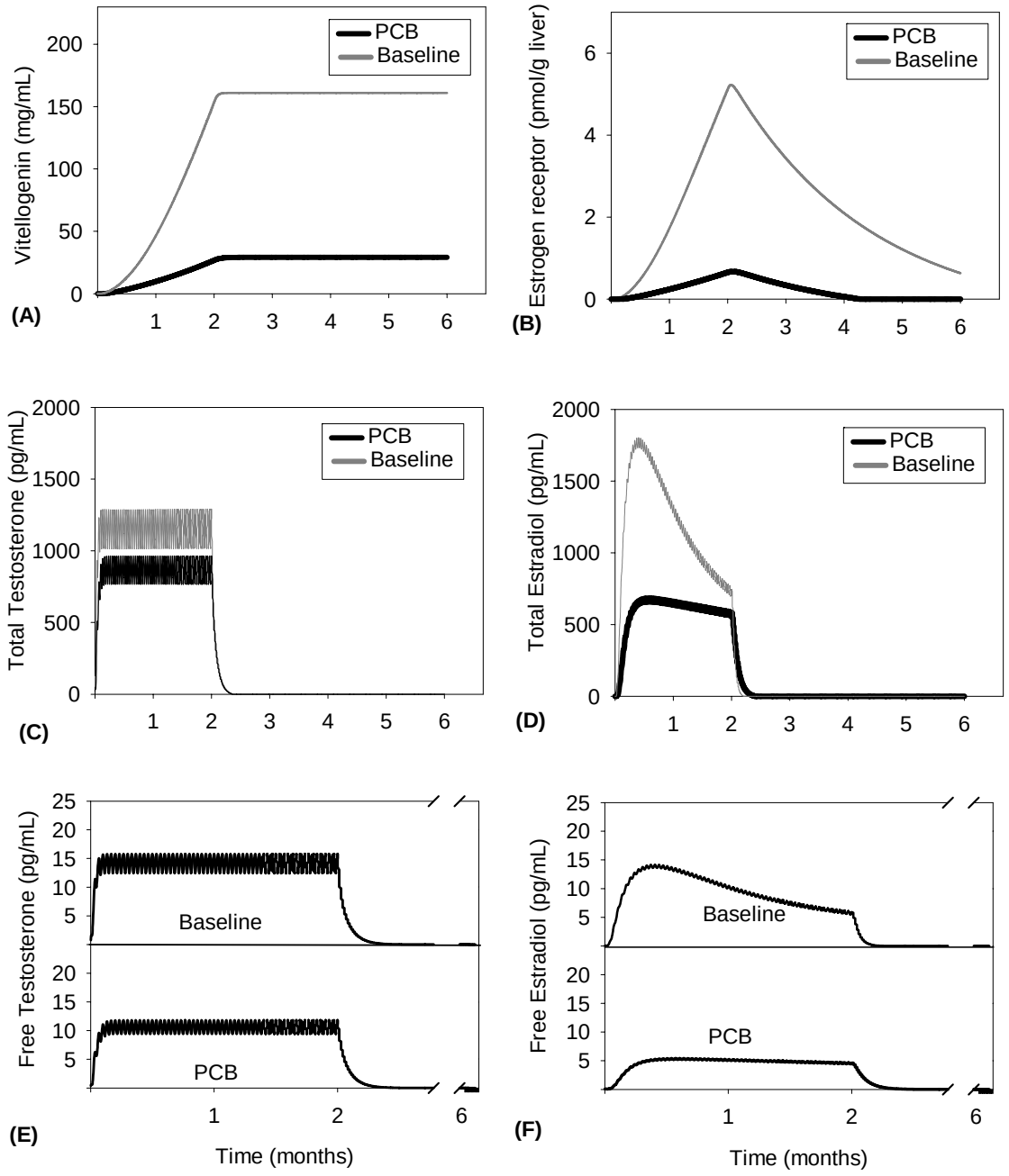

Figure 2.5. Predicted concentrations under PCB exposure and baseline conditions of: (A) vitellogenin, (B) total estrogen receptor, (C) total testosterone, (D) total estradiol, (E) free testosterone, and (F) free estradiol.

cadmium exposure and reached a maximum at 3.3 times that observed under baseline conditions (Fig. 2.6F).

2.4. Discussion

2.4.1. Model Performance and Utility

I developed a model of vitellogenesis for an individual fish, and used the model to predict the effects of two EDCs. The model performed reasonably well. Baseline predictions of maximum concentrations of total steroids and estrogen receptor roughly matched field measurements, and predicted changes in vitellogenin production and estradiol levels under PCB and cadmium exposure generally matched changes observed in laboratory measurements of GSI and estradiol concentrations. The prediction of reduced vitellogenin production under PCB exposure may have been higher than observed in laboratory experiments because the simulation assumed PCB exposure during entire simulation, whereas in laboratory experiments fish were exposed to PCBs for only a portion of the reproductive period Also, based on our experience with measurements in field-caught seatrout, the baseline simulation wrongly predicted a decline to zero concentration of total testosterone and estradiol, rather than to some basal low concentrations, and predicted a peak in total estradiol concentration that occurred a few weeks too early (Fig. 2.4C and D).

My simulations of contaminant effects demonstrated the need to recognize the importance of timing in biomarker measurement. Steroid concentrations in plasma are commonly used as biomarkers of exposure (Monosson, 2000). According to my model simulations, measurements of steroid levels from contaminant exposed fish that were

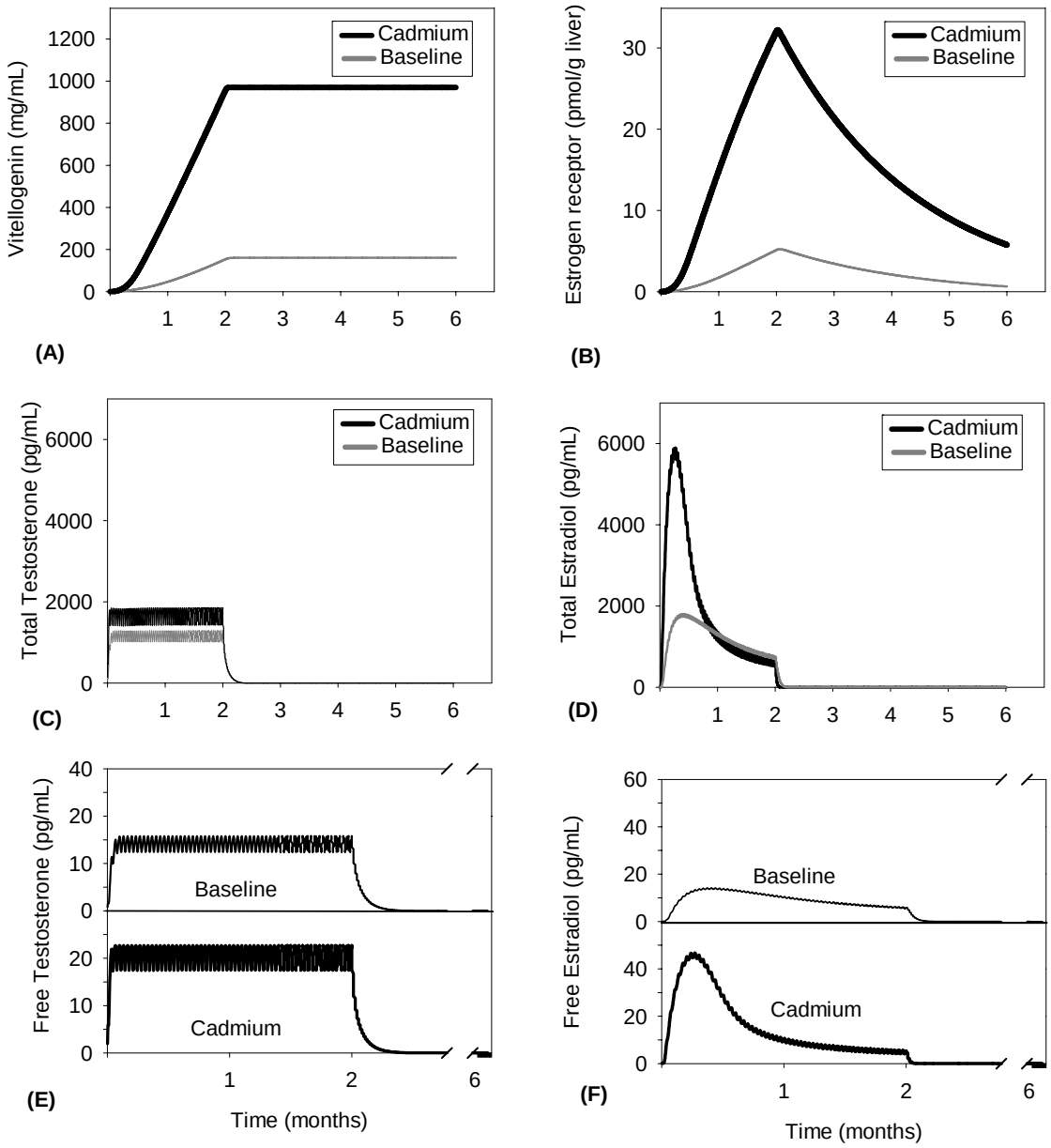

Figure 2.6. Predicted concentrations under cadmium exposure and baseline conditions of: (A) vitellogenin, (B) total estrogen receptor, (C) total testosterone, (D) total estradiol, (E) free testosterone, and (F) free estradiol

taken during the first 2 months of gonadal recrudescence would show the greatest difference from control fish and that estradiol is a more sensitive biomarker than testosterone. Previous research indicates that depressed steroid levels translate into reproductive impairment (e.g., McMaster et al., 2001). Therefore, proper interpretation of estradiol concentrations from field-caught fish is predicated upon knowing the stage in the reproductive cycle of the individual fish.

The simulation of cadmium effects demonstrated how the model could be used to simulate EDCs that affect multiple sites on the hypothalamus-pituitary-gonad-liver (HPGL) axis. Cadmium affects the HPGL axis at the pituitary by stimulating the release of LH, and cadmium also acts on the ovary to enhance steroidogenesis (Thomas and Khan, 1995). I simultaneously imposed both of these effects in our cadmium exposure simulation. I doubled the concentration of gonadotropin in the plasma and doubled the rate of synthesis of testosterone.

A logical extension of how I simulated multiple effects of cadmium would be the simulation of exposure to multiple EDCs. My model can be used to explore the possibility of synergistic and antagonistic effects. Fish in nature are exposed to mixtures of chemicals at various concentrations. For example, kelp bass (*Paralabrax clathratus*) that were collected from Southern California were environmentally exposed to mixtures of DDT and PCBs (Spies and Thomas, 1995). Exposed fish exhibited suppressed gonadotropin secretion from pituitary consistent with PCB effects. But the same fish also showed enhanced ovarian production of testosterone and reduced estrogen receptor affinity to estradiol, effects that could be attributed to other contaminants and may

counteract the effects of PCBs. Spies and Thomas (1999) reported that exposure to DDT and PCBs resulted in no noticeable reduction in vitellogenesis or GSI. *P,p'*-DDE, a metabolite of DDT which binds to the kelp bass androgen receptor (Sperry and Thomas, 1999), exerts antiandrogenic effects in vertebrates (Kelce et al., 1995) . *P,p'*-DDE comprised over 95% of the total DDT detected in the contaminated kelp bass tissues (Spies and Thomas, 1995). Therefore, it would be necessary to include androgen-receptor mediated endocrine disruption in my model to simulate the multiple effects observed in the kelp bass. The model would also require modification for simulating the effects of the large number of chemicals that exert estrogenic actions via binding to the estrogen receptor to alter vitellogenesis and other reproductive processes.

2.4.2. Assumptions and Deficiencies

Despite my use in model development of many laboratory experiments performed over decades, there are several aspects of the model that deserve careful scrutiny and further refinement. Perhaps one of the most useful outcomes of developing a model such as this is the identification of data gaps and assumptions that need further confirmation.

I borrowed techniques from the field of enzyme kinetics (Segel, 1975) to model the dynamics of the estrogen receptor and steroid binding proteins. Enzyme kinetics was the starting point when researchers set out to generate models for epidermal growth factor (EGF) receptor binding and internalization (Wiley et al., 2003). The initial steady state and kinetic models were successful at capturing many of the dynamic features of the EGF binding processes. Once a model framework was built, models were expanded upon as technology improved and more data became available (Wiley et al., 2003). I view my model of vitellogenesis as analogous to the initial kinetic models of the EGF binding

processes. I used simple first and second order rate constants for receptor association and dissociation processes, and I borrowed from an autocatalytic enzyme kinetics model example (Manjabacas et al., 2002) to model the estrogen receptor producing more of itself.

One major uncertainty in my model is the identity of the principal gonadotropin regulating vitellogenesis in the sciaenid fish model. The effects of changes in LH secretion were modeled in this preliminary version of the model. This assumption may be correct for sciaenid fishes as well as some other marine perciform fishes such as European sea bass and red seabream (Okuzawa, 2002). However, the use of LH would clearly be inappropriate for salmonids, and probably some other species in which FSH appears to regulate vitellogenesis (Swanson, 1991). Currently the physiology of FSH secretion during ovarian growth has only been investigated in salmonid fishes due to the lack of immmunoassays for FSH measurement in members of other teleost families. Thus, in the absence of information on the pattern of FSH secretion during vitellogenesis in additional fish species, the role of FSH in the regulation of ovarian growth in teleosts remains unclear.

Experiments that determine the rates of synthesis of testosterone and estradiol in vitellogenic follicles *in vivo* would be useful for model refinement. In my model, rates of synthesis of testosterone and estradiol were calibrated to generate desired maximum concentrations of these steroids in the baseline simulation. However, rates of steroidogenesis may change with time and a gradual decline in rates of steroid synthesis or induction of other mechanisms, such as steroidogenic enzymes, may generate the slow decline in total testosterone and estradiol concentrations observed in field-caught fish.

Further exploration into the mechanisms regulating steroidogenesis is required for more realistic simulations.

Another area in model development that required questionable assumptions was the steroid feedback mechanisms that affected gonadotropin production and release. I know that high doses of estradiol, administered through implants, inhibit the production of gonadotropin, but dose response studies designed to quantify feedback mechanisms are not available. Steroid feedback mechanisms in Atlantic croaker have been studied, but not sufficiently to allow inclusion into our model. Information obtained through gonadectomy and steroid implants showed that during early gonad recrudescence, testosterone and estradiol stimulate LH production. However, when gonads reach maturation, the steroids inhibit the production of LH (Khan et al., 1999). Information on the positive feedback exhibited early in gonadal recrudescence was insufficient, and I therefore only incorporated the negative feedback mechanism into our model. I simply assumed that high concentrations of estradiol would act to reduce gonadotropin levels.

Measurement of the degradation rate for estrogen receptors when estradiol is present would also be helpful. Hepatic estrogen receptor, in the presence of estradiol, undergoes degradation at a different rate than when estradiol is absent (Reid et al., 2002). Therefore, I modified the estrogen receptor degradation rates so that the estrogen receptor concentration approached a maximum concentration near the middle of the baseline simulation. Experiments that determine the degradation rates for estrogen receptor in the absence of estradiol in seatrout would allow more precise parameter values to be used in model simulations.

The apparent disconnect between model predictions of estradiol concentrations and the results of laboratory experiment that used a longer PCB exposure period could be attributed to PCB affecting mechanisms other than gonadotropin release. I greatly simplified the effects of PCBs by assuming PCBs only affect gonadotropin release, whereas in reality PCBs affect many components of the HPGL axis (Thomas, 1990).

The vitellogenesis model was calibrated to simulate baseline conditions from field-caught spotted seatrout, but data from toxicology studies on Atlantic croaker were also used. Although both species are estuarine species from the family Sciaenidae, they exhibit different life history strategies. Spotted seatrout will spawn multiple times in a season, whereas Atlantic croaker will only spawn once (Thomas et al., 1995). Because I am only modeling vitellogenesis and not the production and spawning of eggs, I felt it was reasonable to synthesize information from both spotted seatrout and Atlantic croaker for model development. Also, when I simulated the toxicology experiments I focused on percent changes in hormones rather than on changes in actual concentrations. Regardless, I recognize that hormonal profiles may differ between spotted seatrout and croaker, and these differences act as a source of error in the model.

2.4.3. Future Directions

In addition to model refinement as data gaps are filled, I would also like to extend the model to include simulations of other mechanisms of endocrine disruption, especially those involving binding to nuclear estrogen or androgen receptors and alterations of steroid actions. Many major environmental contaminants bind to the estrogen receptor and are estrogenic (xenoestrogens), and there is extensive evidence of inappropriate induction vitellogenesis in fish by xenoestrogens in both field and laboratory studies.

Endocrine disrupting chemicals can also interfere with later phase of the ovarian cycle such as oocyte maturation and spawning. For example, Kepone and o,p'-DDD bind to the maturation inducing steroid (4-pregnen-17,20β,21-triol-3-one) receptor sites and inhibit final oocyte maturation (Das and Thomas, 1999). Also, as information becomes available, some of the aggregated biochemical reactions, like the Hill functions and the rate of production of vitellogenin and estrogen receptor, can be broken down into their component reactions. The Hill function has been used previously as a surrogate to model detailed biochemical reactions by Schlosser and Selgrade (2000) and it is a reasonable approach because the sigmoid relationship observed between ligand concentration and product has been observed in many biochemical systems. Although the relationship between product and substrate is generally linear, it is convoluted by binding dynamics, degradation, and ligand depletion, thereby indirectly giving rise to the observed sigmoid shape (Wiley et al., 2003). Breaking the Hill function into components would likely increase the realism of the model, and allow one to easily simulate additional endocrine disrupting effects, such as the aromatase impairment associated with hypoxia-exposure (Wu et al., 2003) and effects on steroid binding proteins (Tollefsen, 2002).

I presented deterministic predictions in this paper. In future versions of my model, I plan to use Monte Carlo methods to include stochasticity (natural variability) and uncertainty in model predictions. Monte Carlo methods involve repeated model simulations with input values randomly generated from probability distributions. Model predictions are then presented as probability distributions of outcomes, and correlation analysis can be used to identify the inputs that most contribute to prediction variability (e.g., Jaworska et al., 1997).

Ultimately I would like to couple my model with a bioenergetics model of fish growth. Bioenergetics models are based on dynamic energy budgets and can be used to describe the rates at which individuals allocate energy for maintenance, reproduction, growth, and development (Ney, 1993; Nisbet et al., 2000). In many bioenergetics models, the mechanisms determining energy allocation between somatic growth and reproduction are not well understood and usually determined by simple rules (Hewett and Johnson, 1992). Coupling my vitellogenesis model to a bioenergetics model would allow simulation of the effects of endocrine disruption on energy allocation, and the resulting ecological consequences on reproduction and growth. Incorporation of endocrine disrupting effects into a coupled reproduction-bioenergetics model can eventually be used to relate biomarkers to population and community responses. The model presented in this paper is first step towards a computational biology framework for better understanding endocrine disruption in fish, and for relating reproductive endocrine biomarkers of exposure to reproductive endpoints of ecological relevance.

2.5. References

Barton, B.A., Morgan, J.D., and Vijayan, M.M. 2002 Physiological and condition-related indicators of environmental stress in fish. *In*: Adams, S.M. editor. Biological indicators of aquatic ecosystem stress. Bethesda, Maryland: American Fisheries Society, pp 111-148.

Breton, B., Sambroni, E., Govoroun, M., and Weil, C. 1997. Effects of steroids on GTH I and GTH II secretion and pituitary concentration in the immature rainbow trout *Oncorhynchus mykiss*. *C.R. Acad. Sci. Paris, Sciences de la vie* 320:783-789.

Brown-Peterson, N.J. 2003. The reproductive biology of the spotted seatrout. *In* Bortone S.A. editor. Biology of the Spotted Seatrout. Boca Raton, Florida, Marine Biology Series, pp. 99-133.

Colborn, T., Saalvom, F.S., and Soto A.M. 1993. Developmental effects of endocrine-disrupting chemicals in wildlife and humans. *Environ. Health Perspect*.101:378-384.

Copeland, P.A., and Thomas, P. 1989. Control of gonadotropin release in the Atlantic croaker: evidence for lack of dopaminergic inhibition. *Gen Comp Endocrinol*. 74:474-483.

Copeland, P.A., and Thomas, P. 1993. Isolation of gonadotropin subunits and evidence for distinct gonadotropins in Atlantic croaker (*Micropogonias undulatus*). *Gen. Comp. Endocrinol.* 91:115-125.

Das, S., and Thomas, P. 1999. Pesticides interfere with the nongenomic action of a progestogen on meiotic maturation by binding to its plasma membrane receptor on fish oocytes. *Endocrinol.* 140:1953-1956.

Davis, W.P. 1995. Evidence for developmental and skeletal responses as potential signals of endocrine-disrupting compounds in fishes. *In*: Rolland, R.M., Gilbertson, M. and Peterson R.E., editors. Chemically induced alterations in functional development and reproduction of fishes. Racine, Wisconsin: SETAC Technical Publications Series, pp. 61-72.

Diamond, S.L., Cowell, L.G. and Crowder L.B. 2000. Population effects of shrimp trawl bycatch on Atlantic croaker. *Can J Fish Aquat Sci*. 57:2010-2021.

Diamond, S.L., Crowder, L.B., and Cowell, L.G. 1999. Catch and bycatch: the qualitative effects of fisheries on population vital rates of Atlantic croaker. *Trans Am Fish Soc.* 128:1085-1105.

Dickey, J.T. and Swanson, P. 1998. Effects of sex steroids on gonadotropin (FSH and LH) regulation in coho salmon (*Oncorhynchus kisutch*). *J. Mol. Endocrinol*. 21:291-306.

Donaldson, E.M. 1990. Reproductive indices as measures of the effects of environmental stressors in fish. *Am. Fish. Soc. Symp.* 8:109-122.

Flouriot, G., Pakdel, F. and Valotaire, Y. 1996. Transcriptional and post-transcriptional regulation of rainbow trout estrogen receptor and vitellogenin gene expression. *Mol. Cell. Endocrinol*. 124:173-183.

Hewett, S.J. and Johnson, B.L. 1992. Fish bioenergetics model 2. University of Wisconsin Sea Grant Technical Report. WIS-SG-92-250.

Jaworska, J.S., Rose K.A. and Brenkert A.L. 1997. Individual-based modeling of PCBs effects on young-of-the-year largemouth bass in southeastern USA reservoir. *Ecol. Model.* 99:113-135.

Kelce, W.R., Stone, C.R., Laws, S.C., Gray, L.E., Kemppainen, J.A. and Wilson, E.M. 1995. Persistent DDT Metabolite p,p'-DDE is a potent androgen receptor antagonist. *Nature* 375: 581-585.

Khan, I.A. and Thomas, P. 1999. GABA exerts stimulatory and inhibitory influences on gonadotropin II secretion in the Atlantic croaker (*Micropogonias undulatus*). *Neuroendocrinol*. 69:261-268.

Khan, I.A. and Thomas, P. 2000. Lead and Aroclor 1254 disrupt reproductive neuroendocrine function in Atlantic croaker. *Mar. Environ. Res.* 50: 119-123.

Khan, I.A. and Thomas, P. 2001. Disruption of neuroendocrine control of luteinizing hormone secretion by Aroclor 1254 involves inhibition of hypothalmic tryptophan hydroxylase activity. *Biol. Reprod.* 64:955-964.

Khan, I.A., Hawkins, M.B. and Thomas, P. 1999. Gonadal stage-dependent effects of gonadal steroids on gonadotropin II secretion in the Atlantic croaker (*Micropogonias undulatus*). *Biol. Reprod.* 61:834-841.

Kime, D.E. 2001. Endocrine disruption in fish. Norwell, Massachussets: Kluwer Academic Publishers.

Laidley, C.W. and Thomas, P. 1994. Partial characterization of a sex-steroid binding protein in the spotted seatrout (*Cynoscion nebulosus*). *Biol. Reprod.* 51:982-992.

Laidley, C.W. and Thomas, P. 1997. Changes in plasma sex steroid-binding protein levels associated with ovarian recrudescence in the spotted seatrout (*Cynoscion nebulosus*). *Biol. Reprod*. 56:931-937.

Manjabacas, M.C., Valero, E., Moreno-Conesa, M., Garcia-Moreno, M., Molina-Alarcon, M.and Varon, R. 2002. Linear mixed irreversible inhibition of the autocatalytic activation of zymogens. Kinetic analysis checked by simulated progress curves. *Int. J. Biochem. Cell Biol*. 34:358-369.

McMaster, M.E., Jardine, J.J., Ankley G.T. et al. 2001. An interlaboratory study on the use of steroid hormones in examining endocrine disruption. *Environ. Toxicol. Chem.* 20:2081-2087.

McMaster, M.E., van der Kraak, G.J. and Munkittrick, K.R. 1996. An epidemiological evaluation of the biochemical basis for steroid hormonal depressions in fish exposed to industrial wastes. *J. Great Lakes Res*. 22:153-171.

McQuarrie, D.A. and Rock, P.A. 1987. General Chemistry. Second ed. New York: W. H. Freeman and Company.

Monosson, E. 2000. Reproductive and developmental effects of PCBs in fish: a synthesis of laboratory and field studies. *Rev. Toxicol.* 3:25-75.

Munkittrick, K.R., Portt, C.B., van der Kraak, G., Smith, I.R. and Rokosh, D.A. 1991. Impact of bleached kraft mill effluent on population characteristics, liver MFO activity, and serum steroid levels of a Lake Superior white sucker (*Catostomus commersoni*) population. *Can. J. Fish. Aquat. Sci*. 48:1371-1380.

Nagahama, Y. 1994. Endocrine regulation of gametogenesis in fish. *Int. J. Dev. Biol.* 38:217-229.

Ney, J.J. 1993. Bioenergetics modeling today – growing pains on the cutting edge. *Trans. Am. Fish. Soc.*122:736-748.

Nisbet, R.M., Muller, E.B., Lika, K. and Kooijman, S.A.L.M. 2000. From molecules to ecosystems through dynamic energy budget models. *J. Animal Ecol*. 69:913-926.

Okuzawa, K. 2002. Puberty in teleosts. *Fish Physiol. Biochem*.26:31-41.

Pardridge, W.M. 1981. Transport of protein-bound hormones into tissues *in vivo*. *Endocr. Rev.* 2:103-123.

Patino, R., Yoshizaki, G., Thomas, P. and Kagawa, H. 2001. Gonadotropic control of ovarian follicle maturation: the two stage concept and its mechanisms. *Comp. Biochem. Physiol. B.* 129:427-439.

Petra, P.H., Stanczyk, F.Z., Namkung, P.C., Fritz, M.A. and Novy, M.J. 1985. Direct effect of sex steroid-binding protein (SBP) of plasma on the metabolic clearance rate of testosterone in the rhesus macaque. *J. Steroid Biochem*. 22:739-746.

Reid, G., Denger, S., Kos, M. and Gannon, F. 2002. Human estrogen receptor-α: regulation by synthesis, modification and degradation. *Cell. Mol. Life Sci.* 59:821-831.

Rosner, W. 1990. The functions of corticosteroid-binding globulin and sex hormone-binding globulin; recent advances. *Endocr. Rev*. 11:80-91.

Saligaut, C., Linard, B., Mananos, E.L., Kah, O., Breton, B. and Govoroun, M. 1998. Release of pituitary gonadotrophins GtH I and GtH II in the rainbow trout (*Oncorhynchus mykiss*): modulation by estradiol and catecholamines. *Gen. Comp. Endocrinol.* 109:302-309.

Schlosser, P.M. and Selgrade, J.F. 2000. A model of gonadotropin regulation during the menstrual cycle in women: qualitative features. *Environ. Health. Perspect*. 108:873-881.

Segel, I.H. 1975.Enzyme kinetics. Behavior and analysis of rapid equilibrium and steady-state enzyme systems. New York: John Wiley & Sons, Inc.

Smith, J.S. and Thomas, P. 1990. Binding characteristics of the hepatic estrogen receptor of the spotted seatrout, *Cynoscion nebulosus*. *Gen. Comp. Endocrinol.*77:29-42.

Smith, J.S. and Thomas, P. 1991. Changes in hepatic estrogen-receptor concentration during the annual reproductive and ovarian cycles of a marine teleost, the spotted seatrout, *Cynoscion nebulosus*. *Gen. Comp. Endocrinol*. 81:234-245.

Specker, J.L. and Sullivan, C.V. 1994. Vitellogenesis in fishes: status and perspectives. *In*: Davey, K.G., Peter, R.E. and Tobe, S.S., editors. Perspectives in Comparative Endocrinology. Ottawa: National Research Council. pp. 304-315.

Sperry, T. and Thomas, P. 1999. Identification of two nuclear androgen receptors in kelp bass (*Paralabrax clathratus*) and their binding affinities for xenobiotics: comparison with Atlantic croaker (*Micropogonias undulatus*) androgen receptors. *Biol Reprod.* 61:1152-1161.

Spies, R.B. and Thomas, P. 1995. Reproductive and endocrine status of female kelp bass from a contaminated site in the Southern California Bight and estrogen receptor binding of DDTs. *In*: Rolland, R.M., Gilbertson, M. and Peterson, R.E., editors. Chemically induced alterations in functional development and reproduction of fishes. Racine, Wisconsin: SETAC Technical Publications Series; p. 113-133.

Suzuki, K., Kawauchi, H. and Nagahama Y. 1988. Isolation and characterization of two distinct gonadotropins from chum salmon pituitary glands. *Gen. Comp. Endocrinol.* 71:292-301.

Swanson, P. 1991. Salmon gonadotropins: reconciling old and new ideas. *In*: Scott, A.P., Sumpter, J., Kime, D. and Rolfe, M.S., editors. Proceedings 4th International Symposium on Reproductive Physiology of Fish. University of East Anglia, pp. 2-7.

Thomas, P. and Khan, I.A. 1995. Mechanisms of chemical interference with reproductive endocrine function in sciaenid fishes. *In*: Rolland,R.M., Gilbertson, M. and Peterson, R.E., editors. Chemically induced alterations in functional development and reproduction of fishes. Racine, Wisconsin: SETAC Technical Publications Series. pp. 29-51.

Thomas, P. 1988. Reproductive endocrine function in female Atlantic croaker exposed to pollutants. *Mar. Env. Res*. 24:179-183.

Thomas, P. 1989. Effects of Aroclor 1254 and cadmium on reproductive endocrine function and ovarian growth in Atlantic croaker. *Mar. Env. Res*. 28:499-503

Thomas, P. 1990. Molecular and biochemical responses of fish to stressors and their potential use in environmental monitoring. *Am. Fish. Soc. Symp.* 8:9-28.

Thomas, P., Arnold, C.R. and Holt, G.J. 1995. Sciaenid fishes. *In:* Bromage, N. and Roberts, R.H., editors. Broodstock Management and Egg and Larval Quality. Blackwell Scientific Publishers p. 118-137.

Tollefsen, K-E. 2002. Interaction of estrogen mimics, singly and in combination, with plasma sex steroid-binding proteins in rainbow trout (*Oncorhynchus mykiss*). *Aquat. Toxicol.* 56:215-225.

Tyler, C.R. and Sumpter, J.P. 1996. Oocyte growth and development in teleosts. *Rev. Fish Biol. Fisheries.* 6:287-318.

van der Kraak, G., Suzuki, K., Peter, R.E., Itoh, H. and Kawauchi, H. 1992. Properties of common carp gonadotropin I and gonadotropin II. *Gen. Comp. Endocrinol.* 85:217-229.

WHO. 2002. Global Assessment of the State-of-the-Science of Endocrine Disruptors. *In* Damstra, T., Barlow S., Bergman A., Kavlock R. and van der Kraak G., editors. International Programme On Chemical Safety.

Wiley, H.S., Shvartsman, S.Y. and Lauffenburger, D.A. 2003. Computational modeling of the EGF-receptor system: a paradigm for systems biology. *Trends Cell Biol*. 13:43-50.

Wu, R.S.S., Zhou, B.S., Randall, D.J., Woo, N.Y.S. and Lam, P.K.S. 2003. Aquatic hypoxia is an endocrine disruptor and impairs fish reproduction. *Environ. Sci. Technol.* 37:1137-1141.

Zohar Y. 1982.L'evolution de la pusatilite et des cycles nycthmerau de la secretion gonadotrope chez la truite arc-en-ciel femelle, en relation avec le cycle sexuel annuel et par rapport a l'activite steroidogene de l'ovaire [Ph.D.]. Paris: Universite Pierre et Marie Curie.

CHAPTER 3. HYPOXIA AS AN ENDOCRINE DISRUPTOR: TESTING AND APPLYING A FISH VITELLOGENESIS MODEL TO EVALUATE LAB AND FIELD BIOMARKERS OF HYPOXIA

3.1. Introduction

Evidence in support of reproductive dysfunction in wild populations of fish exposed to environmental contaminants has grown rapidly since the endocrine disruption phenomenon was first recognized (Colborn et al., 1993; Kime, 2001; WHO, 2002; Mills and Chichester, 2005). Initial studies focused on contaminants that acted via the estrogen receptor, either as an antagonist or an agonist, and that caused reproductive abnormalities in exposed wildlife, such as the feminization of male fish in sewage effluent in the United Kingdom (Jobling and Sumpter, 1993; Jobling et al., 1998). However, in addition to disruption of the hypothalamus-pituitary-gonadal axis, there is now evidence that endocrine disruption can also disrupt other systems, such as the hypothalamus-pituitary-interrenal axes and the thyroid systems (e.g., Zhou et al., 2000; Alaru et al., 2004). Also, as the study of endocrine disruption has expanded, the causes of endocrine disruption were found to not only include contamination from naturally occurring and man-made chemicals, but to also include environmental stressors such as low dissolved oxygen (Wu et al., 2003). Detection of endocrine disruption has become increasingly sophisticated, resulting in the development of a plethora of biomarkers, most of which are usually specific to a single mechanism (Rotchell and Ostrander, 2003).

Commonly measured biomarkers of the reproductive system are effective at indicating that an endocrine disruption event has occurred, but biomarkers also possess some limitations. Some commonly measured reproductive biomarkers include plasma concentrations of hormones taken at specified stages during the reproductive process and

gonadosomatic indices (GSI). The reproductive biomarkers are generally static measurements from a dynamic system and it is difficult to extrapolate their significance to higher levels of biological organization, such as to the population or community. Therefore, to determine how such biomarkers indicate individual, population, or community effects, it is often necessary to develop models that can relate biomarker measurements to the entire reproductive cycle and that then can be used to extrapolate measured biomarkers to ecologically relevant endpoints such as the production of eggs.

I previously created a model of vitellogenesis in fish that related reproductive biomarkers to the production of vitellogenin (Chapter 2). Vitellogenin is a yolk-precursor protein that is critical to the production of healthy eggs (Specker and Sullivan, 1994). The model was evaluated by simulating the effects of two environmental contaminants known to affect the hypothalamus-pituitary-gonadal-liver axis (HPGL) in fish: PCBs and cadmium. In this chapter, I perform an additional application of the vitellogenesis model by simulating the effects of hypoxia, an environmental stressor that has also been shown to be an endocrine disruptor (Wu et al., 2003; Thomas et al., 2004). I apply the model to reproductive biomarkers of hypoxia measured in field caught fish. I also use Monte Carlo methods (Rose et al., 1991) to evaluate the sensitivity of model predictions to parameter values under baseline and hypoxia conditions.

Hypoxia has recently been shown to alter the HPGL axis in fish (Wu et al., 2003; Thomas et al., 2004). Observed hypoxic effects on fish include changes in altered steroid levels, reduced gonadotropin secretion, lowered fecundity, and reduced gonadosomatic indices. Although the exact mechanism by which hypoxia acts on the HPGL axis has not been ascertained, studies on Atlantic croaker (*Micropogonias undulatus*) showed reduced

gonadotropin secretion under low dissolved oxygen (DO) conditions, thereby indicating impaired pituitary function (Thomas et al., 2004). The effects of hypoxia on the HPGL axis of fish has also been investigated in the carp (*Cyprinus carpio*), and in these studies, Wu et al. (2003) hypothesized that hypoxia can induce endocrine disruption in fish via its indirect effect on the cytochrome P450 system. The cytochrome P450 system has a number of functions in fish, including involvement in the deactivation and excretion processes of steroid hormones and in gonadal steroidogenesis (Kime, 2001). Aromatase is the enzyme that is primarily responsible for converting testosterone to estradiol and aromatase is cytochrome P450 dependent. If hypoxia indirectly causes a decline in aromatase activity, then less testosterone would be converted to estradiol and the lower estradiol production could result in a decreased production of vitellogenin. A reduced production of vitellogenin would likely result in a lower fecundity and a lower GSI.

Biomarkers of exposure are often developed and tested in the laboratory and then applied to field studies to indicate exposure. Rarely are biomarkers applied to the field able to be used to indicate ecological effects. For example, vitellogenin in the plasma of male fish is often used to indicate that fish in that region were exposed to an estrogenic substance (Cheek et al., 2001; Mills et al., 2003), but it is unknown how such a population is impacted by the exposure (Mills and Chichester, 2005). The vitellogenesis model (Chapter 2) is potentially useful for extrapolating biomarkers measured in the field to ecological metrics that may be early warning indicators of potential long-term population hazards.

In this chapter, I first apply the vitellogenesis model to endocrine responses to hypoxia measured in croaker in laboratory experiments, and then use the model to

evaluate biomarkers of hypoxia measured in field-caught croaker. As part of the field application, I attempt to use the measured biomarkers and modeling results to infer reproductive health of the local population, and the role of hypoxia (versus other stressors) in causing the reproductive health impairments. Finally, I use Monte Carlo uncertainty analysis to determine which parameters most affect the variability of model predictions under baseline and hypoxic conditions.

3.2. Model Simulations

3.2.1. Overview

I used a previously constructed model of vitellogenesis in female fish (Chapter 2) to simulate the effects of low DO on Atlantic croaker. The effects of hypoxia on the reproductive biomarkers of gonadotropin and total estradiol concentrations were obtained from laboratory studies that determined the effects of 6-10 weeks exposure to low dissolved oxygen (DO: 2.7 ppm and 1.7 ppm) on Atlantic croaker (Thomas et al., 2004). Laboratory effects of hypoxia manifested themselves in suppressed gonadotropin, total estradiol, estrogen receptor, and fecundity for both concentrations of low DO. I incorporated the hypoxia effects into the vitellogenesis model simulations, and compared simulated cumulative vitellogenin production to changes in fecundity observed in the laboratory for the 2.7 ppm and 1.7 ppm DO exposures.

I also explored the utility of the vitellogenesis model for interpreting biomarkers of Atlantic croaker measured in the field. Atlantic croaker were collected in and around Pensacola Bay and East Bay, Florida from hypoxic and normoxic sites (Thomas et al., 2004). At each site, estradiol levels and GSI were measured. I imposed the changes in

estradiol levels measured at each site in the model and then compared predicted changes in vitellogenin production to the measured changes in GSI.

Finally, I applied Monte Carlo uncertainty analysis to the vitellogenesis model to explore how variability in model parameter values affects model predictions of cumulative vitellogenin production. Monte Carlo analysis was performed under baseline conditions for three levels of variability in parameter values to determine if parameter importance was robust to increasing variability, and under hypoxia conditions to see if hypoxia caused shifts in which parameters were deemed important.

3.2.2. Model Description

Briefly, the model is a system of eight ordinary differential equations that simulate vitellogenesis in an individual mature female sciaenid fish. The model is driven by the hourly introduction of gonadotropin and the resultant biochemical reactions are simulated for 6 months, resulting in a prediction of the cumulative production of vitellogenin (Chapter 2). There is an equation for the rate of change for the following state variables: free testosterone (T), unbound or free steroid binding protein (SBP), steroid binding protein bound to testosterone (SBP-T), steroid binding protein bound to estradiol (SBP-E2), free estradiol (E2), unbound or free estrogen receptor (ER), estrogen receptor bound to E2 or activated ER (ER-E2), and vitellogenin (Vtg). The model also keeps track of output variables of total testosterone (free plus bound to steroid binding proteins), total estradiol (free plus bound), and total estrogen receptor (free plus bound to estradiol). The output variables are commonly measured biomarkers in laboratory and field studies.

All of the state variable differential equations express the rate of change of a state variable as equal to its synthesis rate minus degradation rate plus inactivation rate minus activation rate. The equations are shown in Table 2.1 of Chapter 2, and baseline parameter values are shown in Table 3.1 of this chapter. All state variables and output variables are expressed as mass (pg or mg) per milliliter of blood (plasma), except for variables involving the estrogen receptor. The free estrogen receptor state variable is modeled in the units of nM units, and converted to pico moles per gram of liver (pmol/g liver) to allow comparison to field measurements.

3.2.3. Laboratory Experiments

The results of two hypoxia laboratory experiments (Thomas et al., 2004) were used in this study and are summarized here. In both experiments, Atlantic croaker (15-17 cm in length) were chronically exposed to three concentrations of dissolved oxygen: 7.0 ppm (control), 2.5 ppm, and 1.7 ppm. Exposure to DO treatments was for 6-10 weeks during the period of gonadal recrudescence. In the first experiment, after exposure to the three dissolved oxygen concentrations, fish were injected with luteinizing hormone releasing hormone analogue (LHRHa), and plasma gonadotropin levels (luteinizing hormone, LH) were measured one hour after the injection. In the second experiment, after exposure to a DO regime, fish were sacrificed, sexed, and the following were measured: plasma concentrations of testosterone, estradiol, and vitellogenin; hepatic estrogen receptor mRNA levels (ERmRNA); fecundity; and GSI.

In the laboratory experiments, low DO had significant effects on most of the measured biomarkers (Thomas et al., 2004). Gonadotropin levels at 2.7 ppm DO were 79% of the values measured in control fish, and at 1.7 ppm were 50% of the values of

control fish (Fig. 3.1A). Testosterone concentrations did not change significantly with low DO (Fig. 3.1B). Estradiol concentrations were significantly reduced from control values; at 2.7 ppm, estradiol concentrations were 41% of control values and at 1.7 ppm estradiol concentrations were 20% of control values (Fig. 3.1C). Hepatic estrogen receptor mRNA (ERmRNA) levels in the livers of females chronically exposed to 2.7 ppm and to 1.7 ppm DO were about 40% of control values (Fig. 3.1D). Fecundity was reduced from control values by 38% under the 2.7 ppm DO and by 13% under the 1.7 ppm DO exposure (Fig. 3.1E). GSI showed a similar dependence on DO concentration as fecundity, although the decline of GSI with decreasing DO was not as dramatic as that measured with fecundity (Fig. 3.1F; Thomas et al., 2004). The model was coded in Fortran90 and solved using a 4^{th} order Runge Kutta algorithm.

3.2.4. Simulated Laboratory Effects of Hypoxia

I simulated the effects of low DO observed in the laboratory experiments in two ways: reduced gonadotropin only and reduced gonadotropin plus an hypothesized impaired aromatase activity. I then compared model predictions of other biomarkers and cumulative vitellogenin to the effects measured in the laboratory experiments. In the first approach, I multiplied the gonadotropin driving variable by 0.79 for the 2.7 ppm DO exposure and by 0.50 for the 1.7 ppm DO exposure. These reductions were those measured in the laboratory experiments (Fig. 3.1). I then compared model predictions of total testosterone, total estradiol, total estrogen receptor, and cumulative vitellogenin to results obtained in the same laboratory experiments. Because the imposition of reduced gonadotropin resulted in model predictions that underestimated the effects on some of the other biomarkers and on vitellogenin production, I also used a second approach that

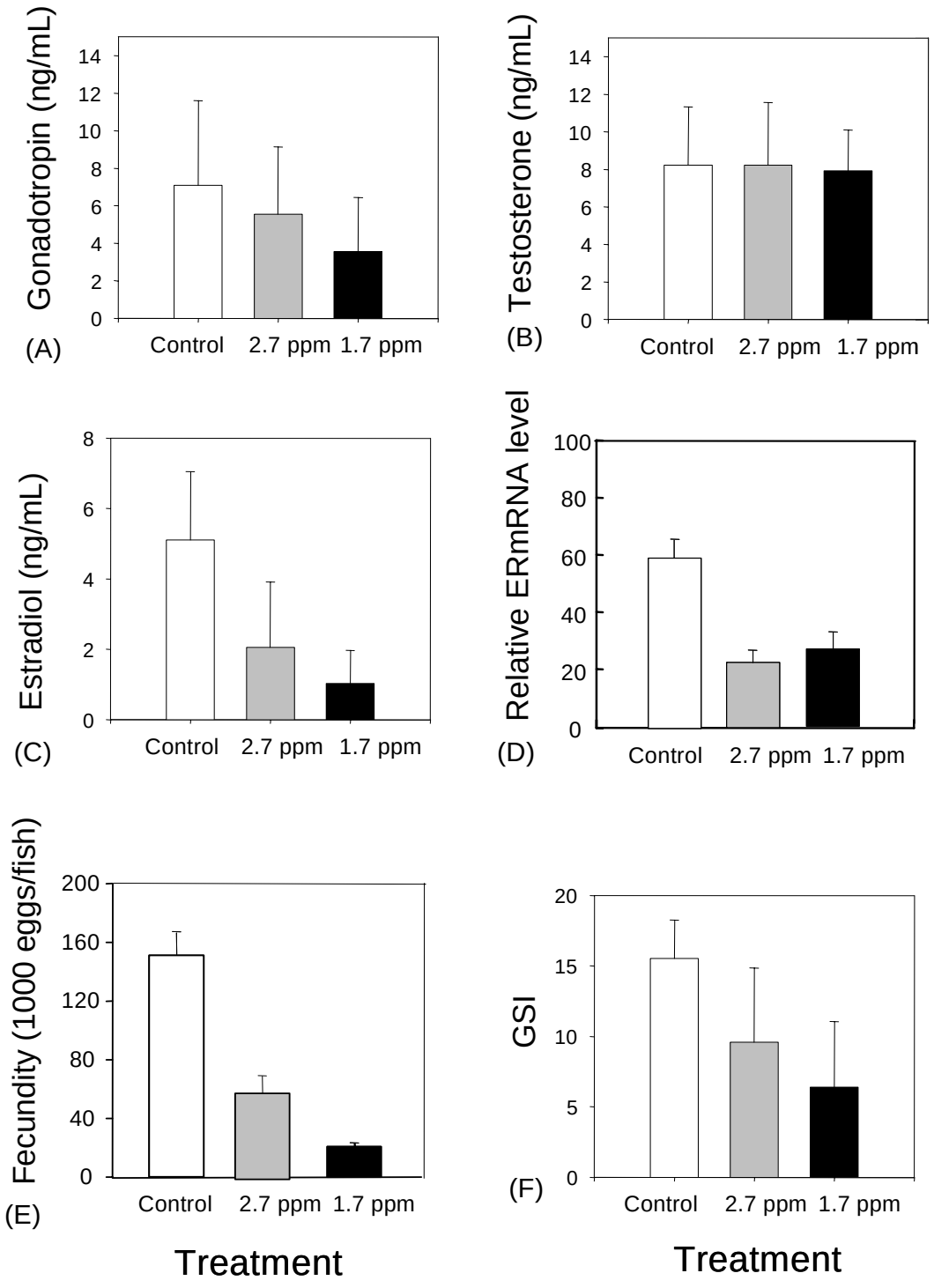

Figure 3.1. Results (mean ± SD) from the control, 2.7 ppm, and 1.7 ppm DO exposure laboratory experiments on Atlantic croaker during gonadal recrudescence. (A) plasma gonadotropin concentrations, (B) plasma testosterone concentrations, (C) plasma estradiol concentrations, (D) relative hepatic ERmRNA levels, (E) fecundity, (F) GSI. The laboratory results are from Thomas et al. (2004, unpublished).

simulated the effects of hypoxia using the same reductions in the gonadotropin driving variable but also included a forced impairment in aromatase activity. The under prediction of effects of low DO suggested that the hypoxia simulations based on reduced gonadotropin only were not capturing the entire hypoxic effect. Hypoxia has also been hypothesized to cause an aromatase impairment (Wu et al., 2003).

To simulate aromatase impairment, I removed a small percentage of free estradiol from the model every time step. The percentage of free estradiol that was removed each timestep was determined iteratively so that the maximum values of total estradiol over the simulation matched the laboratory observed responses of free estradiol, which were 41% of baseline values under the 2.7 ppm exposure and 20% of the baseline value for the 1.7 ppm exposure (Fig. 3.1C). The actual amount of free estradiol removed each timestep of the simulations was 0.01% for the 2.7 ppm DO exposure and 0.0176% for the 1.7 ppm DO exposure. As with the reduced-gonadotropin-only simulations, I compared predicted and measured biomarkers and cumulative vitellogenin production for the reduced gonadotropin plus impaired aromatase activity simulations.

3.2.5. Field Evaluation

Reproductive biomarkers were measured from Atlantic croaker collected from field sites with various concentrations of dissolved oxygen and at different phases of gonad maturation by Thomas et al. (2004; unpublished) and the results are summarized here. Seven field stations in Pensacola Bay and East Bay, Florida, were sampled and DO concentration at the time of sampling ranged from 1.2 ppm to 7.0 ppm among stations. At each sampling station, 30 Atlantic croaker were collected in the morning by trawling in October and in November, 2003. October sampling was done to capture fish in early

stages of gonadal recrudescence, and November sampling was designed to catch fish in late gonad maturation stages. At each sampling station, the DO concentration was also measured. The fish were processed on site, and the tissues, gonads, liver, brain, and blood were removed. Gonadal samples were preserved in formalin and Gilson's solution for one month for histological observation and fecundity estimation from November samples only. Plasma samples were stored on ice, then preserved at -80°C in the laboratory, and later evaluated for hormone concentrations. Also on return to the laboratory, gonadal tissues were weighed and GSIs were calculated. Total estradiol, fecundity, and GSI values for each site were reported as an average from all females collected at that site.

Consistent with the laboratory results, fish that were collected from sites with low DO at the time of sampling also had depressed estradiol levels, GSI, and fecundity (Fig. 3.2; Thomas et al., 2004). Dissolved oxygen concentrations at each of the sampling stations were lower in October compared to November (Fig. 3.2A). Plasma estradiol levels were variable among stations and between October and November, although estradiol seemed to be higher when DO was greater than about 3.0 ppm (Fig. 3.2A). October and November GSI measurements showed similar patterns; sites with the lowest DO concentrations had the lowest GSI values (Fig. 3.2B). November fecundity showed a similar, but more dramatic, decline across stations than GSI (Fig. 3.2C).

The vitellogenesis model was applied to the biomarkers measured in Pensacola and East Bays to help with the interpretation of the field-measured biomarkers. I used data from the two laboratory control experiments as baseline conditions, and re-

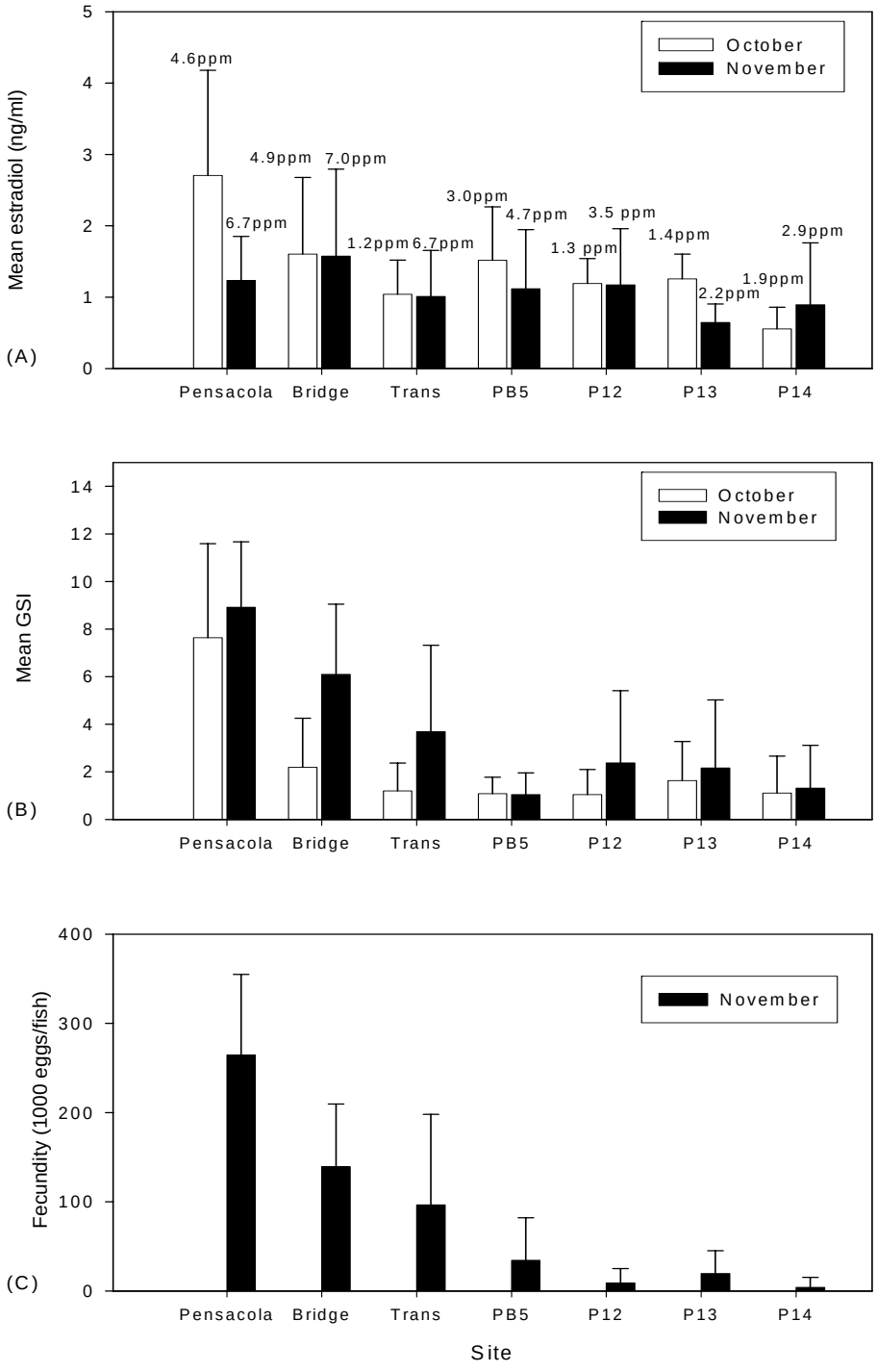

Figure 3.2. Estradiol, GSI, and fecundity (mean ± SD) of female Atlantic croaker collected from Pensacola Bay and East Bay in October and November of 2003. (A) Plasma estradiol concentrations, (B) GSI, and (C) fecundity values for November only. Panel A includes the average DO measured at each site at the time of sampling. Results are from Thomas et al. (2004; unpublished).

expressed the measured mean estradiol at each station as the percent reduction from the laboratory control value and the GSI value at each station as the percent of laboratory control values. Then, using a similar approach as was used to simulate aromatase impairment in the comparison to the laboratory experiments, I simulated a range of percent reductions in estradiol (5% to 92%). For each simulation, the reduction in estradiol was done by removing a small percentage of free estradiol from the simulation every timestep. The model-predicted cumulative vitellogenin produced was expressed as a percent of the cumulative vitellogenin produced under baseline (normoxic) conditions (i.e., relative to 161 mg/mL, Chapter 2). Comparisons thus consisted of predicted vitellogenin production as a percent of the baseline prediction and observed changes in GSI as a percent of the laboratory control value, plotted against percent reductions in estradiol. Model results were normalized by the baseline simulation results and the field data were normalized by the values measured in laboratory controls.

The gonadotropin suppression was not included as part of the hypoxia effect in the field application of the model because the comparisons to field data involved the final predictions of vitellogenin production, and changing estradiol alone based on the changes observed in the field resulted in reasonable agreement with the changes measured in GSI values. Estradiol dynamics in the model operates between the introduction of gonadotropin and the final prediction of vitellogenin production.

3.2.6. Uncertainty Analysis

Monte Carlo simulation was used to propagate variation in model parameters and to express model predictions as probability distributions. The Monte Carlo approach is a procedure involving repeated model simulations with values of parameters randomly

generated from specified probability distributions. I used Latin hypercube sampling (Rose et al., 1991), which is a stratified sampling technique, in order to ensure that extreme values of parameters were included in analysis. The value of the parameters for each simulation were randomly selected from a uniform or normal probability distributions, using the baseline values of the parameters (Chapter 2) as the mean values of the distributions (Table 3.1). I used uniform distributions for most of the model parameters because there was very limited information available to infer more complicated distributions. The exception was for parameters involving steroid binding proteins, where means and standard deviations were reported (Laidley and Thomas, 1994, 1997) and used to define normal distributions.

I performed five independent sets of 300 Monte Carlo iterations to evaluate parameter importance under baseline conditions with increasing levels of variation and to contrast parameter importance under baseline versus hypoxic conditions. The first set of 300 iterations selected all model inputs from normal distributions with means set to baseline values (Table 3.1) and coefficients of variation equal to 1%. The first set was designed to examine parameter importance when parameter values were varied by small amounts (i.e., local sensitivity). The second and third set of iterations were also preformed under baseline conditions but with parameters generated from normal and uniform distributions with baseline means and coefficient of variations equal to 10% and to 25% (Table 3.1). The fourth and fifth sets of Monte Carlo simulations used the situation of the 10% CVs but under 2.7 ppm and 1.7 ppm DO exposures. The two DO exposures used the hypoxia effects assumed to act via both gonadotropin suppression and impaired aromatase activity.

Correlation analysis was used to explore parameter sensitivities (Rose et al., 1991). To determine which parameter contributed most to the variability in cumulative vitellogenin production, I computed Pearson correlation between each of the parameters and cumulative vitellogenin production; the correlation was computed over the 300 model iterations. As a diagnostic to ensure sufficient variability in model predictions could be attributed to parameter variability, I also report the total R^2 from a linear regression model with all parameters included. Model prediction variability was depicted as frequency histograms of cumulative vitellogenin production, and departures from normality were evaluated using a Shapiro-Wilk test. All statistical analyses were using SAS (SAS Institute Inc., 2002).

3.3. Results

3.3.1. Simulated Laboratory Effects of Hypoxia

Predicted cumulative vitellogenin production compared favorably to laboratory results under low DO exposures when both the gonadotropin suppression and aromatase impairment were imposed together (Fig. 3.3A and 3.4A). Under the 2.7 ppm DO exposure conditions, the gonadotropin-suppression-only simulation produced 122.7 mg/mL of vitellogenin, or a 23.8% reduction from baseline (Fig. 3.3A). When the aromatase impairment was added to the hypoxia effect, cumulative vitellogenin produced was 63.4 mg/mL ,or a 60.6% reduction from baseline; laboratory experiments showed a 61.8% reduction in fecundity. Similar results were obtained under the 1.7 ppm DO exposure (Fig. 3.4A); gonadotropin suppression only resulted in a 64.2% reduction in

Table 3.1. Mean, minimum, and maximum values, and the probability distributions, used in the Monte Carlo uncertainty analysis. The mean values were used in all three sets of simulations. The minimum and maximum values and probability distributions were used for the second (CV=10%) and third (CV=25%) sets of simulations. All normal distributions with CV=1% were used for the first set of simulations.

Name	Definition	Mean	Min 1) 2nd iter 2) 3rd iter	Max 1) 2nd iter 2) 3rd iter	Distribution
V_{IT}	Maximum rate of free testosterone production pg/mL/h	80.0	1) 66.1 2) 45.4	1) 93.9 2) 114.6	Uniform
V_{IE}	Maximum rate of free estradiol production pg/mL/h	2300.0	1) 1902.0 2) 1304.1	1) 2697.9 2) 3295.9	Uniform
K_{mT}	Half-saturation of free testosterone production ng/mL	0.3	1) 0.2481 2) 0.1701	1) 0.3519 2) 0.4299	Uniform
K_{mE}	Half-saturation of free estradiol production pg/mL	52.0	1) 43.0 2) 29.5	1) 61.0 2) 74.5	Uniform
h_T	Hill coefficient for free testosterone	1.8	1) 1.489 2) 1.021	1) 2.111 2) 2.579	Uniform
h_E	Hill coefficient for free estradiol	3.5	1) 2.894 2) 1.985	1) 4.106 2) 5.016	Uniform
k_{2m}	Multiplier for rate constant k_2	10.0	1) 8.27 2) 5.67	1) 11.73 2) 14.33	Uniform
k_{2m2}	Coefficient for rate constant k_2	1.15	1) 0.951 2) 0.652	1) 1.349 2) 1.648	Uniform
k_1	Association rate of free estradiol with estrogen receptor $1/10^8$ M/h	7.43	1) 6.145 2) 4.213	1) 8.715 2) 10.647	Uniform
k_{-1}	Dissociation rate of free estradiol with estrogen receptor 1/h	0.81	1) 0.669 2) 0.459	1) 0.950 2) 1.161	Uniform

(Table continued)

k_2	Rate of production of vitellogenin and estrogen receptor 1/h	0.3465	1) 0.287 2) 0.197	1) 0.406 2) 0.497	Uniform
k_{aT}	Association rate of free testosterone with steroid binding protein $1/10^9$ M/h	5.6687	1) 5.102 2) 4.252	1) 6.236 2) 7.086	Normal[a]
k_{dT}	Dissociation rate of free testosterone with steroid binding protein 1/h	27.72	1) 24.948 2) 20.79	1) 30.492 2) 34.65	Normal[a]
k_{aE}	Association rate of free estradiol with steroid binding protein $1/10^9$ M/h	5.6687	1) 5.102 2) 4.252	1) 6.236 2) 7.086	Normal[a]
k_{dE}	Dissociation rate of free estradiol with steroid binding protein 1/h	17.74	1) 15.969 2) 13.307	1) 19.517 2) 22.179	Normal[a]
k_{degT}	Degradation rate of free testosterone 1/h	1.386	1) 1.146 2) 0.786	1) 1.626 2) 1.986	Uniform
k_{degE}	Degradation rate of free estradiol 1/h	1.386	1) 1.146 2) 0.786	1) 1.626 2) 1.986	Uniform
k_{degu}	Degradation rate of free estrogen receptor 1/h	0.00058	1) 0.00048 2) 0.00033	1) 0.00068 2) 0.00083	Uniform
k_{dega}	Degradation rate of activated estrogen receptor 1/h	0.012	1) 0.0099 2) 0.0068	1) 0.0141 2) 0.0172	Uniform
SBP	Free steroid binding protein nM	400.0	1) 360.0 2) 300.0	1) 440.0 2) 500.0	Normal[b]

[a]Laidley and Thomas, 1994
[b]Laidley and Thomas, 1997

cumulative vitellogenin, while adding aromatase impairment resulted in an 88.3% reduction. An 86.6% reduction in fecundity was measured in the laboratory experiments.

As expected, model predictions of total estradiol with just gonadotropin suppression underestimated the laboratory results, and predictions that also included the aromatase impairment effect agreed well with laboratory results (Fig. 3.3D and 3.4D). I used the percent reductions in estradiol as a guide for imposing the aromatase impairment effect in the model simulations so predicted and measured estradiol concentrations should match when the aromatase impairment was included. Simulations involving gonadotropin suppression alone predicted reductions in maximum total estradiol concentrations of 15% for the 2.7 ppm exposure and 44% for the 1.7 ppm exposure, compared to predicted reductions with aromatase impairment included and laboratory-derived reductions of 59% for the 2.7 ppm and 80% for the 1.7 ppm exposures.

Imposing both gonadotropin suppression and aromatase impairment in simulations overestimated the effect on estrogen receptor concentrations when compared to laboratory studies for both the 2.7 ppm (Fig. 3.3B) and 1.7 ppm (Fig. 3.4B) exposures. Predicted reductions were 73.0% for the 2.7 ppm exposure and 93.5% for the 1.7 ppm exposure, compared to a 59% reduction derived from the laboratory experiments. I assumed a proportional relationship between hepatic ERmRNA levels and estrogen receptor concentration.

Simulated and laboratory results showed little change in total testosterone concentrations with increasing hypoxic conditions (Fig. 3.3C and 3.4C), and model predictions showed slightly reduced free testosterone concentrations (Fig. 3.3E and 3.4E)

and reduced free estradiol concentrations (Fig. 3.3F and 3.4F). The largest reductions were predicted for free estradiol levels. Free estradiol was predicted to be reduced by 14.5% for the gonadotropin suppression alone and by 43.8% for aromatase impairment included under the 2.7 ppm exposure, and by 43.2% for gonadotropin suppression alone and by 71.0% for aromatase impairment included under the 1.7 ppm exposure.

3.3.2. Field Evaluation

Simulated results yielded a monotonically decreasing relationship between percent reduction in total estradiol levels and cumulative vitellogenin production as a percent of baseline (Fig. 3.5). As a reference, the results of the laboratory experiments that exposed fish to 2.7 ppm and 1.7 ppm DO are included, expressed as percent reductions in estradiol from laboratory controls and fecundity expressed as a percent of laboratory control values.

When field values were also plotted as percent reductions in estradiol against GSI as a percent of laboratory control values, October values (Fig. 3.5A) more closely matched simulated values than November values (Fig. 3.5B). A possible explanation is that the model simulates vitellogenesis, whereas the November collected fish had finished vitellogenesis.

Measured GSI values (as percents of control values) plotted against percent reductions in total estradiol for October samples showed that all the sites with DO below 2.0 ppm had reduced GSIs, and that estradiol levels that clustered around the simulated line and around the laboratory results measured at the 1.7 ppm DO exposure (Fig. 3.4A).

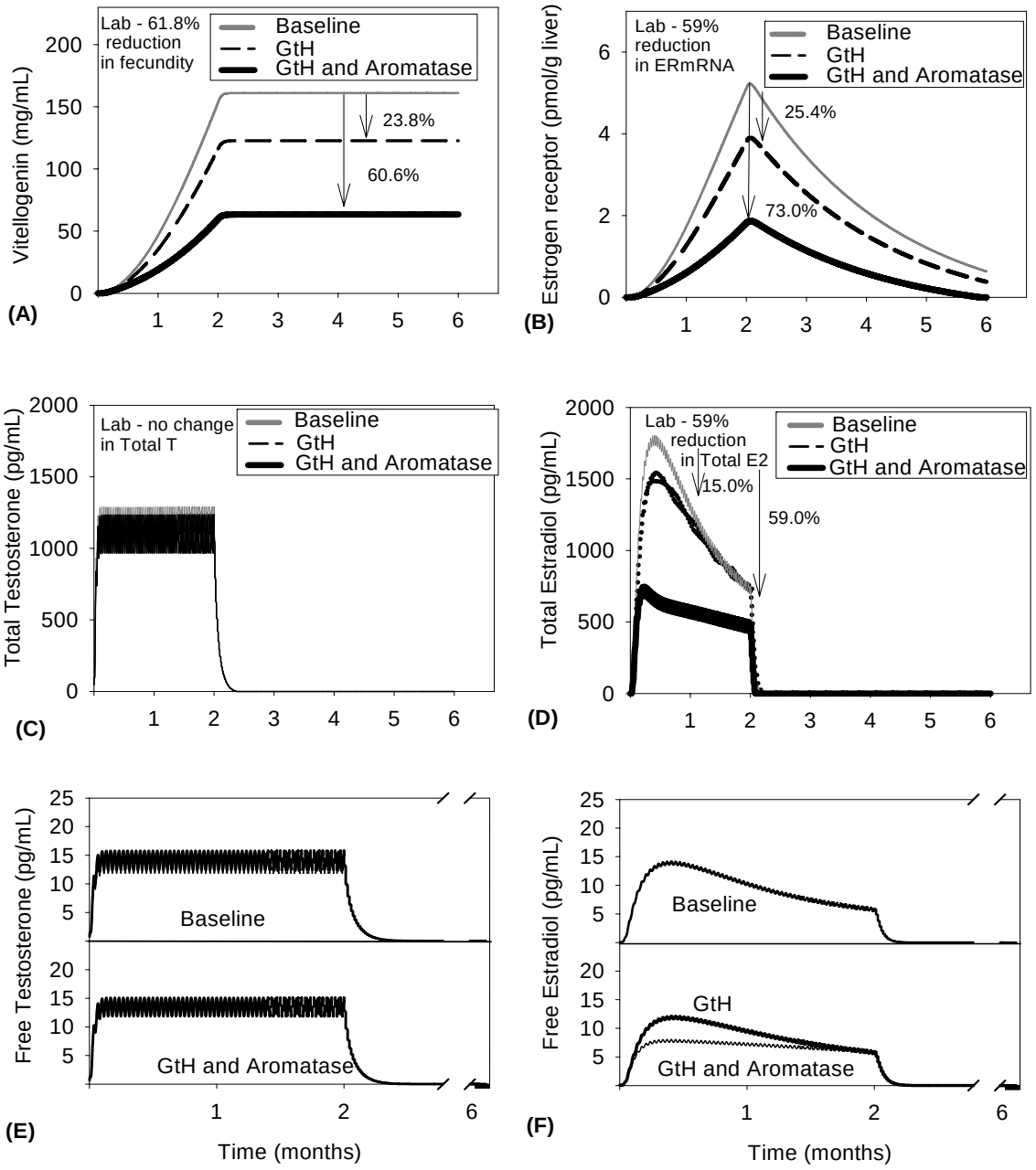

Figure 3.3. Predicted concentrations under baseline conditions and hypoxia exposure (2.7 ppm D.O.) using just gonadotropin (GtH) suppression, and using both GtH suppression and aromatase impairment. (A) vitellogenin, (B) total estrogen receptor, (C) total testosterone, (D) total estradiol, (E) free testosterone, and (F) free estradiol. Percent reductions from peak values are shown for model predictions; percent reductions based on laboratory experiments are shown on each panel for comparison.

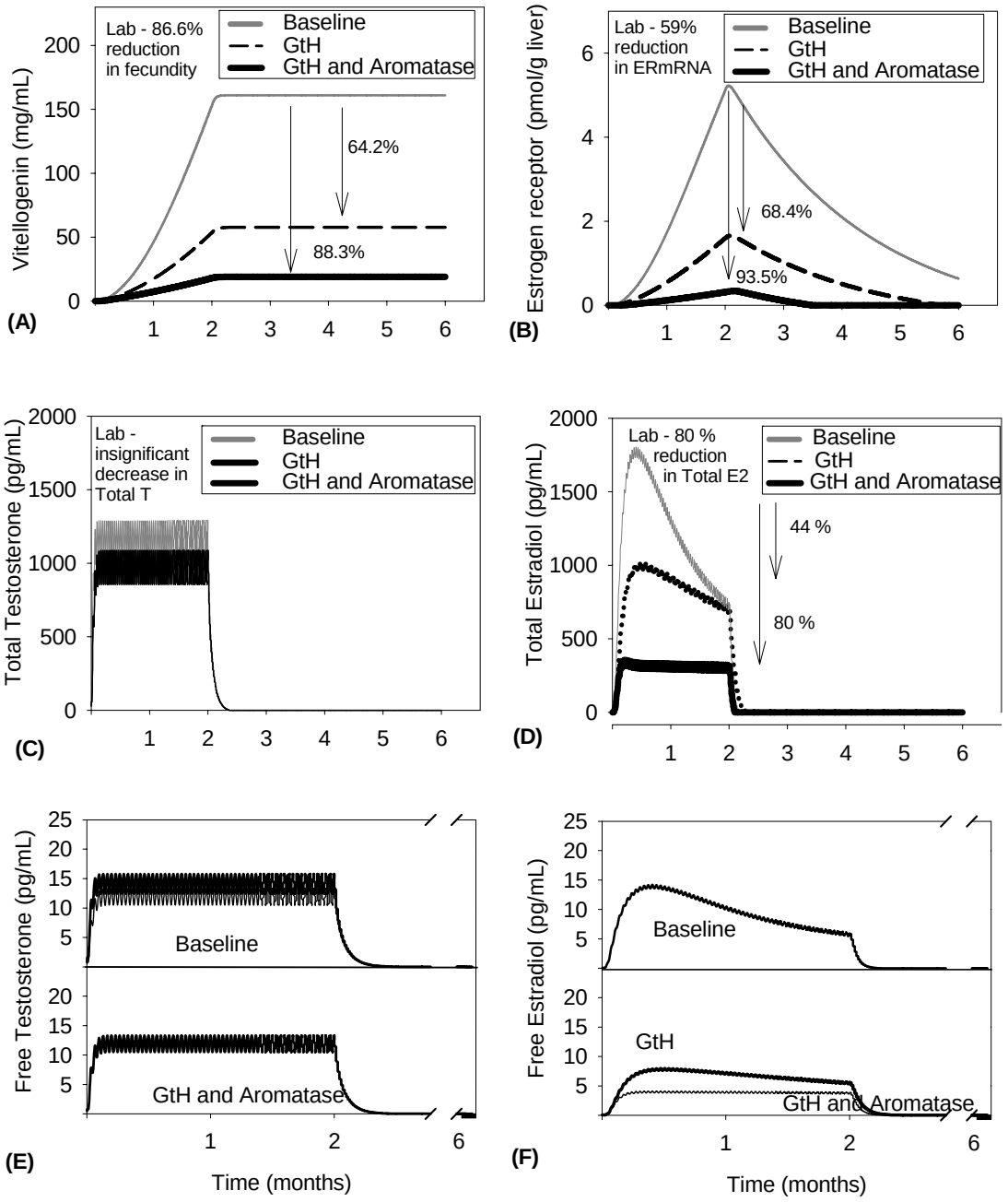

Figure 3.4. Predicted concentrations under baseline conditions and hypoxia exposure (1.7 ppm D.O.) using just gonadotropin (GtH) suppression, and using both GtH suppression and aromatase impairment of : (A) vitellogenin, (B) total estrogen receptor, (C) total testosterone, (D) total estradiol, (E) free testosterone, and (F) free estradiol. Percent reductions from peak values are shown for model predictions; percent reductions based on laboratory experiments are shown on each panel for comparison.

Pensacola Bay, which had a DO value of 4.6 ppm, had higher estradiol levels (i.e., lower percent reductions) and higher GSI values (i.e., higher percent of controls) than the other sites. The low values of measured GSI was consistent with the relatively low vitellogenin production predicted based on the observed reduction in estradiol. Fish collected from the Bridge and PB5 sites, which had DO values of 3.0 ppm and 4.9 ppm, had reduced estradiol and GSI values that differed from the predicted vitellogenin production expected for their measured reductions in estradiol.

3.3.3. Uncertainty Analysis

The coefficient of variation in cumulative vitellogenin production increased with increasing CV values imposed on parameter values (Fig. 3.6A). Mean cumulative vitellogenin production was similar for the CV=1% (160.7 mg/mL) and CV=10% (163.5 mg/ml) sets of simulations, where as the mean was higher (182.5 mg/mL) for the CV=25% set of simulations because the shape of the distribution of vitellogenin production was no longer symmetric. Predicted CV of cumulative vitellogenin increased with increasing variability on parameters (CVs were 3.4% under CV=1%, 34.1% under CV=10%, and 82.3% under CV=25%). Predicted distributions did not demonstrate any significant departure from normality for the CV=1% simulations (Shapiro-Wilk, W = 0.9934, P = 0.2166), but did for the CV=10% (W = 0.9769; P = <0.0001) and CV=25% (W = 0.8928, P < 0.0001) sets of simulations. Under parameter variability of CV=25%, predicted vitellogenin production values under 30 mg/mL were common.

Under CV=10% parameter variability, the mean cumulative vitellogenin production decreased with decreasing DO exposure, but the CV of vitellogenin

Figure 3.5. Simulated cumulative vitellogenin (expressed as percent as baseline model prediction) and field values of GSI (expressed as percent of laboratory control value) versus the associated percent reduction in estradiol (from laboratory control) for 7 field sites located in Pensacola Bay and East Bay, Florida in (A) October 2003 and (B) November 2003. GSI from fish collected in field from each site were averaged and expressed as a percent of laboratory control values. Estradiol associated with the model simulated vitellogenin and with the field measured GSI are expressed as a percent reduction in estradiol from laboratory control fish. Dissolved oxygen measured at each site is included with each data point. Percent GSI and percent reduction in estradiol from two laboratory experiments that exposed female fish to two regimes of low DO (2.7 ppm and 1.7 ppm) for 6-10 weeks is also included.

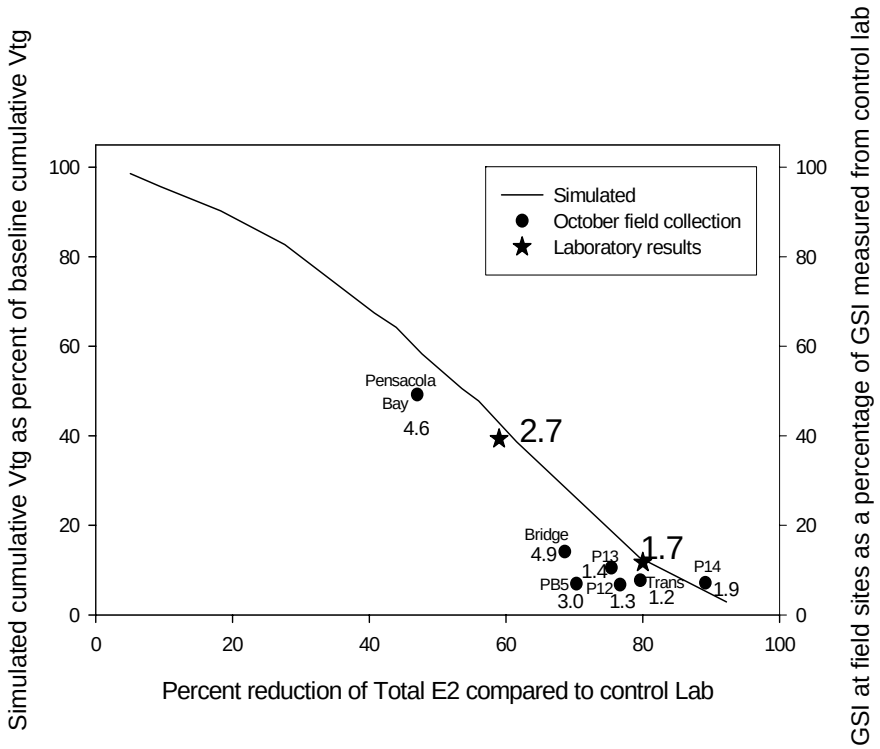
Simulated cumulative Vtg as percent of baseline cumulative Vtg
GSI at field sites as a percentage of GSI measured from control lab
Percent reduction of Total E2 compared to control Lab
Simulated
October field collection
Laboratory results
Pensacola Bay
4.6
2.7
Bridge
4.9
P13
1.4
1.7
P14
1.9
PB5
3.0
P12
1.3
Trans
1.2
0
20
40
60
80
100

(A)

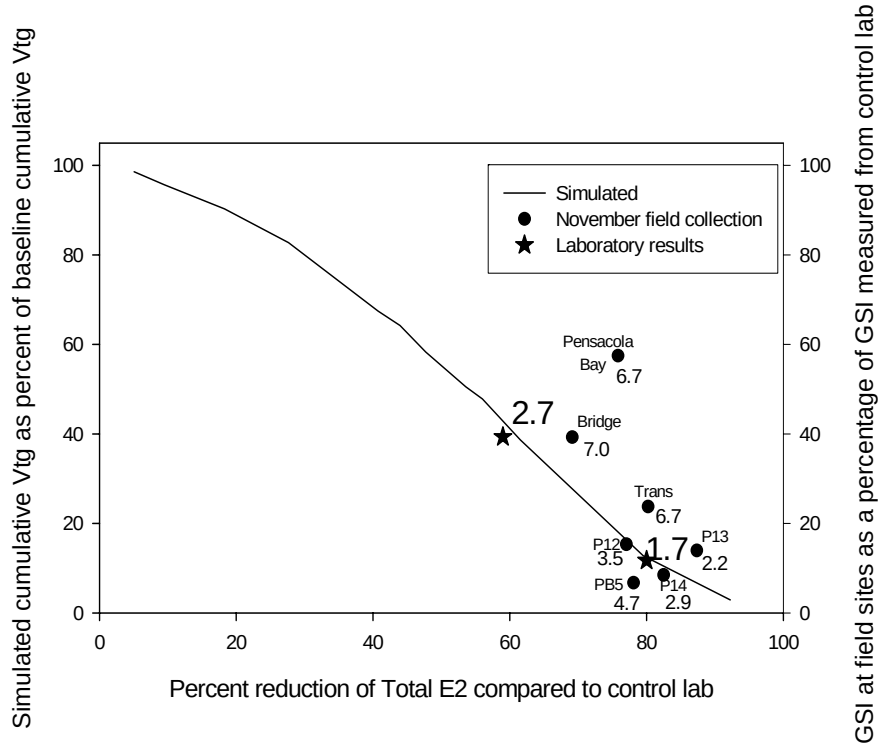
Simulated cumulative Vtg as percent of baseline cumulative Vtg
GSI at field sites as a percentage of GSI measured from control lab
Percent reduction of Total E2 compared to control lab
Simulated
November field collection
Laboratory results
Pensacola Bay
6.7
2.7
Bridge
7.0
Trans
6.7
P12
3.5
1.7
P13
2.2
PB5
4.7
P14
2.9
0
20
40
60
80
100

(B)

production increased with decreasing DO exposure (Fig. 3.6B). Under the 2.7 ppm DO exposure, mean cumulative vitellogenin production decreased, but CV increased over baseline (mean: 68.1 mg/mL versus 160.7, CV: 47.2% versus 34.1%). Low DO exposure of 1.7 ppm predicted a lower mean cumulative production and a higher CV (mean=21.4 mg/mL, CV=55.2%) than under 2.7 ppm and baseline.

Six model parameters were consistently the highest correlated with predicted vitellogenin production under increasing parameter CVs (Fig. 3.7A) and decreasing DO exposures (Fig. 3.7B). Multiple regressions that included all of the parameters varied in the Monte Carlo analyses demonstrated that almost all the variance in the predicted vitellogenin was attributable to the changed model parameters. Total R^2 values were greater than 0.9 for all five sets of Monte Carlo simulations. The important model parameters that consistently explained more than 5% of variance were: maximum rate of free testosterone production (V_{IT}) used in a Hill function, free estradiol production parameters (h_E and K_{mE}) used in a Hill function, association rate of free estradiol with estrogen receptor (k_1), degradation rate of free testosterone (k_{degt}), and the half-saturation of free testosterone production (K_{mT}). In a few cases some other parameters explained slightly more than 5%, but most all other parameters contributed less than 5% to the variance explained. One deviation from the consistency in the important parameters was the replacement of K_{mT} with k_2 (rate of production of vitellogenin and estrogen receptor) under the 2.7 ppm exposure and the replacement of k_{degT} with k_2 under the 1.7 ppm DO exposure (Fig. 3.7B). Although in both cases, the most important parameter remained maximum rate of free testosterone production (V_{1T}).

3.4. Discussion

Predictions of cumulative vitellogenin production under hypoxic conditions using simulations that included both gonadotropin suppression and aromatase impairment compared favorably to laboratory results. Under both the 2.7 ppm and 1.7 ppm DO exposures, cumulative vitellogenin production approximated the observed changes in fecundity measured in laboratory studies of Atlantic croaker (Fig. 3.3A and 3.4A).

Gonadotropin suppression alone was not sufficient to predict the response of cumulative vitellogenin production to hypoxic conditions. Simulations under both the 2.7 and 1.7 ppm DO exposures that involved only altering the gonadotropin driving variable by the magnitudes measured in the laboratory underestimated the effects on cumulative vitellogenin production. A variety of explanations can be offered for this discrepancy. First, the model could be failing to capture the appropriate dynamics involved in vitellogenesis. Chapter 2 included a discussion of model assumptions and limitations, any number of which could cause unrealistic model predictions. Second, I compared cumulative vitellogenin production to fecundity, and therefore may be introducing a source of error. Difficulties arise in using vitellogenin as a biomarker in female fish. The difficulty primarily stems from vitellogenin concentration being in a state of flux; concentrations of vitellogenin in plasma vary over time and depend on the rate of uptake into rapidly growing oocytes (Specker and Sullivan, 1994). In the modeling, I assumed that most of the vitellogenin is taken up by developing oocytes, and therefore I assumed that a reduction in available vitellogenin would result in similar reduction in fecundity. Third, the hypoxia simulation that uses only the gonadotropin

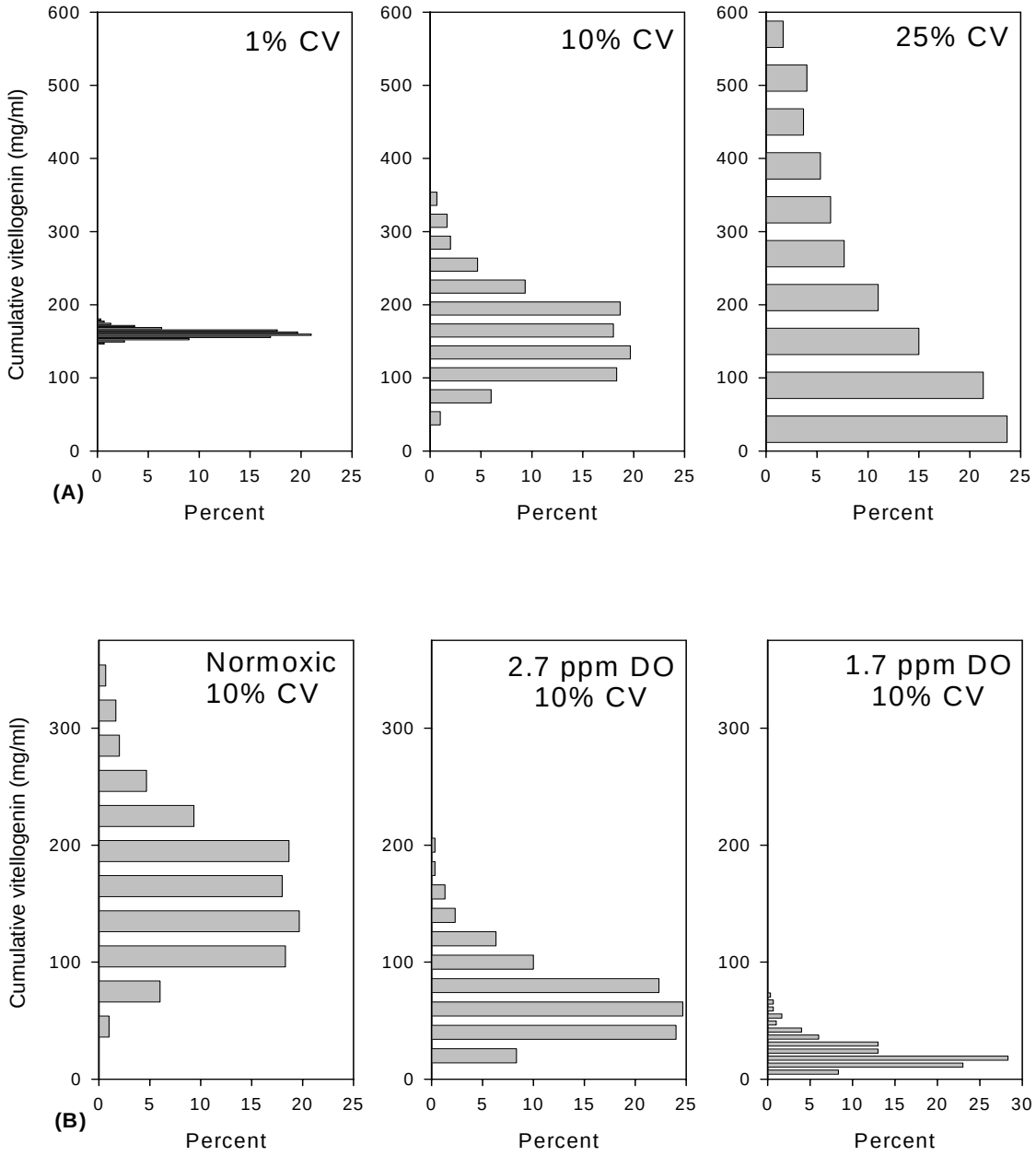

Figure 3.6. Frequency histograms of cumulative vitellogenin production values five sets of 300 Monte Carlo iterations. The top three panels show predicted values under baseline conditions for parameter variability set to: (A) CV=1%, (B) CV=10%, and (C) CV=25%. CV=1% used all normal distributions, while CV=10% and 25% used a mix of normal and uniform distributions. The bottom three panels showed predicted values for the CV=1% case under (A) normoxic (same as baseline), (B) 2.7 ppm DO, and (C) 1.7 ppm DO.

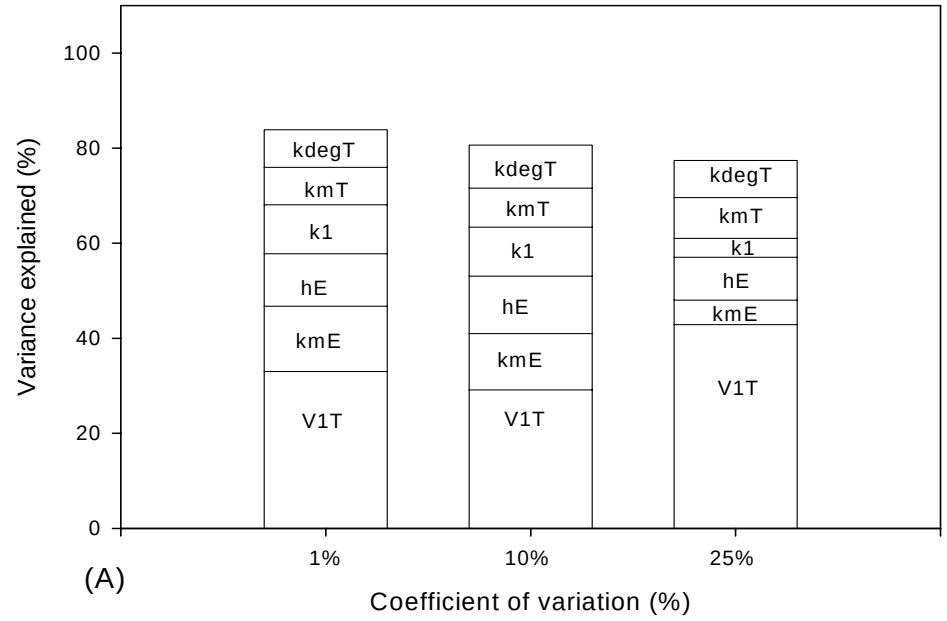

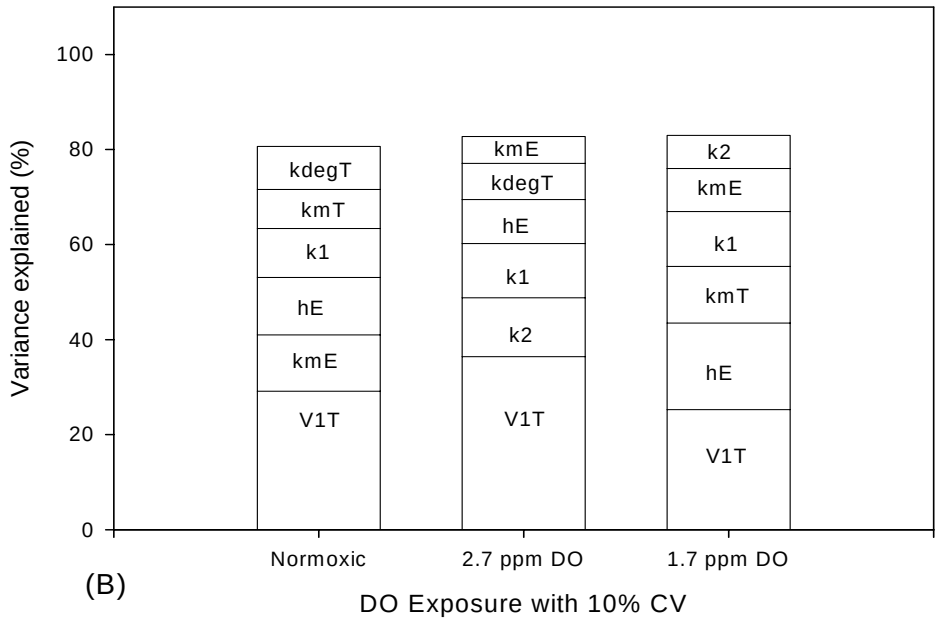

Figure 3.7. The percent variance in predicted cumulative vitellogenin production from Monte Carlo iterations attributed to six top ranked model parameters that accounted for at 5% of the variance. The variance explained is calculated as 100 times the square of the Pearson correlation coefficient between predicted vitellogenin and model parameters over Monte Carlo iterations. (A) CV=1%, 10% and 25% under baseline conditions, and (B) CV=10% for baseline, 2.7 ppm DO and 1.7 ppm DO.

suppression may not be capturing the entire hypoxic effect and may be missing some mechanisms by which hypoxia effects the HPGL axis. As mentioned previously, other studies hypothesized that low DO can indirectly cause aromatase impairment (Wu et al., 2003). It is this third possible explanation that I explored in this chapter. When I added aromatase impairment to the hypoxia effect, by removing a small percentage of free estradiol every timestep, the model did a much better job at predicting the responses in vitellogenin observed via fecundity measurements in the laboratory.

The simulation of hypoxic effects demonstrated how the model can be used as exploratory tool in situations when the mechanisms underlying the effects of the endocrine disruptor are uncertain. Providing the vitellogenesis model accurately predicts hormonal dynamics within a female fish, the model can be used to explore the mechanisms behind an endocrine disrupting event. Often endocrine disrupting events are documented as changes in biomarkers and the exact mechanism behind the effect are unknown. In the hypoxia simulations in this chapter, low dissolved oxygen was hypothesized to affect aromatase function, but the precise mechanism was unknown; the indirect effects of hypoxia manifest as decreases in total estradiol levels and decreases in fecundity. I simulated these indirect effects by decreasing the free estradiol concentration in model simulations so that the correct decrease in total estradiol was predicted. Incorporating indirect effects ensured that the model prediction of the magnitude of the decrease in vitellogenin production under hypoxia was similar to laboratory measurements. New laboratory experiments can be designed to determine if aromatase function in Atlantic croaker is indeed affected by hypoxia, or if hypoxia causes a decline in total estradiol concentrations via other mechanisms.

Although the model was able to simulate appropriate reductions in steroid levels and vitellogenin, the model overestimated the effects of hypoxia on the estrogen receptor concentration. In laboratory studies, ERmRNA levels were reduced by about the same amount for the 2.7 and 1.7 ppm DO exposures (Thomas et al., 2004), whereas the model predicted larger reductions in estrogen receptor than observed (Fig. 3.3B and 3.4B). The model does not appear to capture the dynamics of the estrogen receptor, indicating that additional experimental data or model development is required. In reality, estrogen receptor binding and action is much more complex than simulated here, involving three nuclear receptors subtypes (Hawkins et al., 2000).

This chapter focused on applying the vitellogenesis model to hypoxic conditions. Previous applications of the model involved simulations of PCB and cadmium exposure (Chapter 2). The hypoxia experiments were performed while the vitellogenesis model was being developed, whereas the PCB and cadmium simulations relied on older studies. As a result, the hypoxia simulation was a much better evaluation of the vitellogenesis model because more model-to-data comparisons were possible. The hypoxia simulation explored the dynamics of total testosterone, total estradiol, and hepatic estrogen receptor dynamics compared to laboratory measured values, and predicted vitellogenin production was compared to well-measured GSI values. The PCB and cadmium simulations were compared to fewer steroid concentrations that sometimes were synthesized from a variety of experiments, and the measured GSI values were relatively crude. For example, estradiol concentrations showed somewhat contradictory responses between short-term and long-term PCB experiments (see Chapter 2). The hypoxia simulation suggested that, with the exception of the dynamics of estrogen receptor, the vitellogenesis model

performed well. Further laboratory testing in conjunction with model development will allow for additional improvements in the design of laboratory experiments and increased model realism.

The field application of the vitellogenesis model showed how the model can be used to help interpret biomarkers. Dissolved oxygen concentrations can vary widely in space and time, thereby affecting the exposure of individual fish. DO measured at the time of sampling is snapshot value, whereas fish likely integrate DO exposure over a period of several days (Breitburg, 2002) Biomarkers are excellent measures of exposure and, when coupled with a dynamic simulation model like the model used here, detected exposure can be linked to ecological endpoints such as vitellogenin production. Field measured values indicate that endocrine disruption has occurred but pinpointing the exact cause is often difficult. The degree of agreement between model-predicted vitellogenin production under single or multiple simulated stressors and measured GSI values (e.g., DO as the sole stressor is shown in Fig. 3.5) can provide information on the role of different stressors in causing the observed changes in GSI. In my analyses, if biomarker data collected from a field site fell directly, or close to, the simulated line in Fig. 3.5, the interpretation would be that the site was impacted solely by hypoxic conditions. If the data collected from a site fell far below the simulated line, such as sites PB5 and Bridge collected in October (Fig. 3.5A), the implication is that the site is affected by factors in addition to hypoxic conditions. Also, when reproductive success measures other than the steroid-related biomarkers are not available, the model can translate measured reduction in biomarkers into ecological metrics (e.g., reduced estradiol into cumulative vitellogenin production).

Uncertainty analyses showed that the model is well-behaved under parameter variability. All comparisons of model predictions to laboratory and field data were based upon deterministic simulations. Monte Carlo uncertainty analysis allowed for exploration of model dynamics under variable parameter values. Variance in predicted vitellogenin production increased with increasing CV assumed for parameter values and increased with decreasing DO exposures (Fig. 3.6). Under the CV=10%, and especially under the CV=25% parameter variability conditions, predicted vitellogenin production showed non-normal distributions. These non-normal distributions can be important when interpreting deterministic model predictions (i.e., the deterministic prediction may not be the mode of the distribution when parameters are allowed to vary).

Uncertainty analyses showed that about six of the model parameters consistently played a major role in affecting the variance of predicted vitellogenin production under various assumptions about parameter variability and under normoxic and hypoxic conditions. The most important parameter was V_{IT}, which is used in the Hill function to describe maximum rate of free testosterone production. V_{IT} is a calibrated parameter and realistic ranges were defined based on data collected on goldfish and carp (Chapter 2). Some of the other important parameters were also related to the Hill function for the production of free estradiol (h_E and K_{mE}), and these were involved in steroidogenesis, a process not well understood in Atlantic croaker. Model prediction variability can be reduced by additional research on the appropriateness and parameter values of the Hill function for simulating free testosterone and free estradiol production.

In addition to experiments for refining how testosterone and estradiol production are represented in the model, additional experiments are needed to resolve the most

appropriate way to simulate hypoxic effects in the model. The hypoxia simulation demonstrated that the model can predict vitellogenin production if additional mechanisms, besides gonadotropin suppression, are considered. One key area for further measurements would be experimental data on estrogen receptor, steroidogenesis, and aromatase function to help refine how hypoxia effects are represented in the model.

This study is an excellent example of combining laboratory, field, and modeling efforts to help in the interpretation of biomarkers of stress in fish. The model appeared to perform well and my analysis of the field data demonstrated the potential for the model to be used to evaluate field measured biomarkers and assess population hazards. The benefits to using a dynamic model, such as this one, include predictions of cumulative vitellogenin that do not necessarily follow a linear response to a stressor. The vitellogenesis model provides a method to evaluate biomarkers into the context of a dynamic endocrine system.

3.5. References

Aluru, N., Jorgensen, E.H., Maule, A.G. and Vijayan, M.M. 2004. PCB disruption of the hypothalamus-pituitary-interrenal axis involves brain glucocorticoid receptor downregulation in anadromous Arctic charr. *Am. J. Physiol. Regul. Integr.Comp. Physiol.* 287: R787-R793.

Breitburg, D. 2002. Effects of hypoxia, and the balance between hypoxia and enrichment, on coastal fishes and fisheries. *Estuaries* 25: 767-781.

Cheek, A.O., Hoexum Brouwer, T., Carroll, S., Manning, S., McLachlan, J.A. and Brouwer, M. 2001. Experimental evaluation of vitellogenin as a predictive biomarker for reproductive disruption. *Environ. Health Perspect.* 109: 681-690.

Colborn, T., Saalvom, F.S. and Soto, A.M. 1993. Developmental effects of endocrine-disrupting chemicals in wildlife and humans. *Environ. Health Perspect*. 101:378-384.

Hawkins, M.B., Thornton, J.W., Crews, D., Skipper, J.K., Dotte, A. and Thomas, P.

2000. Identification of a third distinct estrogen receptor and reclassification of estrogen receptors in teleosts. *Proc. Natl. Acad. Sci. USA*. 97:10751-10756.

Jobling, S. and Sumpter, J.P. 1993. Detergent components in sewage effluent are weakly estrogenic to fish – an *in vitro* study using rainbow trout (*Oncorhynchus mykiss*) hepatocytes. *Aquat. Toxicol.* 27: 361-372.

Jobling, S., Nolan, M., Tyler, C.R., Brighty, G. and Sumpter, J.P. 1998. Widespread sexual disruption in wild fish. *Environ. Sci. Technol*. 32: 2498-2506.

Kime, D.E. 2001.Endocrine disruption in fish. Norwell, Massachussets: Kluwer Academic Publishers.

Laidley, C.W. and Thomas, P. 1994. Partial characterization of a sex-steroid binding protein in the spotted seatrout (*Cynoscion nebulosus*). *Biol. Reprod.* 51:982-992.

Laidley, C.W. and Thomas, P. 1997. Changes in plasma sex steroid-binding protein levels associated with ovarian recrudescence in the spotted seatrout (*Cynoscion nebulosus*). *Biol. Reprod*. 56:931-937.

Mills, L.J. and Chichester, C. 2005. Review of evidence: are endocrine-disrupting chemicals in the aquatic environment impacting fish populations? *Sci. Tot. Environ.* 343: 1-34.

Mills, L.J., Gutjahr-Gobell, R.E., Borsay Horowitz, D., Denslow, N.D., Chow, M.C. and Zaroogian, G.E. 2000. Relationship between reproductive success and male plasma vitellogenin concentrations in cunner, *Tautogolabrus adspersus*. *Environ. Health Perspect.* 111: 93-99.

Rose, K.A., Smith, E.P., Gardner, R.H., Brenkert, A.L. and Bartell, S.M. 1991. Parameter sensitivities, Monte Carlo filtering and model forecasting under uncertainty. *J. Forecast*.10: 117-133

Rotchell, J.M. and Ostrander, G.K. 2003. Molecular markers of endocrine disruption in aquatic organisms. *J. Toxicol. Environ. Health B. Crit. Rev.* 6: 453-495.

SAS Institute Inc. 2002 SAS Language Reference, Version 9, Cary, NC: SAS Institute Inc.

Specker, J.L.and Sullivan, C.V. 1994.Vitellogenesis in fishes: status and perspectives. *In*: Davey, K.G, Peter, R.E. and Tobe, S.S., editors. Perspectives in Comparative Endocrinology. Ottawa: National Research Council. pp. 304-315.

Thomas, P., Rahman, S. and Kummer, J. 2004. Reproductive and endocrine responses of Atlantic croaker to moderate hypoxia. Fourth SETAC World Congress, Nov 14-18, Portland Oregon.

WHO. 2002. Global Assessment of the State-of-the-Science of Endocrine Disruptors. *In:* Damstra, T., Barlow, S., Bergman, A., Kavlock, R. and van der Kraak, G. editors. International Programme On Chemical Safety.

Wu, R.S.S., Zhou, B.S., Randall, D.J., Woo, N.Y.S. and Lam, P.K.S. 2003.Aquatic hypoxia is an endocrine disruptor and impairs fish reproduction. *Environ. Sci. Technol.* 37:1137-1141.

Zhou, T., John-Adler, H.B., Weis, J.S. and Weis P.2000. Endocrine disruption: thyroid dysfunction in mummichogs (*Fundulus heteroclitus*) from a polluted habitat. *Mar. Env. Res.* 50: 393-397.

CHAPTER 4. MODELING LARVAL FISH BEHAVIOR: SCALING THE SUBLETHAL EFFECTS OF ENDOCRINE DISRUPTING CHEMICALS TO POPULATION RELEVANT ENDPOINTS

4.1. Introduction

The past few decades of toxicological research have demonstrated that it is difficult to establish a link between sublethal effects of contaminants measured on individuals and indices of population health (Mills and Chichester, 2005). Many contaminants and environmental stressors act as endocrine disruptors, which interrupt normal signaling processes within and between organisms. The effects of endocrine disruption generally manifest themselves as subtle changes in the reproductive endocrine system, molecular biology, physiology, metabolism, homeostasis, and behavior of an organism (WHO, 2002). In efforts to determine the precise mechanism of endocrine disruption, there have been countless studies that measure subtle changes in the endocrine system of animals and the resulting changes in behavior or physiology. However, it often remains unclear as to how such subtle changes translate into an individual's performance in a natural setting. The term "ecological death" has been coined to address this issue. Ecological death is the phenomenon where animals are not overtly harmed by a contaminant, but exposure causes alterations in their behavior or physiology such that the organism is unable to function ecologically as expected (Mesa et al., 1994; Scott and Sloman, 2004).

The effect of contaminants on animal behavior has been well documented (Clotfelter et al., 2004). Behavior is often used as an endpoint in toxicological studies because an animal's behavioral response is an integrated physiological response to its environment (Clotfelter et al., 2004). Usually, toxicological studies that monitor

behavior include behaviors that show disruption of certain physiological mechanisms. For example, in striped mullet (*Mugil cephalus*), methylmercury was shown to decrease levels of serotonin that was then associated with progressive loss of motor control (Thomas et al., 1981). Increasingly, toxicological experiments have been focused on behavioral endpoints that reflect how a contaminant will affect ecological health or fitness. The behaviors selected for such ecological health experiments usually relate to an animal's foraging ability, predator avoidance skills, reproduction, and formation of social hierarchies (Scott and Sloman, 2004). Examples of these ecologically-focused behavioral experiments include contaminant effects on reproductive behavior (Bjerselius et al., 2001), foraging behavior (Weis et al., 2001), and predator avoidance behavior (Weis and Weis, 1995; Zhou and Weis, 1998; Faulk et al., 1999; McCarthy et al., 2003; Alvarez, 2005). Far fewer studies examine the interaction between predator and prey to determine population implications (e.g., Fleeger et al., 2003; Alvarez and Fuiman, 2005).

Individual based models (IBMs) are well suited to link behavioral laboratory results to population relevant indices (Rose et al., 1999; Rose et al., 2003). Individual-based models track each individual; the sum over individuals at any given time is the cohort or the population. Laboratory toxicological effects that are reported for the individual can be easily imposed on processes represented in an individual-based model, either directly or first via some conversion from a statistical model.

In this chapter, an IBM was developed and used to explore the predator-prey interactions between a larval fish and its zooplankton prey and predators under control and contaminant exposure conditions. The contaminant effects include changes to the larval fish's foraging ability and predator evasion skills. The IBM translates these

changes in behaviors of individuals into cohort stage duration and survival. Stage duration and survival provide an ecological context to the behavioral effects of the contaminants, and as demonstrated in Chapter 5, can also be used to change parameter values of population dynamics models to obtain long-term population-level implications of the behavioral effects. The IBM was also used in this chapter to separate the contaminant effects that operate via changes in growth versus mortality, and to determine which process was causing the predicted responses in stage duration and survival.

The ocean larval stage of Atlantic croaker (*Micropogonias undulatus*) is a good model organism on which to base the larval fish IBM and to simulate behavioral effects associated with contaminant exposure. Atlantic croaker spawn offshore in batches and eggs, yolk-sac larvae, and early feeding larvae stages experience high mortality rates while in the ocean (Diamond et al., 1999). Early life stages that exhibit high and variable mortality rates can be important regulators of year class strength and recruitment dynamics (Houde, 1989; Leggett and Deblois, 1994). The ocean larval stage may be especially sensitive to behavioral effects because early ocean larvae have to undergo sufficient development to exhibit successful foraging and predator avoidance. Behavioral experiments have been done in the laboratory to determine how contaminants affect foraging and predator avoidance behaviors of Atlantic croaker ocean larvae (Faulk et al., 1999; McCarthy et al., 2003; Alvarez, 2005).

Several other attributes of Atlantic croaker make it a good species on which to base the modeling efforts. Atlantic croaker is widely distributed and common along the eastern coast of United States and in the Gulf of Mexico. Atlantic croaker also exhibits a complex life history that is typical of many marine fish species. After spending around a

month or more offshore, ocean larvae migrate into the estuary on ocean currents and settle in the marshes as estuarine larvae. For the next year, the estuary larvae grow in the estuary to become juveniles, and eventually migrate offshore to spend the next 8-12 years in the open ocean. The reproduction and larval physiology of the Atlantic croaker has also been studied extensively in the laboratory (Thomas and Khan, 1995; Faulk et al., 1999; McCarthy et al., 2003; Alvarez, 2005), and has been well monitored in long-term field sampling surveys (Diamond et al., 1999, 2000).

In this chapter, I use the IBM to scale the observed effects of maternally transferred polychlorinated biphenyls (PCBs) and methylmercury (MeHg) on larval croaker behavior (McCarthy et al., 2003; Alvarez, 2005) to larval stage duration and survival. PCBs have been shown to alter brain levels of dopamine and norepinephrine and affect locomotor activity in fish (Fingerman and Russell, 1980). In Atlantic croaker larva, PCBs have been shown to inhibit swimming speed, growth rate, and predator evasion skills (McCarthy et al., 2003). MeHg has been shown to reduce serotonin levels in the brain of fish, inhibit normal development of the hypothalamic serotonergic system (Tsai et al., 1995), and to affect locomotor activity and impair prey capture abilities (Smith and Weis, 1997). Specifically in croaker larvae, MeHg has been shown to affect locomotor activity and predatory evasion skills (Alvarez, 2005). Behavioral effects expressed as stage duration and survival help place these sublethal effects in an ecological context, and will be used in Chapter 5 to change parameter values of an Atlantic croaker population dynamics model.

4.2. Methods

4.2.1. Overview of Approach

I applied statistical models to the results from two laboratory studies that examined the effects of maternally-derived PCB and MeHg contamination on larval croaker behavior, and used the output of the statistical models as inputs to a larval stage IBM. The IBM was then used to determine the duration and survival of the larval stage under baseline (unexposed) and under PCB and MeHg exposed conditions. Laboratory studies have shown that maternally-derived contaminants can alter the behavior of larval fish (Faulk et al., 1999; McCarthy et al., 2003; Alvarez, 2005; Alvarez and Fuiman, 2005). The modeling analysis presented in this chapter is derived from an earlier modeling study that was done with preliminary data to demonstrate that the approach was feasible (Rose et al., 2003). The analyses have been expanded here to include two alternative statistical models, a more sophisticated imposition of the contaminant effects within the larval life stage, and an IBM that more realistically simulates the growth and mortality of the larval stage of Atlantic croaker.

4.2.2. Laboratory Studies

Two sets of laboratory experiments that examined how contaminants affect larval croaker survival skills were used in this analysis: PCB effects from a low-dose exposure (McCarthy et al., 2003) and MeHg effects from low and high dose exposures (Alvarez, 2005). Both sets of experiments used video-taping of individual larva to determine larval behavioral responses under control and contaminant-exposed conditions.

4.2.2.1. PCB Experiments

Laboratory experiments were conducted (McCarthy et al., 2003) to determine the effects of maternally-transferred PCBs on larval fish behavior. PCB-treated adult Atlantic croaker were fed ground shrimp containing Aroclor 1254 at a daily dose of 0.4 mg per kg of fish per day for 2 weeks, while control Atlantic croaker were fed regular ground shrimp. This was deemed the low dose exposure in McCarthy et al. (2003). This low dose resulted in Aroclor 1254 concentrations in treated fish of approximately 8250 ng per gram of dry weight of liver, which was a high concentration compared to concentrations in field-caught fish and close to the highest PCB concentrations measured in fish from contaminated sites (Rose et al., 2003). Female croaker transferred Aroclor 1254 into their eggs, resulting in concentrations in eggs of 3.2 ± 2.6 μg per gram of eggs or approximately 0.66 ± 0.54 ng per egg (McCarthy et al., 2003).

Eggs from control and PCB-treated fish were hatched in the laboratory and the developing larvae were used in behavior experiments that were designed to test larval survival skills. At days 5, 9 and 13 days after hatching, subsets of larval fish from control and PCB-exposed fish were removed from rearing tanks, their lengths measured for later determination of growth rates, and tested using a series of behavioral assays. Behavioral assays included using video-taping to measure swimming speed, percentage of time active, active swimming speed, and responsiveness to a vibratory startle stimulus (McCarthy et al., 2003). Results from the PCB experiments showed significant decreases in growth rates in PCB exposed fish compared to control fish (Fig. 4.1A). PCB exposed larvae also showed slightly slower, but not statistically significant, swimming speeds at day 13 (Fig. 4.1A). Other significant PCB effects manifested themselves at day 13,

including a reduced percent responding, decreased mean burst speed, and decreased maximum burst speed (McCarthy et al., 2003). The IBM, and associated statistical analyses I performed, utilized the measured PCB effects on growth rates, swimming speed, and vibrational response distance (summarized in Fig. 4.1A).

4.2.2.2. MeHg Experiments

The effects of MeHg on larval fish behavior were evaluated using two realistic doses of MeHg (Alvarez, 2005). Control adult Atlantic croaker were fed uncontaminated shrimp for one month, whereas low-dose treated Atlantic croaker were fed blue marlin for one month that had a concentration of 0.05 mg MeHg per kg in its muscle tissue. The high dose of MeHg was attained by feeding Atlantic croaker MeHg-treated blue marlin and MeHg contaminated shrimp for one month to attain a final dosage of 0.1mg MeHg per kg (Alvarez, 2005). The adults were spawned for both the low and high dose treatments, eggs were collected, and MeHg concentrations in eggs were measured. MeHg concentrations in eggs from the low and high dose treatments could be placed into seven distinct groups, ranging from 0.04 to 4.6 ng per g of spawned eggs. These MeHg concentrations were deemed to be environmentally realistic when compared to MeHg contaminated fish from the field (Alvarez, 2005). All eggs with MeHg burdens less than 0.05 ng per gram of spawned eggs were included in a control (unexposed fish) group. Concentrations of MeHg in eggs that fell between 0.05 and 1.0 ng per g of spawned eggs were put into what was termed a low dose MeHg group, and eggs with MeHg burdens greater than 1.0 ng per g of spawned eggs were grouped as into what was termed a high dose MeHg group (see Alvarez, 2005 for details).

After spawning, eggs from the control, low, and high MeHg dose treatments were hatched in the laboratory and evaluated for growth rates and survival skills (Alvarez, 2005). At days 1, 3, 6, 11, and 17 after hatching, larvae were removed from rearing tanks and their lengths were measured. Day 3 larvae had just completed yolk absorption and were labeled as "yolk" larvae. The oil globule had been completely absorbed by day 6, and these larvae were labeled as "oil" larvae. Day 11 and Day 17 larvae mark 4 and 11 days after oil absorption, subsequently these larvae were labeled "oil+4" and "oil+11."

Yolk, oil, oil+4 and oil+11 larvae from control, low dose, and high dose MeHg treatments were evaluated for routine behavior, such as swimming speed (mm/s), active swimming speed (mm/s), net-to-gross displacement ratio, and percent activity (Alvarez, 2005). The four age groupings of larval fish were also subjected to visual startle stimulus and vibratory startle stimulus. In these startle stimulus assays, Alvarez (2005) used video-taping to determine responsiveness, response distance (mm), response duration (s), average response speed (mm/s), maximum response speed (mm/s), and visual reactive distances (mm) for control, low dose, and high dose larvae. In these experiments, MeHg had no effect on growth rates, but resulted in significantly reduced swimming speeds for yolk and oil+4 ages (Fig. 4.1B). MeHg also significantly reduced the rate of active swimming speed of oil-aged larvae, and decreased the activity of yolk and oil+4 aged larvae (Alvarez, 2005). Other significant MeHg effects included increased visual startle responsiveness for oil+4 larvae, decreased vibrational response speed for yolk, oil+4, and oil+11 larvae, and increased vibrational response duration for oil+4 larvae. Visual reactive distances were slightly reduced in MeHg exposed yolk and oil+4 larvae and were slightly increased in MeHg exposed oil and oil+11 larvae, but the effects were not

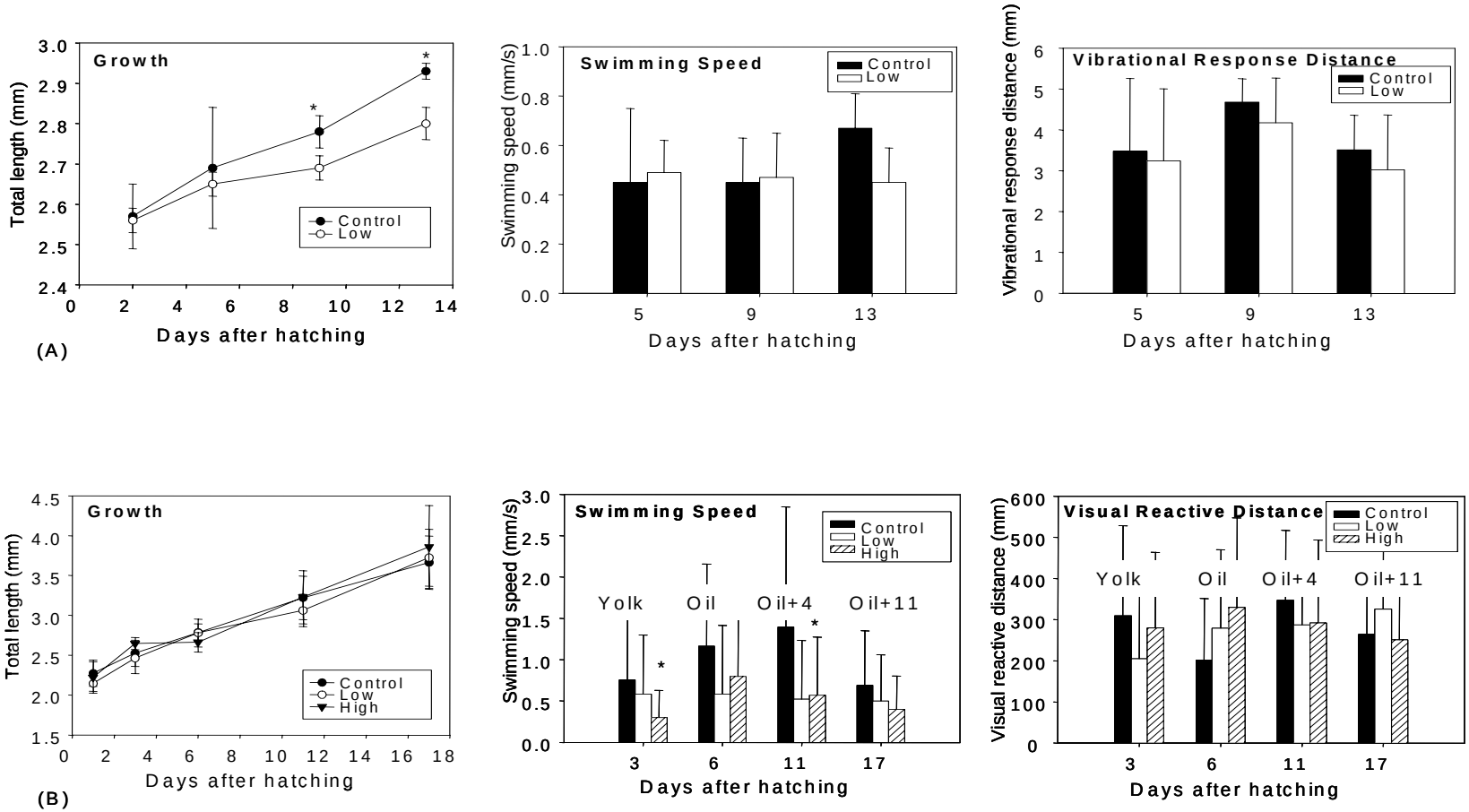

Figure 4.1. Laboratory results from PCB and MeHg experiments whose results are used in the model. (A) Results from control and low dose PCB exposure experiments on growth, swimming speed, and vibrational response distances (McCarthy et al., 2003), and (B) Results from control, low and high dose MeHg experiments on growth, swimming speed, and visual reactive distances (Alvarez, 2005). * = significantly different (P<0.05)

statistically significant (Fig. 4.1B). Data used in the IBM, and associated statistical analyses, included the MeHg effects on swimming speed and visual reactive distances (Fig. 4.1B).

4.2.3. Statistical Models

4.2.3.1. Statistical Modeling Overview

The laboratory studies provided measurements of swimming speeds and larval responses to startle stimuli for control and contaminant-exposed larvae, but the challenge was to convert these behaviors into ecologically relevant responses. Measurements of larval swimming speed under control and contaminant-exposed conditions could be directly inputted into an individual based model of larval fish behavior; swimming speed affects larval encounter rates with predators and prey. The other effects measured in the PCB and MeHg studies (e.g., responsiveness, reaction distances) are more difficult to directly relate to the predator-prey interactions simulated in the IBM. Therefore, I used the results of another laboratory study on red drum larvae (*Sciaenops ocellatus*) that measured both these sets of survival skills variables and the probability of the same larva actually avoiding a real predator (Fuiman et al., in press). I used two alternative statistical approaches (regression tree (RT) and a linear regression using logits (LRL)) to relate the measured values of the survival skills to the probability of escaping an attack from a real fish predator. Both approaches required standardizing the RT and LRL statistical models so that survival skills measured on croaker could be incorporated into the relationships determined from measurements based on red drum. I used two approaches to explore the importance of additional behaviors to the probability of

escaping a predator; LRL only used swimming speed as a predictor variable, and RT used other behavioral measures in addition to swimming speed as predictor variables.

4.2.3.2. Probability of Escaping a Fish Predator

The predation component of the individual-based model is based on the principle that the vulnerability of a larval fish (i.e. the probability of being consumed by a predator) can be viewed as the product of three component probabilities (Fuiman, 1989):

$$P(eaten) = P(encounter) \bullet P(attack \mid encounter) \bullet P(capture \mid attack)$$

where the bar indicates a conditional probability. The *P*(*encounter*) term is computed in the IBM using a modified Gerritsen-Strickler (1977) formulation to accommodate non-negligible larva prey size (Bailey and Batty, 1983; Cowan et al., 1996); the formulation uses predator and prey lengths, swimming speeds, and reactive distances to estimate encounter rates. The *P(attack | encounter)* term was specified as a constant in the IBM, and was arbitrarily assigned a value of 50%. The *P(capture | attack)* term is also calculated in the IBM using empirically derived formulas. The P(*capture | attack)* can be restated as the *P(escape)* = 1 - *P(capture | attack*). The laboratory experiment that examined both the survival skills and avoidance of predation by a fish predator was used to modify the *P(escape)* term in the IBM for control and contaminant exposure simulations.

The experiment used to relate survival skills to probability of escaping predation involved video-taping of red drum larvae to obtain values of their survival skills and then placing each larva in a tank with a real predator and recording the number of attacks and escapes (Fuiman and Cowan, 2003; Fuiman et al., in press). The survival skills measured

on the red drum were similar to those measured on Atlantic croaker in the PCB and MeHg experiments. *P(escape)* was calculated by dividing the number of times a larval red drum fish escaped by the number of times the larval fish was attacked by a fish predator. Using results measured on red drum for croaker was partially justified as they both belong to the same Sciaenidae family.

4.2.3.3. Use of a Regression Tree to Estimate Probability of Escape

To relate survival skills to the probability of escaping a predator, I modified a RT relationship previously developed from a study on red drum larva (Fig. 4.2A; Fuiman et al., in press). The advantage of RT analysis over regular regression technique is that it is not necessary to assume a linear relationship over the entire range of data (Breiman et al., 1998). Fuiman et al. (in press) fitted a RT to the data using *P(escape*), weighted by the number of attacks, as the response variable, and survival skills as the predictor variables (Fig. 4.2A). The specific predictor variables used included routine swimming speeds and the survival skills of visual and acoustic responsiveness to artificial predators; distance, duration, and speed of response to visual and acoustic stimuli; and visual reactive distance.

I modified the RT so that it could be applied to use the measured survival skills of croaker larvae under control and contaminant exposure experiments to predict how contaminants would affect a larva's probability of escaping a fish predator. To standardize the red drum RT, the variables used in the RT were analyzed for normality, and those variables that were not normal were transformed to fit a normal distribution. For the red drum data, the swimming speed was the only variable that failed to fit a normal distribution, and a simple log transformation was applied. The RT reported by

Fuiman et al. (in press) was then refit using the log-transformed swimming speed; the result was the same tree as before but with the swimming speed node splitting on a different value. The split-values for each node were then converted to a z-score from a normal distribution using the following formula: $\left(\hat{Y} - \bar{Y} \right) / sd$ (Fig. 4.2B).

To use the RT model developed for red drum to predict the effects of MeHg on the probability of a croaker larva escaping a predator involved first transforming the measured croaker survival skills required by the RT to fit a normal distribution, and then calculation of z-scores for each survival skill. Swimming speed was square root transformed, and visual reactive distance was transformed using a Box-Cox transformation with λ of 0.4 (SAS Institute Inc., 2002). The transformed values were converted to z-scores using the mean and standard deviation from the transformed control data for swimming speed and visual reactive distance. Probabilities of escape were predicted from survival skills of larvae for each age grouping (yolk, oil, oil+4, and oil+11) separately for control, low dose, and high dose MeHg exposures.

The effects of PCBs on a larvae's probability of escaping a predator was determined by first calculating z-scores for control and PCB-exposed larvae (by age grouping) for the survival skills of swimming speed and a substitute skill for visual reactive distance. A substitute survival skill was needed for the visual reactive distance used in the RT because it was not measured in the PCB experiments. I used the distance traveled in response to a vibratory stimulus as a substitute for visual reactive distance. Analysis of the MeHg data showed a significant, albeit weak, correlation between normalized visual reactive distance and normalized distance traveled in response

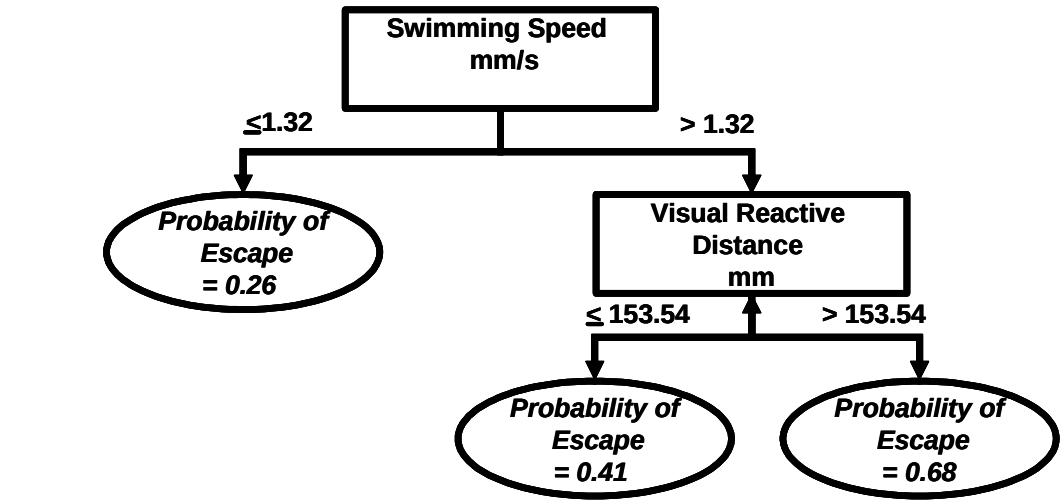

(A)

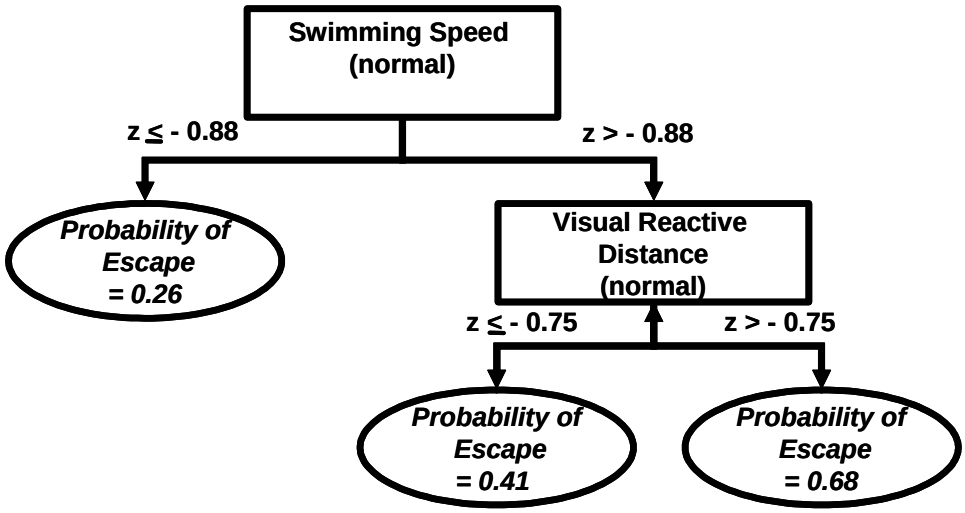

(B)

Figure 4.2. Regression tree relating the probability of escaping a real predatory fish attack to the swimming speed and visual reactive distance. (A) Regression tree developed for red-drum (Fuiman et al., in press), and (B) Regression tree adjusted to use z-scores.

to a vibratory stimulus (r = 0.076, *P*=0.0185). Swimming speed and distance traveled in response to a vibratory stimulus were converted to z-scores using the mean and standard deviation from the control group for each age grouping. Probabilities of escape were predicted for larvae by age grouping (day 5, 9, and 13) for control and low-dose PCB exposure.

4.2.3.4. Use of Linear Regression using Logits to Estimate Probability of Escape

As an alternative to the RT analysis, I also analyzed the same red-drum-laboratory experiment using LRL to relate the probability of escaping a predator attack to the single predator variable of swimming speed. The swimming-speed variable was measured in all three (red drum, PCB, MeHG) experiments, and was an important variable in the regression-tree analysis (Fig. 4.2). The red drum data was used to initially create the LRL model because the dataset included the measurements of swimming speed and *P(escape)* on the same larvae. The *P(escape)* was linearized using a logit transformation: $\pi_i = \ln(P_i/(1-P_i))$, where π_i is the logit, and P_i is the *P(escape)*. When P_i is equal to 0 or 1, then the logit transformation is undefined, and in those instances, P_i was modified so that: $P_i = 1/10 \cdot$attacks, when $P_i = 0$, and $P_i = 1\text{-}1/10 \cdot$attacks, when $P_i = 1$. The number of attacks was multiplied by 10, instead of 2, as has been reported for other models (e.g., Bessin et al., 1990), because the number of attacks was generally a very low number, and multiplying by 2 failed to produce a significant model. I then applied a linear regression to the logits with swimming speed as the predictor variable (SAS Institute Inc, 2002). I did not apply a weighted least-squares regression to the logit transformed data, as is commonly applied to logit regressions to correct for nonconstant variance, because non-weighted least squares regression produced the most normally distributed residuals.

To apply the LRL model fitted to red drum data to croaker larvae, the swimming speed measured for croaker larvae in the MeHg and PCB experiments had to be scaled to match the swimming speed of red drum used in the LRL model. The swimming speeds reported for red drum were fit to a lognormal distribution (mean = 8.96, sd = 17.90), with a scale parameter of 1.39 and a shape parameter of 1.27. I then fit the swimming speeds of croaker from the controls of the PCB and MeHg experiments to lognormal distributions. I scaled each swimming speed reported for each age grouping for the MeHg and PCB experiments by first multiplying each swimming speed by a constant that would make the shape parameter match that of red drum (1.27), and then adding a constant to make the scale parameter match that for red drum (1.39). The scaled swimming speeds were used in the LRL, and the resulting logits were converted into the probability of escaping a predator using the following formula: $1/(1+e^{-\pi i})$. Probabilities of escaping a predator were predicted for each age grouping (yolk, oil, oil+4, and oil+11) for the control, low dose, and high dose MeHg exposed larvae, and for each age grouping (days 5, 9, and 13) for the control and low dose PCB exposed larvae.

4.2.3.5. Multipliers for Individual Based Model

Swimming speed and the probability of escaping a predator (predicted by the RT or LRL model) were converted into multipliers for use in the IBM. First, in an effort to make the control groups from the MeHg and PCB experiments result in similar IBM-predicted larval stage growth and mortality rates, I squared the swimming speed for larvae in the control and low dose PCB experiment. This resulted in swimming speed values of the controls group from the PCB experiment being very similar to the swimming speed from the MeHg control group (Table 4.3). I modified the swimming

speed of the PCB experiment because the MeHg experiment had larger sample sizes. Second, each swimming speed value was divided by the mean swimming speed of the control larvae from each age grouping. The same procedure was applied to probability of escape values, resulting in multipliers for swimming speed and probability of escape for each of the four age groupings in the control, low dose, and high dose MeHg experiment and for each of the three age groupings in the control and low dose PCB experiment.

The swimming speed and probability of escaping multipliers were used with the IBM. For the MeHg simulations (control, low dose, and high dose) and the PCB simulations (control and low dose), each larval fish in the simulation was assigned a multiplier for swimming speed and a multiplier for probability of escaping a fish predator initially and then was randomly assigned new values as the larva entered subsequent age groupings. Multipliers were randomly assigned to model larvae from the appropriate pool of measured larval values (i.e., same exposure and age grouping).

4.2.4. Individual Based Model

4.2.4.1. Individual Based Modeling Overview

I configured an individual-based model (IBM) to track daily growth and mortality of Atlantic croaker larvae as larvae grow from 2.5 mm to 11 mm (Fig. 4.3), and used the model, with the swimming speed and probability of escape multipliers, to determine how PCB and MeHg exposure affect larval stage duration and survival. The parameter values used in the IBM were derived from laboratory and field data, and the IBM was assumed to represent larval dynamics typical of the mid-Atlantic Bight (MAB) and the Gulf of Mexico (GOM). The 2.5 to 11.0 mm size interval corresponds with the ocean-larva stage

of development for croaker (Diamond et al., 1999, 2000). The model was coded in Fortran90.

The model begins with 10,000 individual larval fish. Each day, for 150 days, individual larvae encounter prey (invertebrate eggs, nauplii, copepodites and adult copepods) and predators (medusa, ctenophores and fish) in a 20,000 m^3 well-mixed volume of water. The volume was chosen to simulate realistic densities of Atlantic croaker ocean larvae (Morse, 1989). Daily growth of larvae was simulated using a bioenergetics model with terms for consumption, assimilation, metabolism, egestion, and specific dynamic action. Daily consumption was determined by simulating encounter rates of larva with zooplankton prey. Larval are assumed to be too dilute to affect their prey densities (i.e., model was density-independent). Starvation mortality occurred if the condition of larva was below a threshold value. Mortality due to predation was determined by simulating larval vulnerability to predators based on encounters and captures with the three common predators of fish larvae. Swimming speed influenced growth rate (via affecting encounters with prey) and predation mortality (via encounters with predators); probability of escape influenced predation mortality only. The multipliers of swimming speed and probability of escaping a predator, obtained from the RT and LRL regression analysis, were used to simulate the effects of MeHg and PCB exposure on ocean larval stage duration and survival.

4.2.4.2. Growth

The growth component of the IBM was a foraging and bioenergetics model adapted from the model described in Letcher et al. (1996) and later modified by Rose et al. (2003). For temperature-dependent processes, I assumed that the ocean larvae in the

Mid-Atlantic Bight would experience 15 °C temperature (Stegmann et al., 1999). Gulf of Mexico ocean larvae would experience temperatures 5-10 °C warmer than MAB larvae (Seamap, 2001, 2002). The same model formulation was used to simulate both the MAB and GOM populations.

Table 4.1. Length (mm), weight (μg), density (number/mL) for each of the four zooplankton prey types used in the IBM.

Prey Type	Prey Number	Length (mm)	Mass (μg dry)	Density (number/mL)
Invertebrate Eggs	1	0.11	0.250	0.3
Nauplius	2	0.25	0.282	0.08
Copepodite	3	0.5	1.410	0.008
Copepod	4	1.0	7.700	0.0008

Stage survival and stage duration for Mid Atlantic Bight ocean larvae is approximately 0.9 % and ranges from 31-44 days, while stage survival for GOM larvae is approximately 1.7% and stage duration is estimated to be 46 days (Diamond et al., in prep; Chapter 5).

The bioenergetics model simulates the daily change in weight of an individual larva based on assimilation efficiency, ingestion, metabolic costs, and egestion:

(4.1) $\Delta W = W_{t+1} - W_t = A \cdot I - M - E$

where A is the assimilation efficiency, I is ingestion (μg/day), M is total metabolic cost (μg/day), egestion and specific dynamic action were combined in the term E, and E was

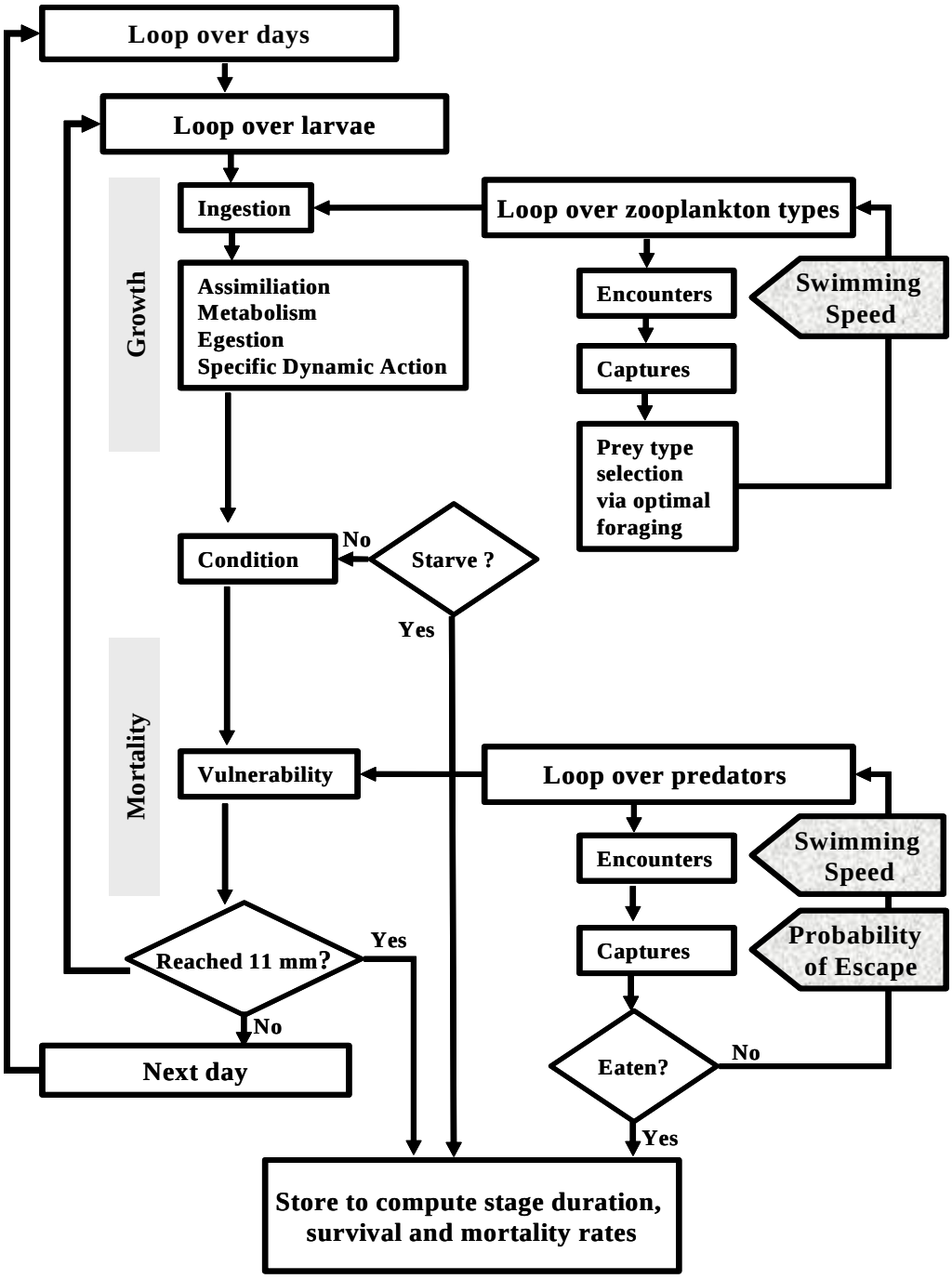

Figure 4.3. Schematic diagram of the individual-based model larval cohort model. The IBM simulates the daily growth and mortality of ocean larvae as they grow from 2.5 mm to 11 mm. Growth is based on bioenergetics principles, with ingestion dependent on encounter rates of larvae with three types of zooplankton. Mortality was based on the encounter and capture of larvae by sea nettles, ctenophores and predatory fish. PCBs and MeHg influenced larval swimming speed, which affected encounter rates of larvae with zooplankton and with predators, and influenced the probability of escaping a predatory fish attack (After Rose et al., 2003)

assumed to be 30% of ingestion: $E = 0.3*I$ (μg/day). Equation (4.1) was solved as a difference equation with a time step of one day. Each day, weight was converted to length for each larva using a length-weight relationship:

(4.2) $$Weight = 0.1674\, length^{3.837}$$

The length of the larva was updated if the weight gain was positive and the larva had reached at least the average weight expected for its length.

Assimilation efficiency was a function of fish mass. I lowered the assimilation efficiency maximum from Letcher et al. (1996) because croaker grew much slower than the generic marine larval fish simulated in the original Letcher et al. model.

(4.3) $$A = 0.6(1 - 0.25e^{-0.002(Mass-10)})$$

Total metabolic cost (M) included routine metabolism and activity metabolism. Total metabolism was defined as a function of larval fish mass:

(4.4) $$M = \frac{4500 \cdot Mass}{45000 + Mass} + 2.5\left(\frac{4500 \cdot Mass}{45000 + Mass}\right) Light$$

where *Light* is the number of hours of daylight (assumed to be 13).

4.2.4.3. Foraging and Ingestion

The ingestion term of the bioenergetics equation (I in equation 4.1) was determined by simulating the foraging of a larva and its encounters, captures, and diet selection with four types of zooplankton prey. The four prey types were: invertebrate eggs, nauplii, copepodites, and adult copepods (Table 4.1). All four prey items were found in stomachs of larval Atlantic croaker shorter than 10 mm (Govoni et al., 1986). Length and mass of nauplii, copepodites, and copepods were estimated from information reported in Letcher et al. (1996); nauplii and copepodite sizes were used directly, while I

used the length and mass corresponding to a larger 1.0 mm copepod. I used larger copepods than Letcher et al. (1996) because larval Atlantic croaker consumed larger zooplankton than most marine larvae (Govoni et al., 1986; Rose et al., 2003). Invertebrate eggs were included as a prey type because they were found in the stomachs of larvae Atlantic croaker (Govoni et al., 1983; Govoni et al., 1986). The length and weight of invertebrate eggs were roughly estimated from copepod eggs (Kiorboe and Sabatini, 1994). Relative order of magnitudes for the densities of the prey types were estimated from plankton surveys conducted offshore in the Gulf of Mexico (Al-Yimani, 1988) and in the mid Atlantic Bight (Kane, 2003); the actual values were adjusted within their reported ranges to yield appropriate larval growth rates (Table 4.1).

Encounter rates with each individual prey type (number of encounters in 13 hours), was a product of the search volume (SV, mm^3/sec), density of prey type (ρ, Table 4.1), conversion factor to convert mL to mm^3 (0.001), and the number of seconds of daylight in one day (46,800.0).

(4.5) $ER_{preytype} = SV \cdot \rho \cdot 0.001 \cdot 46800.0$

Search volume for each larval fish was a product of the swimming speed of the larval fish (SS, mm/s), and the reactive area (RA, mm^2).

(4.6) $SV = SS \cdot RA$

Swimming speed was dependent on length of the fish, and averaged about 1 body length/s (Miller 1988).

(4.7) $SS = 0.776\, length^{1.07}$

The reactive area for the larval fish was a half circle (0.5) with radius equal to the reactive distance (RD, mm) defined for each prey type.

(4.8) $RA = (RD_{preytype})^2 \cdot \pi \cdot 0.5$

Reactive distance for each prey type was defined as a function of the length of prey and larval length (Breck and Gitter, 1983). The reactive distance for each prey type is defined by the length of the prey type (mm, Table 4.1), divided by twice the tangent of one-half the angle of acuity (degrees).

(4.9) $$RD = \frac{L_{preytype}}{2 \cdot \tan(\frac{\alpha}{2})}$$

The angle of acuity is calculated using the length of the larval fish.

(4.10) $\alpha = (0.0167 \cdot e^{9.14 - 2.4 \cdot \ln(length) + 0.229 \cdot (\ln(length))^2})$

Finally, realized encounter rates *($ER_{realized}$)* were calculated as deviates from a Poisson random distribution with mean and variance equal to $ER_{preytype}$. Encounter rates were computed daily between a larva and each of the four zooplankton prey types.

Once given prey were determined to be encountered ($ER_{realized}$), the next step was to determine which of the encountered prey were also captured. I altered the capture success function of Letcher et al. (1996) to allow croaker to capture larger prey items at smaller sizes (Govoni et al., 1986; Rose et al., 2003). Atlantic croaker larvae consume copepods until croaker reach approximately 10 mm in length, and then shift to much larger mysids at lengths greater than 10 mm (Govoni et al., 1983, Govoni et al., 1986; Soto et al., 1998). The modified capture success (*CS*) functions (Fig. 4.4) resulted in realistic diet shifts to larger prey with increasing larval size. Capture success was used in the diet selection algorithm and then also used to determine how many of the encountered prey were successful captured.

The final step in going from encounters to actual ingestion was to use a diet selection algorithm to determine which of the encountered and captured prey types were ingested. I used an optimal foraging algorithm developed for marine larval fish (Letcher et al., 1996) to determine diet selection. Optimal foraging operates on the principle that larva select the most profitable prey items out of all prey items encountered. The most profitable prey items are those that render the most energy, when handling time and capture success of particular prey items are taken into consideration.

For each larva on each day, handling time and capture success were calculated for each prey type and used to determine which prey types were actually consumed. Handling time of each prey type (Walton et al., 1992) depended on prey and larval lengths:

$$HT_{preytype} = e^{0.264 \cdot 10^{7.0151(\mathrm{Pr}\, eylength\, /\, larvallength)}} \quad (4.11)$$

Prey types were then ranked using the following relationship:

$$\frac{Mass_{preytype} \cdot CS_{preytype}}{HT_{preytype}} \quad (4.12)$$

Prey items that provided the greatest mass per unit of time required to ingest a single prey item received the highest rank (Letcher et al., 1996). Once prey items were ranked, each ranked prey was assigned a profitability score based on a benefit-cost ratio:

$$\frac{Energy_{preytype}}{Time_{preytpe}} = \frac{\sum_{preytype} Mass_{preytype} \cdot ER(\mathrm{Re}\, alized)_{preytype} \cdot CS_{preytype}}{1 + \sum_{preytype} ER(\mathrm{Re}\, alized)_{preytype} \cdot HT_{preytype}} \quad (4.13)$$

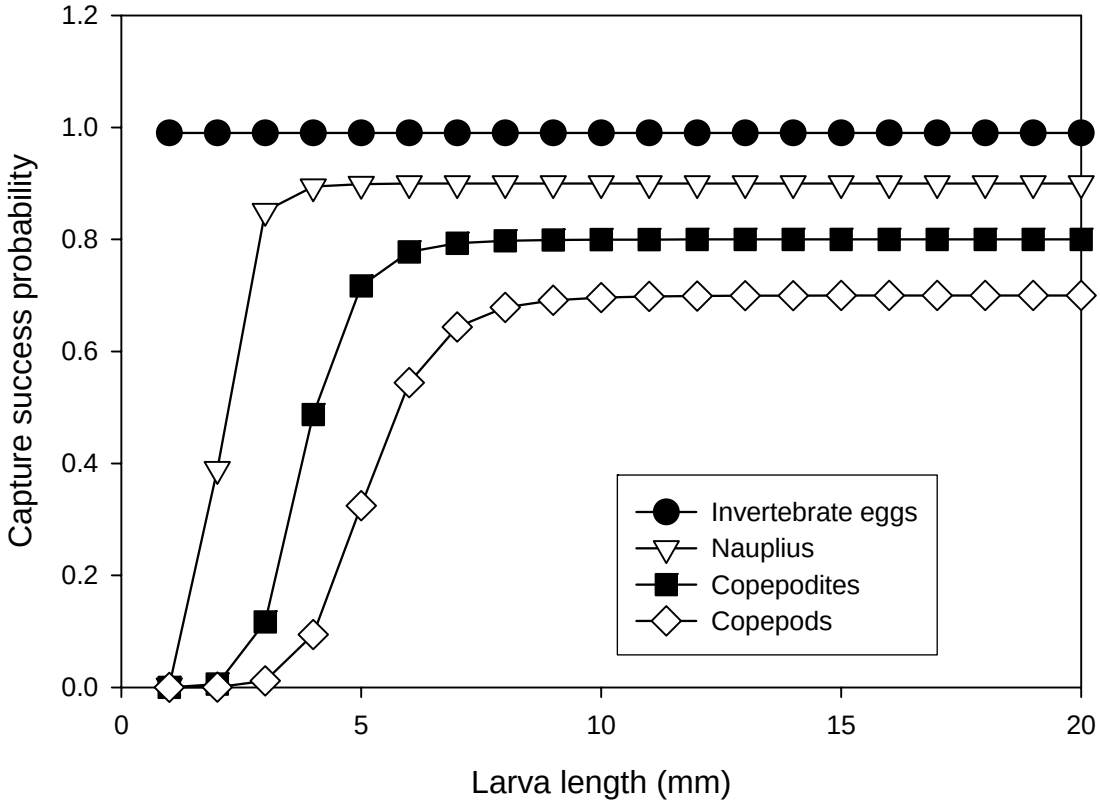

Figure 4.4. Capture success as a function of fish length for Atlantic croaker larvae feeding on different prey items in the IBM.

Profitability was essentially the ratio of energy consumed of each prey type divided by the time required for handling those prey. The diet of an individual larval fish on a given day was determined by including prey types sequentially through their ranked ordering based on mass per unit time until profitability began to decrease, after which prey types with lower profitability were not ingested.

Daily ingestion was computed from the realized number of prey encountered and capture success for those prey types determined by the diet selection algorithm to be included in the diet. The number of prey actually ingested was determined by generating a random deviate from a binomial distribution, with number of trials equal to the realized

encounter rate per day ($ER_{realized}$) and with probability of success equal to capture success (CS). Ingestion was the sum of the number of prey actually ingested, times their weight, for all of the prey types included in the diet, up to a maximum consumption rate. The maximum daily consumption was related to the weight of the larval fish:

(4.14) $$C_{\max} = 2.8275 \cdot Mass_{larvae}^{0.8496}$$

4.2.4.4. Starvation

Starvation mortality occurred when a larva lost too much weight. I simulated this by keeping track of each larva's maximum weight, and when a larva's weight on subsequent days went to less than 25% of its maximum weight, the larva was assumed to die from starvation. I used the same algorithm as Letcher et al. (1996) to adjust weight loss when a larva was feeding at less than maintenance levels to reflect lowered metabolism (Wiesser et al., 1992; Letcher et al., 1996, Kiorboe et al., 1997). The algorithm was based on starvation occurring after a desired number of days of no feeding (i.e., point of no return). Atlantic croaker ocean larvae exhibit slower growth rates than assumed in the Letcher et al. (1996) model. Thus, I used a relatively low 25% threshold for starvation and a weight loss algorithm tuned to allow a size-dependent estimate of days of no feeding before starvation.

4.2.4.5. Mortality by Predation

Mortality by predation occurred when larvae were encountered and captured by individuals of three common predators types: ctenophores, jellyfish medusae, and predatory fish (Cowan et al., 1996; Rose et al., 2003). Mean lengths and diameters of the three types of predators were taken from a previous model that examined the effects of larval size on larval vulnerability to predation (Table 4.2; Cowan et al., 1996). Lengths

were randomly assigned to each individual of a predator type from a normal distribution with the appropriate mean and standard deviation for that predator type. I lowered the assumed predator densities and increased the density of medusae relative to ctenophores from the densities used by Cowan et al. (1996) for their Chesapeake Bay application. Predators are generally found in lower densities in offshore environments (e.g., SEAMAP, 2001, 2002; Suchman and Brodeur, 2005), and offshore trawls in the GOM during late fall and early winter indicated that medusae were at higher concentrations than ctenophores (Seamap 2001, 2002). The final predator densities used in simulations were roughly calibrated to produce appropriate mortality rates estimated for Atlantic croaker ocean larva (i.e., stage survival of 0.9-1.7%; Diamond et al., 1999, 2000). The final predator numbers in the 20,000 m^3 volume were 255 medusae, 100 ctenophores and 30 individual juvenile fish.

The encounter rate of each larval fish with each individual predator was computed based on larval and predator lengths and swimming speeds. I used the equations reported in Cowan et al. (1996), which were a modification of the Gerritson-Strickler formulation (Gerritson and Strickler, 1977). On each day of the simulation, the model calculated the encounter rate of a larva with each individual of the three predator types (Table 4.2):

$$(4.15)\quad ER_{predatortype} = \pi(R_L + R_P)^2 C(10^{-9}/V)$$

where ER is the encounter rate of a larva with an individual predator (number of encounters/24 hours), R_L is the encounter radius of larva (mm), R_P is the encounter radius of the predator (mm), C is the foraging rate (mm/sec), and V is the volume of water modeled in the simulation (20000 m^3). The encounter radius of larva was computed as:

$$(4.16)\ R_L = \frac{2L_l}{\pi^2}$$

where L_l is the length of larva (mm). The encounter radius of each predator type was derived from empirical studies (Table 4.2). The foraging rate (C) was determined as:

$$(4.17) \quad C = \begin{cases} \dfrac{D_L^2 + 3D_P^2}{3D_P} & \text{if } D_P \rangle D_L \end{cases}$$

$$C = \begin{cases} \dfrac{D_P^2 + 3D_L^2}{3D_L} & \text{if } D_P \langle D_L \end{cases}$$

where D_L is the distance swum in a day by a larval fish (mm) and D_P is the distance swum in a day by a predator (mm). The distance swum in a day by a larval fish was calculated by:

$$(4.18) \quad D_L = SS \cdot 46800.0$$

where 46800 is equal to the number of seconds in 13 hours; larval fish assumed to be active only during the day, and SS is the swimming speed of the larval fish (mm/sec). The calculation of D_P depended upon the swimming speeds of predators, which in turn depended upon the lengths for each of the three predator types (Table 4.2). Predators were assumed to be active for all 24 hours in a day.

Realized number of encounters a larva with an individual predator was generated as a random deviate from a Poisson distribution. The number of realized encounters that were successful was then randomly drawn from a binomial distribution with the probability of success equal to the capture success for that predator type. Capture success for each predator type was determined using empirically derived formulas based on larval and predator lengths (Table 4.2). On each day, each larva's encounters and potential capture was evaluated for all of the individual predators. If a larva was successfully encountered and captured by any of the individual predators of any of the three predator types, that larva was considered eaten and was removed from the simulation.

4.2.5. Contaminant Effects on IBM-Simulated Growth and Mortality

Three contaminant effects were simulated in the IBM: reduced growth due to PCBs affecting metabolism, altered multipliers of swimming speed, and altered multipliers of probability of escaping a fish predator attack.

Laboratory studies showed that PCBs, but not MeHg, affected the growth rate of larval fish (Fig. 4.1). I assumed that the PCBs were causing a disruption in metabolic processes over and above how altered swimming speeds affected growth. I adjusted metabolism in the model based on the relative difference in growth rates observed between control and PCB exposed fish reared in the laboratory (McCarthy et al., 2003). Using growth equations derived by McCarthy et al. (2003), I calculated that after 13 days, a low-dose PCB exposed larva would be 2.804 mm in length compared to 2.954 mm in control conditions, or a 5% reduction in length. To determine the magnitude of the metabolic cost, I repeatedly ran the IBM without predators (to mimic laboratory conditions) until the forced increase in daily metabolism resulted in the desired increase in stage duration corresponding to a 5% reduction in growth rate (45.4 days to 48.2 days). The determined value of 6.9% decrease in change in weight was imposed for the low dose PCB simulations.

The multipliers of swimming speed and the multipliers of probability of escape were imposed for the control, low dose, and high dose MeHg conditions, and for the control and low dose PCB conditions. Larvae received a new set of multipliers on the day they entered each age grouping (yolk, oil, oil+4, oil+11 for MeHg; days 3, 7, and 11 for PCB). The swimming speed of each larva (*SS* in equations 4.7 and 4.18) was adjusted by being multiplied by the multiplier of the swimming speed. This affected the larva's

encounter rates with each zooplankton prey (equation 4.7) and with each of its predators (equation 4.18). The probability of a larva escaping an encounter with a fish predator was adjusted by first converting probability of capture to probability of escape (escape = 1-capture), multiplying by the multiplier of the probability of escape, and then recomputing probability of capture for encounters with individual fish predators. Multipliers were applied to fish predator only because the red drum laboratory study only examined fish predators.

4.2.6. Simulations

Four sets of model simulations (involving 17 different conditions) were performed to explore the effects of contaminants on ocean larval stage duration and survival (Table 4.3). The first set of simulations explored baseline conditions and involved four conditions. Baseline simulations (conditions 1-4) were the four combinations of swimming speed and probability of escape multipliers from the PCB and MeHg controls with the probability of escape multipliers either predicted by the RT or LRL statistical models.

The second set of simulations explored the effects of low dose PCB exposure and involved six conditions (Table 4.3). All of the PCB simulations used multipliers derived from low-dose PCB experiment. Conditions 5 and 6 used probability of escape multipliers from the RT or LRL analyses, with both conditions including the extra metabolic costs due to PCB exposure. Condition 7 was the same as condition 6 but without the imposition of the extra metabolic costs. Conditions 8 and 9 investigated whether the predicted response to PCB exposure were due to growth or predation

Table 4.2. Lengths (mm), distance swum (mm/day; Cowan and Houde, 1992), encounter radius (mm; Cowan and Houde, 1992) and realized capture probability (Adamack, 2003) of the three predator types (ctenophores, medusae and predatory fish) used in the IBM. L_C is the length of ctenophore predator, L_M is the diameter of medusae predator, and L_P is the length of predatory fish. L_L is the total length of larval prey in mm. 86400 is the number of seconds in a day.

Predator type	Length/Diameter mean ± s.d (mm) Min/Max (mm)	Distance swum (D_P) (mm/day)	Encounter radius (R_P) (mm)	Realized Capture Probability
Ctenophore	45.0 ± 10.0 30.0/60.0	$0.025L_C \cdot 86400$	$0.33L_C$	$0.813 - 4.416\frac{L_L}{L_C}$
Medusa	75.0 ± 10.0 60.0/90.0	$(1.2 + 0.04L_M) \cdot 86400$	$0.5L_M$	$0.505 + 4.653\frac{L_L}{L_M} - 66.215\left(\frac{L_L}{L_M}\right)^2 + 155.377\left(\frac{L_L}{L_M}\right)^3$
Predatory fish	35.0 ± 5.0 25.0/45.0	$3.0L_P \cdot 86400$	$0.8L_P$	$0.029 + 0.015L_L - 0.003\ L_L^2 + 0.0001\ L_L^3$

mortality effects. LRL predicted probabilities of escape and no extra metabolic costs were used in both conditions. Condition 8 had the PCB-derived swimming speed multipliers only affect larva encounters with zooplankton; control-derived multipliers of swimming speed and probability of escape were used to simulate encounters with predators. Condition 9 had the PCB-derived swimming speed and probability of escape multipliers affect larva encounters with their predators; control multipliers of swimming speed were used to affect larva encounters with zooplankton.

The third and fourth sets of simulations involved predicting the effects of the low and high dose MeHg exposures (Table 4.3). Conditions 10 and 11 explored the results of low dose MeHg exposure and used multipliers of probability of escape from the RT or LRL. As was done with the low dose PCB exposure, two additional simulations (conditions 12 and 13) were performed using multipliers of probability of escape from the LRL with multiplier effects imposed for growth only and for predation mortality only. The same four conditions were simulated for the low dose MeHg exposure were repeated but using the multipliers derived from the high dose MeHg exposure (conditions 14-17).

Three replicate simulations that used different random number sequences were performed for each of the 17 conditions. Model predictions were very similar among the three replicate simulations for each condition simulated. Predicted larval stage survival (%) and duration (days) are presented as the average of the three replicates for all 17 conditions. For clarity in some tables and figures, I show results for one of the replicate simulations. Baseline results are shown in more detail than the other conditions to illustrate several auxiliary outputs of the model besides stage duration and survival (e.g., diets, length frequency histograms through time, mean lengths of live and dead larvae).

Because of the high variance in larval lengths at snapshots during the simulation, larvae ranging in length from 3 to 10 mm were present on some days during the simulation. I therefore summarized some information (diets, mean growth rates, and mean mortality rates) based on larval length. To help understand the different effects of PCBs and MeHg on stage duration, I present numbers entering, growth rates, percent starving, and percent eaten by age groupings.

Table 4.3. Features of the 17 different conditions simulated using the IBM under control, low dose PCB, low dose MeHg, and high dose MeHg exposures, with two sources of control multipliers (PCB or MeHg), two sources of multiplier estimates (regression tree (RT) or linear regression using logits (LRL)), whether growth (G), predation (P), or both processes are affected by the multipliers, and whether the added metabolic costs of PCB exposure are included. NA means not applicable.

Number	Simulation	Source of Multipliers	Statistical source for multipliers of probability of escape	Processes affected by multipliers	Extra metabolic costs of PCBs
1	Baseline	PCB control	RT	Both	NA
2			LRL	Both	NA
3		MeHg control	RT	Both	NA
4			LRL	Both	NA
5	Low dose PCB	Low dose PCB	RT	Both	Yes
6			LRL	Both	Yes
7			LRL	Both	No
8			LRL	P only	No
9			LRL	G only	No
10	Low dose MeHg	Low dose MeHg	RT	Both	NA
11			LRL	Both	NA
12			LRL	P only	NA
13			LRL	G only	NA
14	High dose MeHg	High dose MeHg	RT	Both	NA
15			LRL	Both	NA
16			LRL	P only	NA
17			LRL	G only	NA

4.3. Results

4.3.1. Statistical Models

4.3.1.1. Regression Tree Analyses

RT analysis of the low dose PCB exposure larvae suggested that maternal exposure to PCBs caused a decrease in the probability of escape that was largest for older larvae. Predicted probability of escape was similar between control and low dose exposed larvae at day 5, and was lower at day 7 (mean of 0.51 in control versus 0.44 in exposed) and at day 13 (0.56 versus 0.42) (Fig. 4.5). Associated with this decrease in probability of escape, were shorter vibrational reactive distances for day 7 and 13 larvae (Fig. 4.1), and slower swimming speeds for day 13 larvae (Fig. 4.5). The predicted decrease in probability of escape with older larvae was due to a combination of PCB caused changes in swimming speed and in vibrational response distance.

RT predicted probabilities of escape for MeHg-exposed larvae showed little clear dependence on the MeHg dose. Similar to the PCB analysis, the RT analysis on MeHg-exposed larval fish integrated the effects of MeHg on the swimming speed and on visual reactive distance, but because these did not vary consistently together, no obvious pattern in probability of escape related to MeHg dose was predicted (Fig. 4.6). Swimming speed was slowed in the low and high dose exposures relative to control swimming speeds (Fig. 4.6). However, visual reactive distances varied such that the probability of escape was roughly similar for yolk age larvae for all treatments, and slightly lower for oil and oil +4 age larvae for both low and high MeHg treatments. The oil+11 larvae were the only group that showed the lowest survival probability at the highest dose of MeHg (Fig.4.6).

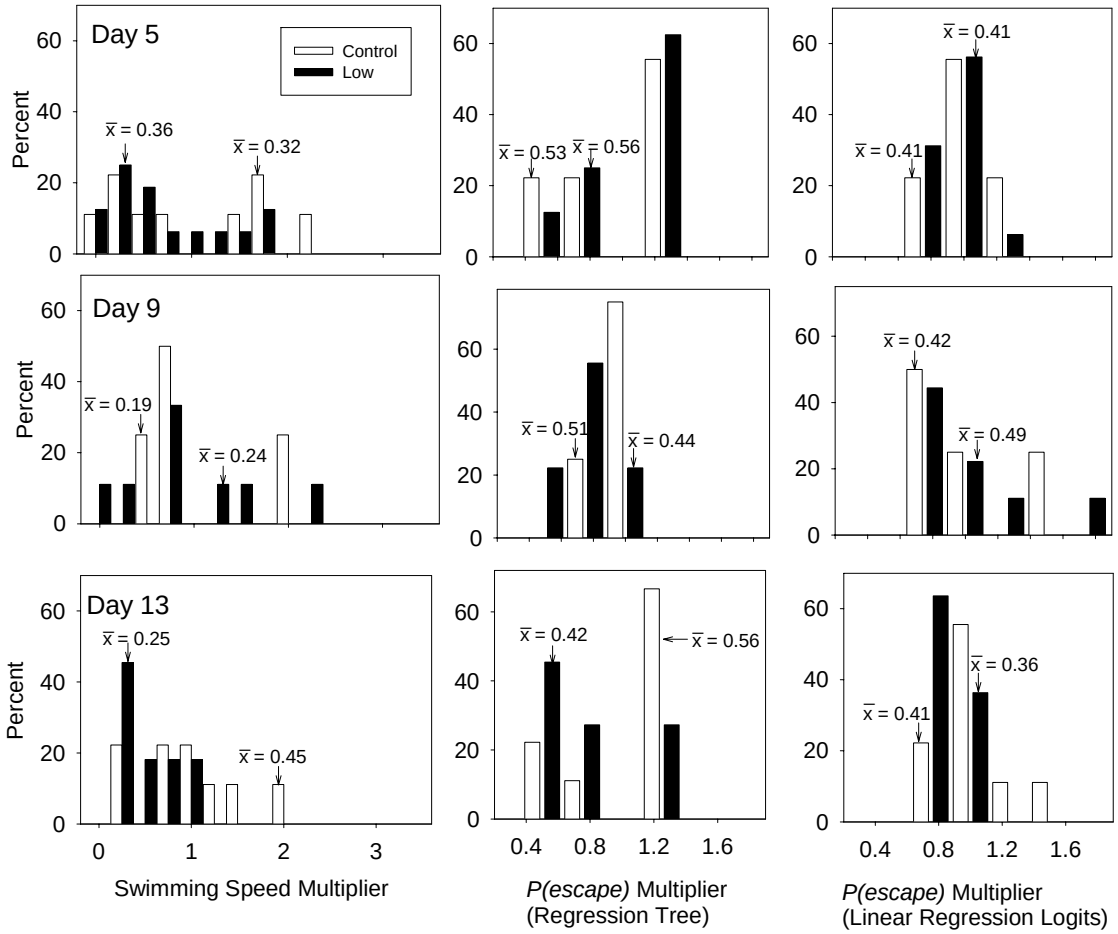

Figure 4.5. Mean values of swimming speed (mm/s) and probability of escape and frequency histograms of multipliers for control and low-dose PCB treatments that were used in the IBM. The probability of escape multipliers were derived via regression tree or linear regression using logits analyses. Multipliers were created by dividing each swimming speed and probability of escape value for every age (Day 5, 9 and 13), treatment and statistical analysis by the mean of the swimming speed or probability of escape for every age, treatment and statistical analysis. Arrows indicate the treatment group for the mean swimming speed and probability of escape for each age

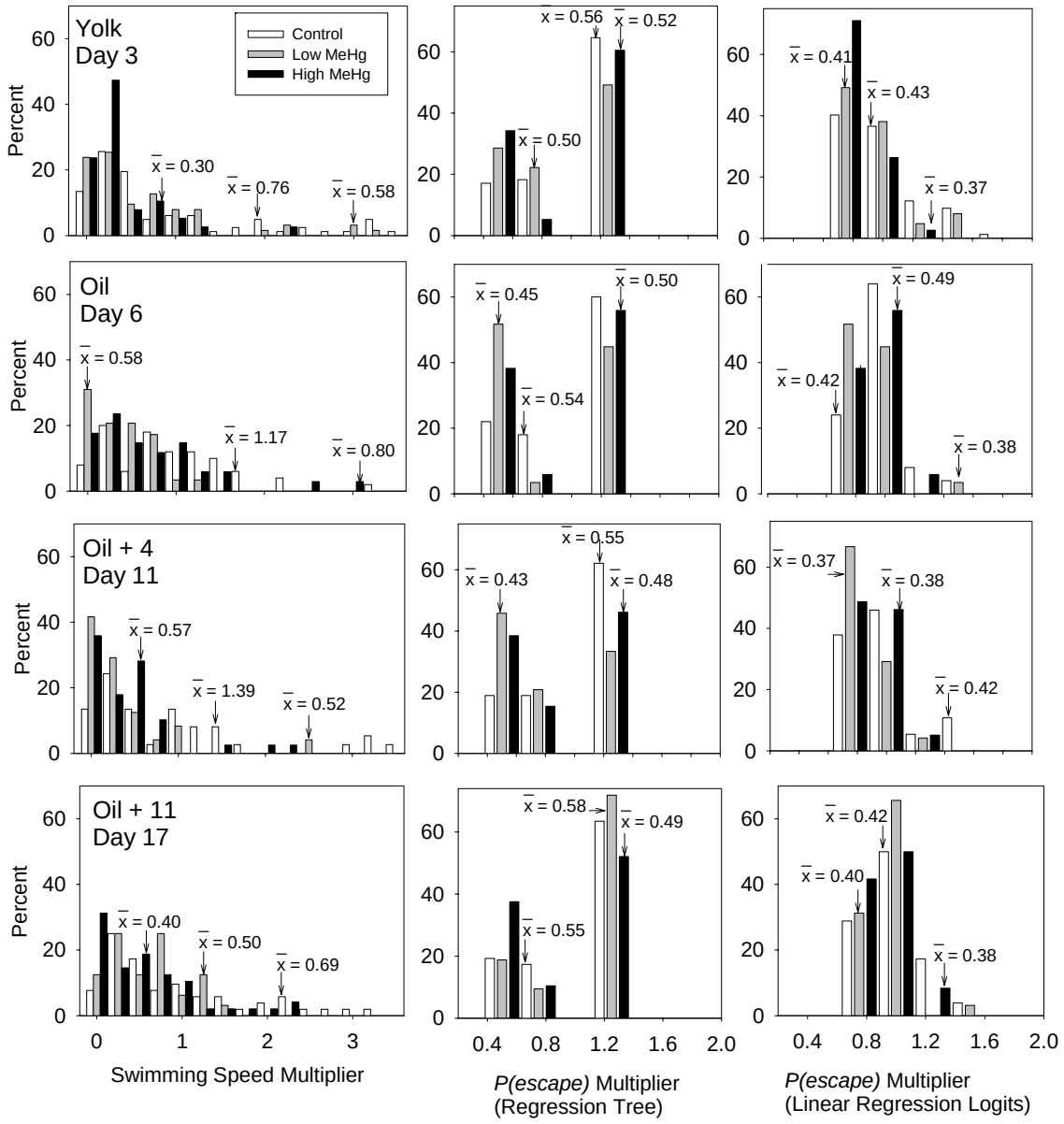

Figure 4.6. Mean values of swimming speed (mm/s) and probability of escape and frequency histograms of multipliers for control, low and high dose MeHg treatments that were used in the IBM. The probability of escape multipliers were derived via regression tree or linear regression using logits analyses. Multipliers were created by dividing each swimming speed and probability of escape value for every age (Day 3, 6, 11 and 17), treatment and statistical analysis by the mean of the swimming speed or probability of escape for every age, treatment and statistical analysis. Arrows indicate the treatment group for the mean swimming speed and probability of escape for each age.

4.3.1.2. Linear Regression using Logits

The LRL model related the swimming speed to the probability of escaping a real fish predator ($F_{1,92} = 6.53$, $P = 0.0122$, $R^2 = 0.0663$).

(4.21) $\pi_i = 0.04838(\text{Swimming Speed}) - 0.68519$

Logits from the regression model were converted to the probability of escape using the following formula: $P(escape) = 1/(1+e^{\pi i})$. The LRL model predicted an almost linear increase in probability of escape with increasing swimming speed, with some minor curvature at the faster swimming speeds (Fig. 4.7).

LRL predicted probabilities of escape showed only small effects of PCBs (Fig. 4.5) that were similar to those predicted by the RT analysis. LRL predictions followed changes in swimming speed as this was the only predictor variable in the LRL model. Low dose PCB exposure resulted in a slight decrease in the probability of escape for day 13 larvae (Fig. 4.5). Probabilities of escape predicted from the LRL model were generally 10% lower than those predicted from the RT analyses.

For all age groupings of larvae, LRL predicted probabilities of escaping that were consistently lower under MeHg exposure compared to control values, although the magnitude of the decrease was small (Fig. 4.6). Predicted probabilities of escaping decreased with increasing MeHg concentration for the yolk and oil+11 age groupings. Caution is needed in interpreting the predicted decreases in probability of escaping; while the decreases were consistent in pattern, they were also very small in magnitude.

4.3.2. IBM Simulations

4.3.2.1. Baseline Simulations

Predicted stage duration and stage survival were similar between baseline simulations that used LRL-derived multipliers from PCB controls and multipliers from MeHg controls. Predicted stage survival over three replicates was 1.6, 1.7, and 1.4% for baseline simulations that used PCB controls and slightly lower (1.1, 1.2, and 1.2 %) for MeHg controls; average stage durations over three replicates were 32.0, 32.4 and 31.7 days for PCB controls and 30.5, 30.3, 31.2 days for MeHg controls.

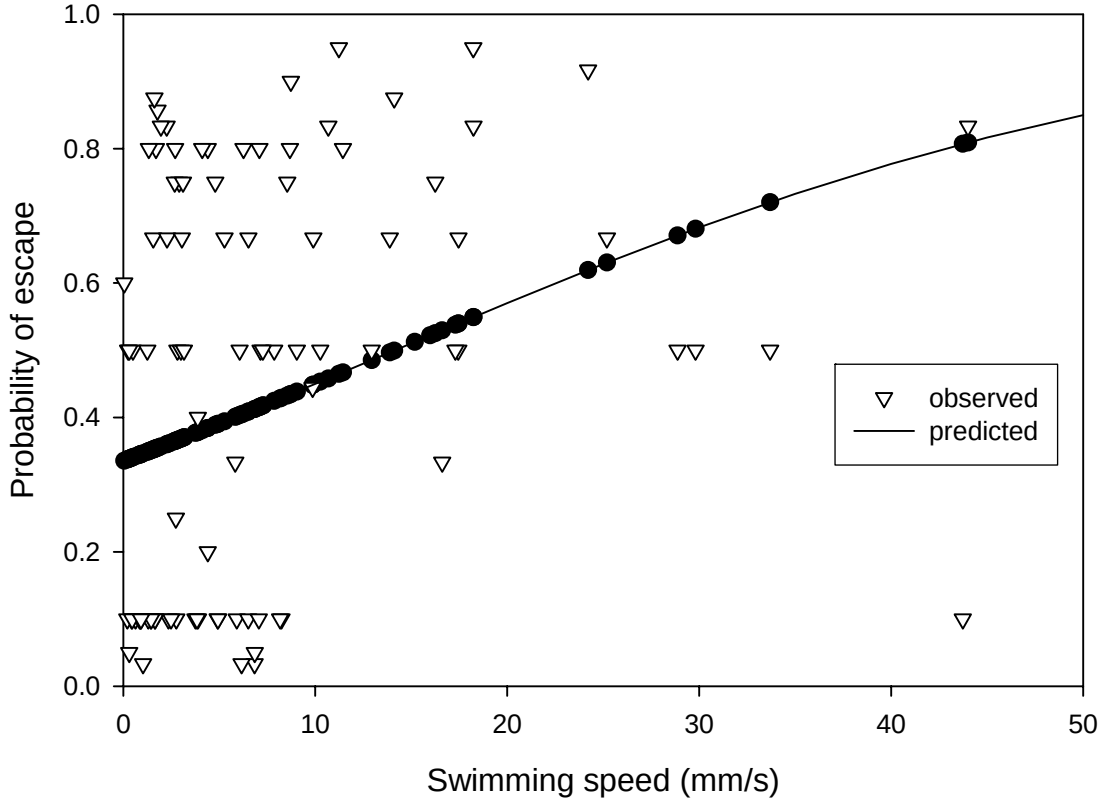

Figure 4.7. Linear regression model using logits for predicted and observed (Fuiman et al., in press) probabilities of red drum larvae escaping a fish predator attack versus swimming speed ($R^2 = 0.0663$, $P = 0.0122$).

Detailed examination of the single replicate of the baseline simulation, based on the MeHg control results and LRL-predicted probabilities of escape, demonstrated realistic diets of larvae (Fig. 4.8A). Very small larvae (about 3 mm) tended to eat the smaller zooplankton groups. By the time a control larva reached about 6 mm in length, the bulk of the biomass of the larval fish diet consisted of copepods. This shift from smaller to larger zooplankton is typical of Atlantic croaker larvae and of marine larvae in general (Govoni et al., 1986).

Length frequency distributions showed that individuals exhibited highly variable growth rates (Fig. 4.8B). The predicted length distribution was very broad by day 20, with some individuals having exhibited little growth and others having reached 11.0 mm. By days 40 and 60 of the simulation, the length frequencies were irregular, with a significant proportion of the survivors below 4.0 mm and had few nearing 11.0 mm.

Mean daily growth rate increased as larval fish grew longer, but daily mortality rates remained relatively constant with larval length (Fig. 4.8C and 4.8D). As the individual larval fish grew larger, the growth rate also increased. Growth rates were very slow in the first few days of feeding (about 3 mm) and they rapidly increased for those that survived the initial period of first feeding (Fig. 4.8C). In contrast, mortality rates did not show any obvious relationship with larval length, indicating that mortality rate was relatively constant for all size classes (Fig. 4.8D).

Mortality rates of simulated larval fish were high, as evidenced by the rapid decline in the number of survivors over time, and predation, especially by medusae, was the dominant source of mortality (Fig. 4.8E). High mortality rates occurred during the first 20 days of the simulation. Cumulative numbers of larvae, categorized by their cause

of death, showed that about 64% of all initial larvae were consumed by predation and about 35% of the larvae starved to death. Of those that died by predation, 93% were consumed by medusae, 6% by predatory fish, and 0.5% by ctenophores. Starvation mostly occurred during days 6 to 10 in poorly-fed larvae, due to the adjusted rate of weight loss to starvation relationship. Less than 65 individuals starved after day 20.

Mean lengths of live larvae versus those that died on each day showed that mortality was size selective during days 10 to 30, corresponding to a large pulse of starvation of small larvae (Fig. 4.8F). During the first 10 days of the simulation all individuals were of similar lengths. From days 10 to about 30, the mean length of those individuals that die each day was consistently shorter than those alive on the same day. After day 30, mean length of individuals that died was highly variable. While only 86 individuals died after day 30, mortality from predation occurred on large as well as small larvae.

4.3.2.4. PCB and MeHg Effects: Stage Survival and Duration

PCB and MeHg derived control multipliers of swimming speed and probability of escape yielded similar predictions of stage duration and survival (Fig. 4.9). Regardless of whether RT or LRL was used, simulations that used multipliers derived from PCB control experiments had, on average, a survival rate of 1.6% (RT and LRL), which was similar to the average of 1.1% from both RT and LRL-derived multipliers in MeHg control simulations. Predicted stage durations for the PCB and MeHg controls were also similar (29.9-33.0 days).

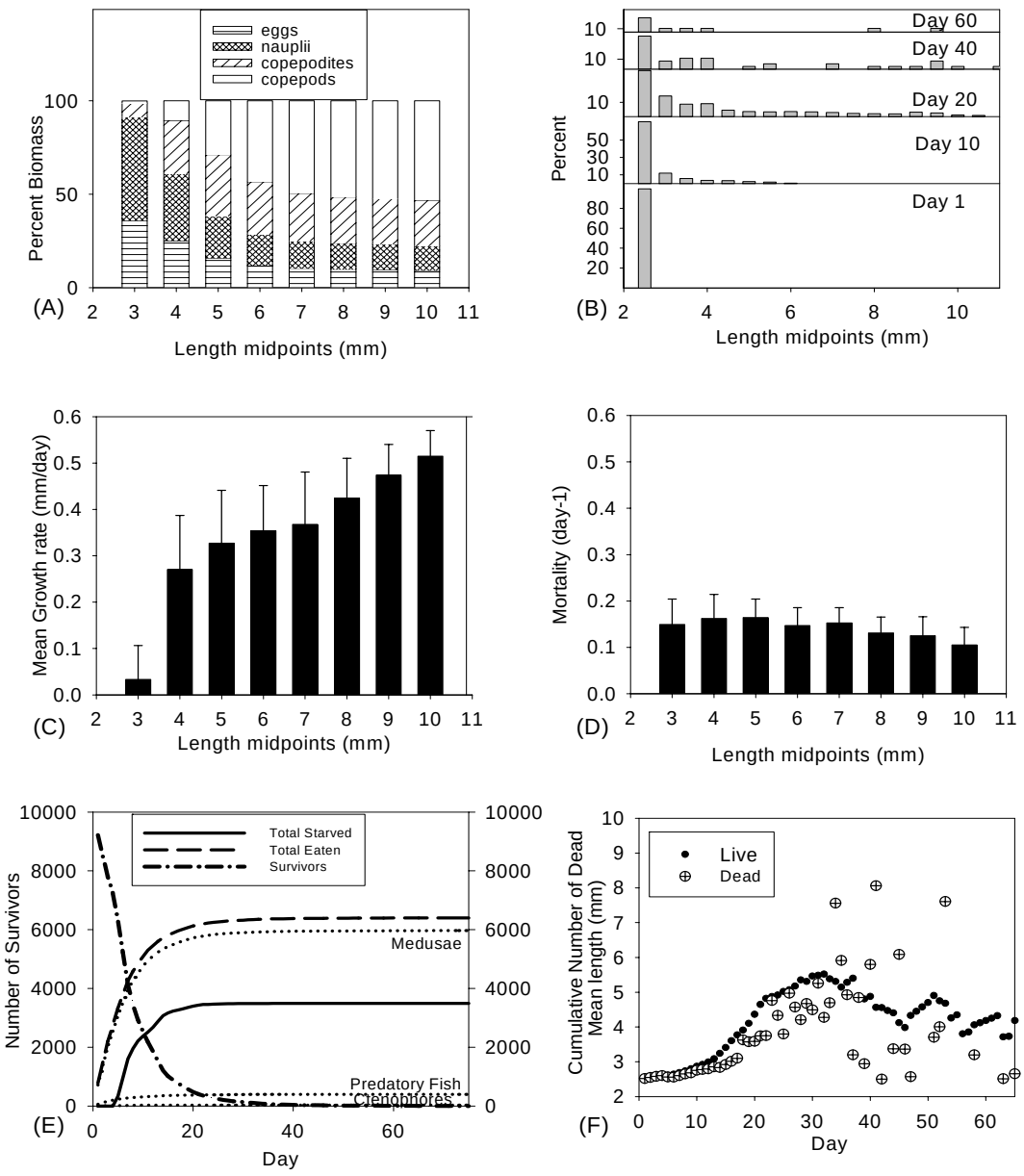

Figure 4.8. Results from a single replicate simulation under baseline conditions that used swimming speed and probability of escape multipliers derived from the control MeHg experiment. (A) Mean biomass of the four zooplankton prey types consumed by size class of larvae expressed as a percent of total biomass consumed, (B) Length frequency distributions of larval fish at days 1, 10, 20, 40 and 60, (C) Mean growth rate (mm/day) by size class of live larvae (D) Mortality rate by size class of dead larvae, (E) Numbers surviving (left axis) and cumulative number eaten by predator type (right axis), dotted lines refer to number eaten by a specific predator type, (F) Mean length of live larvae and dead larvae each day.

The inclusion of an added metabolic cost associated with PCB exposure had a small effect on predicted stage survival and duration (Fig. 4.9). Predicted survival was slightly higher and stage duration slightly shorter when the added metabolic costs were not imposed. Faster growth due to lower metabolism reduced starvation mortality.

Both PCBs and MeHg exposures resulted in reduced larval stage survival, but had different effects on stage duration (Fig. 4.9). Predicted survival rate was approximately halved from the control rate for the low dose PCBs, and by about 85% for the low dose MeHg and by 95% for the high dose MeHg. However, predicted stage duration decreased by about 20% under low dose PCB, was similar to control for low dose MeHg, and increased by 15% for high dose MeHg. These results were consistent for the multipliers derived from RT and LRL, and whether PCB effects included an additional metabolic cost or not.

The opposite effects of PCBs and high-dose MeHg on predicted stage duration was due to differences in when (which age-groupings) the contaminants affected swim speed (Tables 4.4 and 4.5). PCBs did not affect swim speeds until the last age grouping (day 13 and older), when PCBs caused a large reduction in swim speeds. In fact, swim speeds under PCB exposure were slightly faster than control values for the age-9 grouping. PCB exposed larvae grew similar to, or faster than, control larvae for the first two age groupings (0.026 mm/day versus 0.026 and 0.068 versus 0.034). The third age-grouping, which was the longest period, had slowed growth initially due to the slowed swim speed, and starvation mortality increased (51% versus 23%) that culled the slow growers (Table 4.4). The survivors were those that exhibited fast growth and thus stage duration was reduced under PCB exposure.

For the high dose MeHg, swim speeds were reduced throughout all of the age-groupings, which caused increased starvation in every age grouping (greater than 50% versus less than 33% under control; Table 4.5). The only few remaining survivors were those that had slow growth rates; hence, stage duration increased under the high dose MeHg. The low dose MeHg exposure also had slowed swim speeds compared to controls for all age groupings, but not as severe as under the high dose MeHg exposure. Growth rates were similar to controls, and starvation increased relative to controls (like the high dose) but not in the last and longest age-grouping. Thus, under the low dose MeHg exposure, survival was reduced but stage duration was about the same as control values.

The effects of PCBs and MeHg on stage survival and duration were almost entirely due to swim speed effects on prey encounters and resulting growth rates; swim speed and probability of escape had little effects on predation (Fig.4.9). When swimming speed and survival multipliers derived from PCB and MeHg exposed fish were applied to the predation component of the IBM only and control multipliers for swimming speed were applied to the growth component, the predicted stage survival and duration was similar to control conditions of about 1.1% survival and 31 days (PCB: 1.6% survival, 31.7 days duration; MeHg low: 1.0% and 30.6 days; MeHg high: 1.1% and 29.8 days; Fig. 4.9). In contrast, when the contaminant-affected multipliers were applied to larvae encountering their zooplankton prey only, predicted stage survival and duration was very similar to the values predicted when contaminants affected both growth and predation Predicted averaged survival and duration was 1.6% and 32.0 days under control versus 1.1% and 25.0 days under PCB exposure, and 1.1% and 30.7 days under control versus

0.13% and 30.2 days under low dose MeHg and 0.07% and 34.8 days under high dose MeHg exposures (Fig. 4.9).

4.4. Discussion

4.4.1. Contaminant Effects on Cohort Stage Survival and Duration

Both maternally-transferred contaminants, PCBs and MeHg, altered the survival and growth rates of simulated cohorts of Atlantic croaker ocean larvae, and each contaminant and dose had different effects on survival and growth (Fig. 4.9). The subtle differences observed between contaminants and exposures (doses) manifested as significant differences at the cohort level (Fig. 4.9). Low dose PCB simulations showed a moderate reduction in survival and stage duration whereas low dose MeHg had a much larger reduction in stage survival, but did not affect stage duration significantly. High dose MeHg had a severe effect on stage survival and the very few remaining slow growing individuals extended the stage duration of the cohort.

The differences in stage survival and duration that were evoked by the two contaminants were due to contaminant effects differing among age groupings. Low dose PCB and High dose MeHg had opposite effects on the stage duration because PCBs did not affect swim speeds until the last age grouping, while high dose MeHg exposure affected swim speeds at all age groupings. If the contaminant effects were uniformly imposed on all ages, it is likely that the simulations would predict very different results that presented here; PCBs and MeHg would likely show effects that occur in the same direction, but at different magnitudes. The age-groupings that were chosen for this study were designed to help determine the role of mobilization of yolk and oil globule in the

sublethal behavioral effects imposed by contaminants (Alvarez, 2005). The behavioral effects were variable and dependent on the age groupings and the IBM provided a means

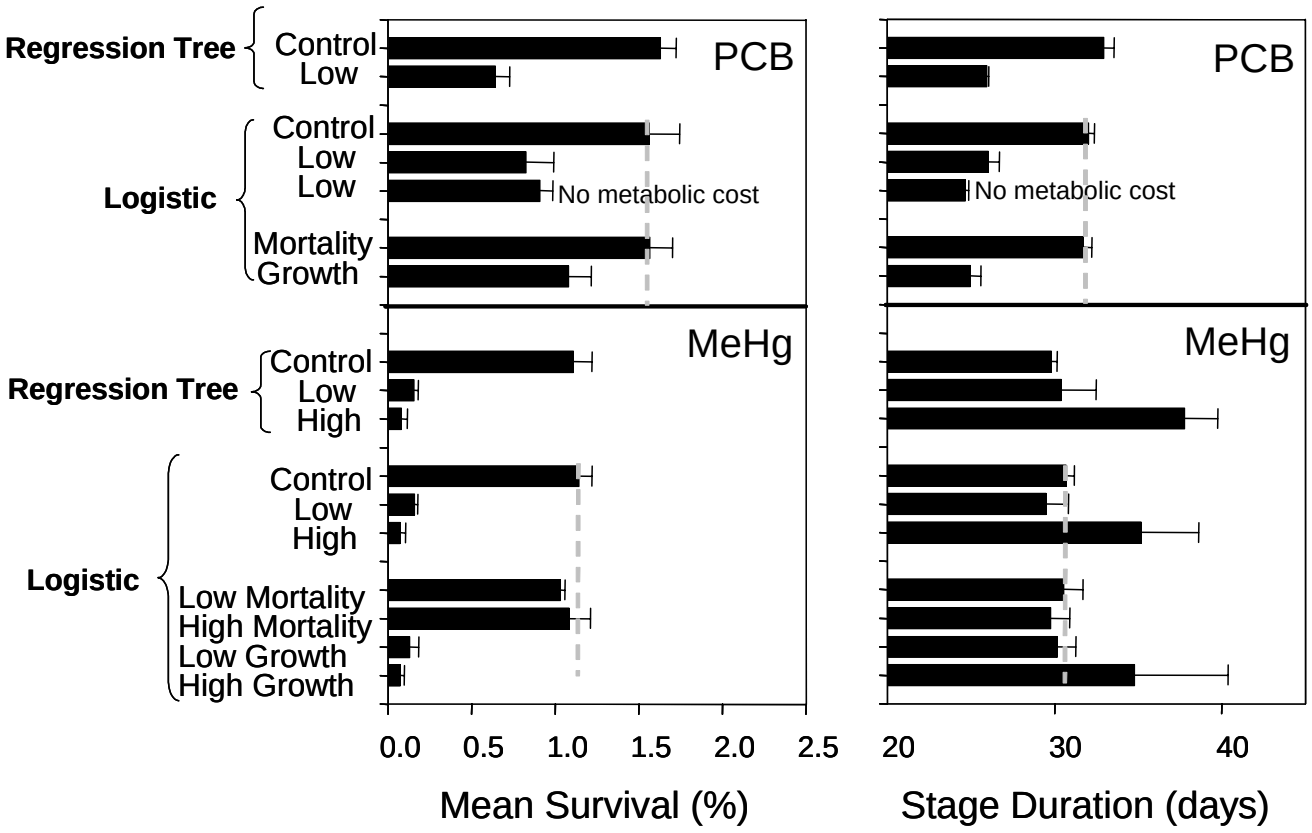

Figure 4.9. Mean (± SD) of survival and duration of the ocean larval stage predicted by the IBM for three replicate simulations for various combinations of baseline (control), low dose PCB, and low dose and high dose MeHg exposures. Probability of escape multipliers were either from the regression tree or linear regression using logits model. Baseline predictions used either the multipliers of swim speed and probability of escape from the control PCB or MeHg experiments. PCB exposures were performed without and with added metabolic costs to mimic growth reduction observed in the laboratory experiment. The final set of simulations were designed to predict stage survival and duration when PCBs and MeHg only affect growth and only affect predation. The vertical dotted line shows the baseline results based on the linear regression using logits analysis for the multipliers.

Table 4.4. Averaged values by age grouping of swim speed (mm/s), growth rate (mm/day), numbers entering, and percent mortality due to predation and starvation for a single replicate simulation under control (C) and low dose PCB exposure.

Age-group	Swim Speed		Growth rate		Number entering		Percent of entering that were eaten		Percent of entering that starved	
	C	PCB	C	PCB	C	PCB	C	PCB	C	PCB
5	8.96	7.12	0.026	0.026	10,000	10,000	37	38	16	13
9	7.73	8.05	0.034	0.068	4,708	4,793	26	25	15	28
13	6.81	2.12	0.388	0.543	2,732	2,246	70	46	23	51

Table 4.5. Averaged values by age grouping of swim speed (mm/s), growth rate (mm/day), numbers entering, and percent mortality due to predation and starvation for a single replicate simulation under control (C), low dose MeHg (L), and high dose MeHg (H) exposures.

Age-group	Swim Speed			Growth rate			Number entering			Percent of entering that were eaten			Percent of entering that starved		
	C	L	H	C	L	H	C	L	H	C	L	H	C	L	H
3 (yolk)	8.01	6.26	3.38	0.028	0.019	0.002	10,000	10,000	10,000	22	22	22	0	0	0
6 (oil)	7.49	4.02	5.39	0.040	0.045	0.013	7,794	7,761	7,810	37	29	31	31	57	52
11 (oil+4)	7.56	3.30	3.54	0.123	0.128	0.039	2,540	1,051	1,320	32	24	24	33	60	62
17 (oil+11)	7.32	5.53	4.50	0.54	0.63	0.43	887	161	192	57	60	47	29	29	51

to integrate all effects to ultimately determine the stage survival and stage duration of a cohort affected by potentially age-dependent contaminant effects.

Contaminant effects on swimming speeds manifested as a reduced ability to encounter enough food to sustain growth during the early period of the larval stage. Low dose PCBs appeared to select for faster growers because growth rate was increased for all age groupings but the percent that starved to death increased under PCB exposure (Table 4.4). Low dose MeHg did not change the growth rate of survivors much, but did increase the percent that starved for the oil and oil+4 age groupings (Table 4.5). High dose MeHg decreased growth rates substantially for all age groupings and increased starvation rates for all age groups except for yolk (Table 4.5). The dominant source of mortality remained as predation for low dose PCBs, but switched from predation to starvation for both doses of MeHg-exposed fish. However, interpretation of a switch in mortality from predation to mortality for low dose MeHg should be viewed with caution because the model was calibrated to a moderately high baseline level of starvation (35% of total mortality).

4.4.2. Growth versus Predation Effects

Contaminant exposures primarily affected growth processes of the simulation. While multipliers derived from contaminant experiments were applied to both mortality and growth processes of the IBM, the multipliers derived from contaminant experiments had the greatest effect on growth and minimal effects on mortality (Fig. 4.9). The only component affected by contaminants in the growth processes of the IBM were larval fish swimming speeds. Larval fish swimming speeds are important determinants of encounter rates with prey items.

Certain model assumptions that are related to larva encounters with predators and zooplankton prey provide an explanation for why contaminants predominantly affect growth processes in these simulations. In these simulations, larvae are active and swimming for only 13 hours per day, whereas predators are active for 24 hours; a situation that reduces the impact that changes in swimming speed in larval fish would have on encounter rates with predators. Additionally, it is not likely that small contaminant-induced changes in swimming speed would have much of an impact on predation because larva swim much slower in comparison to their major predators: medusa and juvenile fish. Swimming speeds of larval fish and ctenophore predators are more comparable, but the simulated ctenophore encounters were lower than those with the other predator types. The model assumptions suggest that changes in larval fish swimming speed will have just a small effect on predation. If a larval fish swims slower, then it encounters predators less frequently. However, this small effect may be at least partially offset by a contaminant induced decreased probability of escaping a predator. Interestingly, the proportion of larval fish consumed by fish predators, out of all larval fish consumed by predators, increased slightly under contaminant exposure, while the proportion of consumption by invertebrate predators decreased (predictions not shown). The increase in predation by fish predators suggested that the multipliers derived from the low dose contaminant experiments that were applied to the *P(escape)* of a fish predator were having only a small effect. In contrast, while larvae swim speeds also affect encounter rates with zooplankton prey, the zooplankton prey are not moving. Therefore, if the larval swimming speed is reduced because of contaminant exposure, then encounter rates will also be reduced by a proportional amount. My goal was to

demonstrate a method that links larval behavior to population relevant indices. In other situations, such as later life stages and estuarine environments, behavioral effects may produce much greater effects on predation.

The statistical technique used to develop *P(escape*) multipliers had minimal effects on the IBM simulation results in this study. Both sets of multipliers from different statistical techniques yielded similar results, confirming that the IBM was not sensitive to the changes to *P(escape)*. However, if predation was more important in this model, the particular statistical analyses used to determine *P(escape)* could influence the results. For PCB analyses, *P(escape)* was affected consistently in day-13-age larvae, regardless of the statistical technique. The predictions of *P(escape)* from the MeHg analyses more depended on the type of statistical model used. When LRL was used, swimming speeds and escape probabilities declined with MeHg exposure at every stage. A dose-response relationship was only found when using LRL, and the dose- response relationship was only manifested in the youngest and oldest stages (yolk and oil +11). When RT analyses were used with the MeHg data, escape probabilities declined with swimming speeds for every age except for the oldest stage of oil +11. The differences resulting from the two alternative statistical analyses of the MeHg-laboratory results, had only minor effects in model simulations because of the unimportance of predator encounters. The MeHg simulations that used multipliers derived from RT analyses predicted a slight increase in stage duration in low- dose-MeHg-exposed fish, when compared to control. In contrast, MeHg simulations that used multipliers derived from the LRL analyses predicted a slight decrease in stage duration in low-dose-MeHg exposed fish when compared to control

(Fig. 4.9). These differences may become more important in situations where changes in predation due to contaminant exposure are more important.

In this study, both RT and LRL techniques were applied to evaluate survival probabilities and to compare each method. The main advantage to using a RT analysis is the incorporation of more information from potentially non-linear relationships. The survival probability derived from the RT analysis was a more integrated response; the calculated survival probability incorporated responses reported for the visual reactive distances as well as swimming speed. The disadvantage to using a RT approach is that the predicted escape probability lacked resolution and was grouped into one of three values. In contrast, LRL did not use other behavioral measures and only required swimming speed to predict escape probability as a continuous variable. In this study, it was useful to use a single predictor variable because the experimental design of the PCB and MeHg experiments only allowed for the single common variable of the swimming speed. Therefore, to adequately compare the two data sets, I also used LRL to compare the MeHg and PCB data instead of using a weakly correlated variable as a surrogate to visual reactive distance. The two types of statistical models that were explored in this study may have utility in future studies.

4.4.3. Corroboration of Baseline Predictions

The simulated cohort of Atlantic croaker larva under baseline conditions demonstrated similar patterns in growth to growth patterns reported in the literature for larval fish. The high variability in growth rates observed under control conditions (Fig. 4.8B) is comparable to natural systems. Cohorts of fish reared in the laboratory and in large enclosures that had the same birth date, show high variability in growth rates, and

an establishment of a size hierarchy with time (see Fuiman et al., 2005 for review). It has also been documented that faster growers tend to survive (Houde, 1996). Once simulated larva are able to initiate feeding and survive the vulnerable period, their growth rates increase rapidly with size. The model prediction of an increase in the growth rate with size is supported by studies that demonstrated that RNA/DNA ratios measured from larval fish increased with larval size or age (Buckley, 1982, Buckley et al., 1984). Both control and contaminant exposed simulated larvae demonstrated an increase in growth rate with size.

Most species of larval fish are known to have difficulties with capturing prey during the period of time when larval fish switch from endogenous to exogenous food sources (Hjort, 1914; Ware et al., 1981; Blaxter, 1986). Starvation is a serious risk during this period because of high mass-specific metabolic rates and the low energy reserves of fish larvae (Fuiman, 2002). Patchily distributed food sources can also increase the likelihood of starvation for some individuals (Houde, 1989). Robinson and Ware (1988), using RNA/DNA ratios, calculated a window of time in which larval herring are vulnerable to starvation. In the presence of prey items, the time to irreversible starvation averaged 11 days for the studied group of herring larva. In the absence of food, the time to irreversible starvation declined to an average of six days. In the IBM simulations under control conditions, the majority of individuals died of starvation by day 20.

It is possible that a third of Atlantic croaker ocean larva will starve to death in the ocean. Laboratory studies on related species and field-based studies on Atlantic croaker suggest that larval croaker have high starvation potential. Laboratory studies using

RNA/DNA ratios for larval red drum, a related species, demonstrated that red drum have a critical period during which starvation is a serious risk. In the critical period, larval red drum switch from endogenous to exogenous food sources and have difficulties capturing prey. As a result, the RNA/DNA ratios measured on larval red drum decline rapidly until first feeding (Ware et al., 1981; Westerman and Holt, 1994). Furthermore, otolith studies on Atlantic croaker suggest that wild Atlantic croaker that were spawned in September and October in the MAB during periods of falling plankton abundance and increased prey patchiness have much slower growth rates and are prone to starvation (Nixon and Jones, 1997). Additionally, field-caught newly settled estuarine Atlantic croaker have much higher percentages of empty stomachs than other settling larva (Govoni et al., 1983), suggesting that by the end of the life stage, Atlantic croaker are close to, or at the end of, their stored energy reserves.

IBM simulations under control conditions showed that larval feeding and growth patterns are similar to published studies, but it is unknown if mortality of croaker ocean larvae are dominated by predation or starvation. The predicted diet of control Atlantic croaker larva was dominated by copepods (Fig. 4.8A), which is similar to field reported diets. Soto et al. (1987) reported that pelagic Atlantic croaker less than 10 mm length ingested almost only calanoid copepods. Control ocean larval Atlantic croaker grew slowly and had stage durations of approximately 31 days; a duration that was within the range of time reported for croaker ocean larvae (Diamond et al., 1999). The relatively long stage duration and slow growth rates of croaker are typical for fish species that show dispersal over long ranges (Bradbury and Snelgrove, 2001). In the baseline simulations presented here, the source of ocean larva mortality appeared to be dominated by

predation (Fig. 4.8E). Other studies suggest that predation dominates the mortality of many marine species (Cushing, 1974; Hunter, 1981).

4.4.4. Corroboration of Contaminant Predictions

The predicted decline in stage survival of larval fish due to the effects of contaminants on growth processes is an expected effect given the current model structure and prior sensitivity analyses. The model used in this study was based primarily on a model developed by Letcher et al. (1996) for generic marine larva. Sensitivity analyses of individual parameters performed for the generic marine larva model suggested that the intrinsic variables regulating growth had the largest effects on survival. Slight variations in metabolic rates or sensitivities to starvation would determine if a larval fish dies from predation or starvation (Letcher et al., 1996). Houde (1987) also identified growth rate as an important regulator of cohort survival, and suggested that isolating the sources of growth variability should contribute most to the understanding of survival of young fish. Model sensitivity analyses also suggested that larval encounter rates with prey items were more important to survival and growth than actual prey density, a result consistent with my contaminant simulations (Letcher et al., 1996). The predicted effects of contaminants were impaired ability to capture food, a consequence of decreased encounter rates because of slower swimming speeds. The total number of food items that were consumed decreased, which had a direct effect on metabolism.

The simulation results presented here also agree, in part, with previous findings from a study on larval striped bass, *Morone saxatilis,* which concluded that larval condition is a more important determinant of cohort survival than predation (Chick and van den Avyle, 2000). In the striped bass study, the authors conducted laboratory

experiments to determine the effect of food density on routine swimming speeds and then simulated larval fish responsiveness to predators based on their laboratory results. Chick and van den Avyle (2000) concluded that growth rates substantially influenced mortality; faster growing cohorts had higher stage survival rates. The apparent benefits of faster growth rates outweighed the costs associated with an increased encounter rates with predators (Chick and van den Avyle, 2000). Chick and van den Avyle (2000) also suggested that swimming speed was a function of larval fish condition, and that larval fish that are in better condition (i.e. faster swimmers), grew faster and had a higher survival rate. The conclusions derived from the striped bass study are consistent with conclusions from our study. In the simulations presented here, poor condition contaminant–exposed larvae swam slower, had lower survival rates and, for the high-dose MeHg treatment, grew slower. The slower swim speed resulted in lower encounter rates with food items, and subsequently lower food intake.

However, in contrast to the striped bass study, the simulations presented here suggest that growth rate has no relationship to predation mortality. Chick and van den Avyle (2000) suggested that growth rate was related to predation mortality and that faster growing larvae escaped predation. My simulations of contaminant exposure suggest that during the ocean larval stage, if larval swimming speeds are slow and predator swimming speeds are fast, then growth can become decoupled from predation. If growth and predation processes were linked, contaminants would affect both processes. Instead, in these simulations, contaminants affected growth but not predation. Empirical studies on red drum larva also support the finding that growth processes and predation mortality are separate processes and are not related. Fuiman et al. (2005) examined growth rate and

other survival skills of red drum larvae and found no relationship between growth rate and vulnerability to predation.

Direct evidence in support of the predicted population effects of PCBs and MeHg on cohort growth and survival is generally unavailable. Most laboratory studies examined growth and survival of fish exposed to MeHg or PCBs in controlled laboratory conditions, where doses of contaminants were measured and fish were fed to satiation. In laboratory studies on Atlantic croaker and the mummichog (*Fundulus heteroclitus*) growth was reduced by PCBs (Black et al., 1998; McCarthy et al., 2003) but the measured effect on growth was likely due to a disruption in metabolic processes instead of foraging ability because food was supplied in high concentrations and competition was minimized. In contrast, MeHg did not affect growth of laboratory studied Atlantic croaker (Alvarez, 2005), larval and juvenile walleye (*Stizostedion vitreum*) (Friedmann et al., 1996; Latif et al., 2001), larval fathead minnows (*Pimephales promelas*) (Hammerschmidt et al., 2002), or zebrafish larvae (*Danio rerio*) (Samson et al., 2001).

Qualitative changes in growth and decreased survival of a cohort of Atlantic croaker exposed to low dose PCBs and MeHg because of impaired foraging abilities are indirectly suggested by behavioral experiments and field studies. PCBs have been reported to reduce food consumption in laboratory reared mummichogs and to reduce growth of field-caught mummichogs (Black et al., 1998). Methylmercury decreased feeding and impaired the competitive abilities of grayling (*Thymallus thymallus*) (Fjeld et al., 1998), reduced prey capture ability of zebrafish (Samson et al., 2001), reduced swimming ability and prey capture ability of mummichogs (Weis and Weis, 1995 a,b; Zhou and Weis, 1998), and the swimming ability of minnows (Kolok et al., 1998).

Models provide a mechanism for quantitatively relating changes in swimming speed and foraging behavior into population relevant measures, such as stage survival and growth.

4.4.5. Model Limitations

In addition to obvious potential errors introduced from an unrealistic IBM, two other sources of potential error were the treatment of age grouping in simulations and the use of a red drum experiment to infer croaker reponses to contaminant exposure. Although the structure of the IBM facilitated the incorporation of the contaminant effects on different developmental stages, the simulations lacked individual characteristics that could be tracked throughout a larva's entire development. Laboratory results only tracked the contaminant effects on behavior through a single age grouping (e.g., yolk, oil, etc.). Multipliers of swimming speed and escape probabilities were applied at every age grouping, but multipliers were randomly assigned to each individual independently of the individual's multiplier values from the previous age grouping. This meant that an individual fish that had above average multipliers assigned at one age grouping (i.e., a fast swimmer), could possibly be assigned average, or below average, multipliers at the next age grouping. Ideally, data from laboratory experiments that track individuals and their characteristics throughout all developmental stages are needed, but whether it is logistically feasible to acquire such data remains a challenge.

Another potential source of error in the model is that the experiments used to create the statistical models were done on red drum instead of Atlantic croaker. Ideally, escape probabilities derived from experiments done with croaker would provide the best predictions. Unfortunately, experiments from croaker were not available, therefore I used data collected from red drum instead; red drum are closely related to Atlantic croaker.

From the red drum data, I was able to create a standardized RT by normalizing the data and splitting each node on z-scores. I was also able to create a LRL from red drum data that could be applied to croaker after transforming the swimming speeds of croaker to fit the lognormal distribution of red drum. The standardized RT model or the LRL model may be applicable to larval fish from other species, but this hypothesis requires support from additional laboratory studies.

4.4.6. Conclusions

The results of this study suggest that, under certain conditions, contaminants have the potential to impact the survival and duration of the important larval stage. The focus of this study was the ocean larva stage because this stage has a high mortality rate and deterministic matrix projection models suggest that Atlantic croaker populations were sensitive to changes in the survival and durations of the ocean larval stage perturbations (Diamond et al., 1999, 2000). Ocean larva can also be reared in the laboratory and monitored for subtle changes in behaviors that are induced by contaminants. The change in behavior induced by contaminants was then inputted into statistical models and an IBM to estimate a change in stage duration and survival. The change in survival of pre-recruits can be a key factor in determining population abundances in species like Atlantic croaker that have substantial annual recruitment variability (Houde, 1987; Nixon and Jones, 1997). Relatively small differences in growth (duration) and mortality rates, such as a few percent per day, can result in large differences in the number of individuals entering the reproductive age (Houde, 1987). Many factors influence survival, and there is increasing evidence that starvation may be a major source of mortality; a lack of food, or a mismatch between spawning and prey production, may be a principle cause of poor

year class strength (Hunter, 1981). Starvation has been suggested to be one of the main causes of mortality in marine fish larvae (Cushing, 1974; Lasker, 1975; Leggett and Deblois, 1994). This study suggests that contaminants can potentially shift the source of mortality from predation to starvation and to increase overall mortality during the critical larval life stage.

This study demonstrated that the sublethal effects of contaminants on behavior of croaker can be converted into population relevant endpoints. The laboratory measured subtle behavioral changes of fish exposed to contaminants, and the statistical model and IBM, which were made to be as realistic as possible, converted these changes into changes in larval stage duration and survival. In Chapter 5, the relative changes in stage duration and survival are used to change the parameters of the ocean larval stage in a matrix projection population model. The matrix model is then used to predict the effects of the low dose PCB exposure and the low and high-dose MeHg exposures on the long-term population dynamics of the Mid Atlantic Bight and Gulf of Mexico croaker populations.

4.5. References

Adamack, A. T. 2003. Quantifying habitat quality of larval bay anchovy (*Anchoa mitchilli*) in Chesapeake Bay by linking an individual-based model with spatially-detailed field data. MS thesis, Louisiana State University, Baton Rouge, Louisiana.

Alvarez, M. C. 2005. Significance of environmentally realistic levels of selected contaminants to ecological performance of fish larvae: effects of atrazine, malathion, and methylmercury. PhD Dissertation. University of Texas, Austin, Texas.

Alvarez, M. C., and Fuiman, L. A. 2005. Environmental levels of atrazine and its degradation products impair survival skills and growth of red drum larvae. *Aquat. Toxicol*. 74:229-241.

Al-Yimani, F. Y. 1988. Distributional ecology of zooplankton and fish larvae (spot, croaker, menhaden) in the northern Gulf of Mexico. PhD Dissertation. University of Miami, Goral Gables, Florida.

Bailey, K.M. and Batty, R. S. 1983. A laboratory study of predation by *Aurelia aurita* on larval herring (*Clupea harengus*): experimental observations compared with model predictions. *Mar. Biol.* 72: 295-310.

Bessin, R. T., Moser, E.B, Reagan, T. E. and White, W.J. 1990. Analysis of percent bored internode data collected from sugarcane borer varietal resistance e valuations. *J. Am. Soc. Sugar Cane Tech*. 10:8-22.

Bjerselius, R., Lunstedt-Enkel, K., Olsen, H, Mayer, I. and Dimberg, K. 2001. Male goldfish reproductive behaviour and physiology are severely affected by exogenous exposure to 17β-estradiol. *Aquat. Toxicol*. 53:139-152.

Black, D. E., Gutjahr-Gobell, R, Pruell, R. J., Bergen, B., Mills, L. and McElroy, A. E. 1998. Reproduction and polychlorinated biphenyls in *Fundulus heteroclitus* (Linnaeus) from New Bedford Harbor, Massachusetts, USA. *Environ. Toxicol. Chem.* 17:1405-1414.

Blaxter, J. H. S. 1986. Development of sense organs and behaviour of teleost larvae with special reference to feeding and predator avoidance. *Trans. Am. Fish. Soc*. 115:98-114.

Bradbury. I. R. and Snelgrove, P.V.R. 2001. Contrasting larval transport in demersal fish and benthic invertebrates: the roles of behaviour and advective processes in determining spatial pattern. *Can. J. Fish. Aquat. Sci*. 58:811-823.

Breck, J. E. and Gitter, M. J. 1983. Effect of fish size on the reactive distance of bluegill (*Lepomis macrochirus)* sunfish. *Can. J. Fish. Aquat. Sci.* 40: 162-167.

Breiman, L., Friedman, J.H., Olshen, R. A. and Stone, C. J. 1998. Classification and Regression Trees. Chapman and Hall/CRC, Boca Raton, Fl, USA.

Buckley, L. J. 1982. Effects of temperature on growth and biochemical composition of larval winter flounder *Pseudopleuronectes americanus*. *Mar. Ecol. Prog. Ser.* 8:181-186.

Buckley, L. J. 1984. RNA-DNA ratio: an index of larval fish growth in the sea. *Mar. Biol.* 80:291-298.

Chick, J. H. and Van Den Avyle, M. J. 2000. Effects of feeding ration on larval swimming speed and responsiveness to predator attacks: implications for cohort survival. *Can. J. Fish. Aquat. Sci*. 57:106-115.

Clotfelter, E. D., Bell, A. M. and Levering, K. R. 2004. The role of animal behaviour in the study of endocrine-disrupting chemicals. *Anim. Behav*. 68:665-676.

Cowan, J. H. Jr. and Houde, E. D. 1992. Size-dependent predation on marine fish larvae by ctenophores, scyphomedusae, and planktivorous fish. *Fish. Ocean.* 1:113-126.

Cowan, J. H. Jr., Houde, E. D. and Rose, K. A. 1996. Size-dependent vulnerability of marine fish larvae to predation: an individual-based numerical experiment. *ICES J. Mar. Sci*. 53:23-37.

Cushing, D. H. 1974. The natural regulation of fish populations. In: Harden-Jones, F. R. ed. Sea Fisheries Research. Elek Science, London. pp. 399-412.

Diamond, S. L., Cowell, L.G. and Crowder. L. B. 2000. Population effects of shrimp trawl bycatch on Atlantic croaker. *Can J Fish Aquat Sci*. 57:2010-2021.

Diamond, S. L., Crowder, L.B. and Cowell, L. G. 1999. Catch and bycatch: the qualitative effects of fisheries on population vital rates of Atlantic croaker. *Trans. Am. Fish. Soc*. 128:1085-1105.

Faulk, C. K., Fuiman, L. A. and Thomas, P. 1999. Parental exposure to ortho, para-dichlorodiphenyltrichloroethane impairs survival skills of Atlantic croaker (*Micropognias undulatus*) larvae. *Environ. Toxicol. Chem*. 18: 254-262.

Fingerman, S. W., and Russell, L. C. 1980. Effects of the polychlorinated biphenyl Aroclor 1242 on locomotor activity and on the neurotransmitters dopamine and norepinephrine in the brain of the gulf killifish, *Fundulus grandis*. *Bull. Environm. Contam. Toxicol*. 25:682-697.

Fjeld E., Haugen, T. O, and Vollestad. L. A. 1998. Permanent impairment in the feeding behavior of grayling (*Thymallus thymallus*) exposed to methylmercury during embryogenesis. *Sci. Total Environ*. 213: 247-254.

Fleeger, J.W., Carman, K.R. and Nisbet, R. M. 2003. Indirect effects of contaminants in aquatic ecosystems. *Sci. Total Environ*. 317: 207-233.

Friedmann, A. S., Watzin, M.C., Brinck-Johnsen, T. and Leiter, J.C. 1996. Low levels of dietary methylmercury inhibit growth and gonadal development in juvenile walleye (*Stizostedion vitreum*). *Aquat. Toxicol*. 35:265-278.

Fuiman, L. A. 1989. Vulnerability of Atlantic herring larvae to predation by yearling herring. *Mar. Ecol. Prog. Ser*. 1989:291-299.

Fuiman, L. A. 2002. Special consideration of fish eggs and larva. In: Fishery Science. The Unique Contributions of Early Life Stages. Fuiman L. A and R.G. Werner. Eds.Blackwell Publishers, Malden, MA. pp1-32.

Fuiman, L. A. and Cowan, J. H. Jr. 2003. Behavior and recruitment success in fish larvae: repeatability and covariation of survival skills. *Ecology* 84:53-67.

Fuiman, L. A., Cowan, J. H. Jr., Smith, M. E. and O'Neal, J. P. 2005. Behavior and recruitment success in fish larvae: variation with growth rate and the batch effect. *Can. J. Fish. Aquat. Sci*. 62: 1337-1349.

Fuiman, L. A.,Rose, K. A., Cowan, J. H. Jr. and Smith, E. P. Survival skills required for predator evasion by fish larvae and their relationship to laboratory measures of performance. *Anim. Behav*. (in press)

Gerritsen, J., and Strickler. J. R. 1977. Encounter probabilities and community structure in zooplankton: a mathematical model. *J. Fish. Res. Board Can.* 34:73-82.

Govoni, J. J., Hoss, D. E. and Chester. A. J. 1983. Comparative feeding of three species of larval fishes in the northern Gulf of Mexico: *Brevoortia patronus, Leiostomus xanthurus,* and *Micropogonias undulatus*. *Mar. Ecol. Prog. Ser*. 13: 189-199.

Govoni, J. J., Ortner, P. B., Al-Yimani, F. and Hill. L. C. 1986. Selective feeding of spot, *Leistomus xanthurus* and Atlantic croaker, *Micropogonias undulatus*, larvae in the Northern Gulf of Mexico. *Mar. Ecol. Prog. Ser.* 28: 175-183.

Hammerschmidt, C. R., Sandheinrich, M. B., Wiener, J. G. and Rada, R.G. 2002. Effects of dietary methylmercury on reproduction of fathead minnows. *Environ. Sci. Technol*. 36:877-883.

Hjort, J. 1914. Fluctuations in the great fisheries of northern Europe viewed in the light of biological research. *Rapp. P. –v. Reun. Cons. Int Explor. Mer* 20: 1-228.

Hunter, J. R. 1981. Feeding ecology and predation of marine fish larvae. In: Marine fish larvae: morphology, ecology and relation to fisheries. Lasker, R. Ed. University of Washington Press, Seattle, Wash. Pp. 33-77.

Houde, E. D. 1989. Subtleties and episodes in the early life of fishes. *J. Fish Biol.* 35 (Supplement A**)**:29-38.

Houde, E. D. 1996. Evaluating stage-specific survival during the early life if fish. In: Survival Strategies in Early Life Stages of Marine Resources. Watanabe, Y., Y. Yamashita, and Y. Oozeki. Eds. Rotterdam, Balkema. Pp. 51-66.

Kane, J. 2003. Spatial and temporal abundance patterns for the late stage copepodites of *Metridia lucen*s (Copepoda: Calanoida) in the US northeast continental shelf ecosystem. *J. Plank. Res*. 25:151-167.

Kiorboe, T., Munk, P.and Richardson, K. 1987. Respiration and growth of larval herring

Clupea harengus: relation between specific dynamic action and growth efficiency. *Mar. Ecol. Prog. Ser*. 40: 1-10.

Kiorboe, T. and Sabatini, M. 1994. Reproductive and life cycle strategies in egg carrying cyclopoid and free spawning calanoid copepods. *J. Plank. Res*. 16: 1353-1366.

Kolok, A. S., Plaisance, E. P. and Abdelghani, A.1998. Individual variation in the swimming performance of fishes: an overlooked source of variation in toxicity studies. *Environ. Toxicol. Chem.* 17:282-285.

Lasker, R. 1975. Field criteria for survival of anchovy larvae: the relation between inshore chlorophyll maximum layers and successful first feeding. *Fish. Bull.* 73**:** 453-462.

Latif, M. A., Bodaly, R.A., Johnston, T. A. and Fudge, R. J. P. 2001. Effects of environmental and maternally derived methylmercury on the embryonic and larval stages of walleye (*Stizostedion vitreum*). *Environ. Pollut*. 111:139-148.

Leggett, W. C. and Deblois, E. 1994. Recruitment in marine fishes: is it regulated by starvation and predation in the egg and larval stages? *Neth. J. Sea. Res*. 32:119-134.

Letcher, B. H., Rice, J.A., Crowder, L. B. and Rose, K. A. 1996. Variability in survival of larval fish: disentangling components with a generalized individual-based model. *Can. J. Fish. Aquat. Sci*. 53:787-801.

McCarthy, I. D., Fuiman, L.A., and Alvarez, M.C. 2003. Aroclor 1254 affects growth and survival skills of Atlantic croaker *Micropogonias undulatus* larvae. *Mar. Ecol. Prog. Ser*. 252:295-301.

Mesa, M. G., Poe, T. P., Gadomski, D.M. and Petersen, J. H.. 1994. Are all prey created equal? A review and synthesis of differential predation on prey in substandard condition. *J. Fish Biol*. 45 (Suppl. A):81-96.

Miller, T. J., Crowder, L. B., Rice, J. A. and Marschall, E. A. 1988. Larval size and recruitment mechanisms in fishes: toward a conceptual framework. *Can. J. Fish. Aquat. Sci*. 45:1657-1670.

Mills, L. J., and Chichester, C. 2005. Review of evidence: are endocrine-disrupting chemicals in the aquatic environment impacting fish populations? *Sci. Tot. Environ.* 343:1-34.

Morse, W. W. 1989. Catchability, growth and mortality of larval fishes. *Fish. Bull. U.S.* 87:417-446.

Nixon, S. W., and Jones, C.M. 1997. Age and growth of larval and juvenile Atlantic

croaker, *Micropogonias undulatus*, from the Middle Atlantic Bight and estuarine waters of Virginia. *Fish. Bull*. 95:773-784.

Purcell, J. E., and Decker, M. B.. 2005. Effects of climate on relative predation by scyphomedusae and ctenophores on copepods in Chesapeake Bay during 1987-2000. *Limnol. Oceanogr*. 50:376-387.

Robinson, S. M. C. and Ware, D.M. 1988. Ontogenetic development of growth rates in larval Pacific herring *Clupea harengus pallasi*, measured with RNA-DNA ratios in the Strait of Georgia, British Columbia. *Can. J. Fish. Aquat. Sci.* 45:1422-1429.

Rose, K. A., Cowan, J. H. Jr., Clark, M. E.,Houde, E. D. and Wang, S. –B. 1999. Simulating bay anchovy population dynamics using an individual based approach. *Mar. Ecol. Prog. Ser*. 185: 113-132.

Rose, K. A., Murphy, C. A., Diamond, S. L., Fuiman, L. A. and Thomas, P. 2003. Using nested models and laboratory data for predicting population effects of contaminants on fish: a step toward a bottom-up approach for establishing causality in field studies. *Hum. Ecol. Risk Assess.* 9:231-257.

Samson, J. C., Goodridge, R., Olobatuyi, F. and Weis, J. S. 2001. Delayed effects of embryonic exposure of zebrafish (*Danio rerio)* to methylmercury (MeHg). *Aquat. Toxicol.* 51:369-376.

SAS Institute Inc. SAS Language Reference,Version 9, Cary, NC: SAS Institute Inc; 2002

Scott, G. R., and Sloman, K. A. 2004. The effects of environmental pollutants on complex fish behaviour: integrating behavioral and physiological indicators of toxicity. *Aquat. Toxicol.* 68:369-392.

SEAMAP, 2001. Enviromental and Biological Atlas of the Gulf of Mexico.1999. Gulf States marine Fisheries commission. No. 82.

SEAMAP, 2002. Enviromental and Biological Atlas of the Gulf of Mexico.2000. Gulf States marine Fisheries commission. No. 101.

Smith, G. M., and Weis, J. S. 1997. Predator-prey relationships in mummichogs (*Fundulus heteroclitus* (L.)): effects of living in polluted environment. *J. Exp. Mar. Biol. Ecol*. 209:75-87.

Soto, M. A., Holt, G. J., Holt, S. A. and Rooker, J. 1998. Food habits and dietary overlap of newly settled red drum (*Sciaenops ocellatus*) and Atlantic croaker (*Micropogonias undulatus*) from Texas seagrass meadows. *Gulf. Res. Rep*. 10:41-55.

Stegmann, P. M, Quinlan, J. A. and Werner, F.W. et al, 1999. Atlantic menhaden recruitment to a southern estuary: defining potential spawning regions. *Fish. Oceanog*. 8: (Suppl 2): 111-23.

Suchman, C. L., and Brodeur, R. D. 2005. Abundance and distribution of large medusae in surface waters of the northern California current. *Deep-Sea Res. II* 52:51-72.

Thomas P. and Khan, I. A. 1995. Mechanisms of chemical interference with reproductive endocrine function in sciaenid fishes. In: Rolland R. M, Gilbertson M, Peterson RE, eds. Chemically induced alterations in functional development and reproduction of fishes. Racine, Wisconsin: SETAC Technical Publications Series; p p. 29-51.

Thomas, P., Wofford, H.W. and Neff, J. M. 1981. Biochemical stress responses of striped mullet (*Mugil cephalus* L.) to fluorine analogs. *Aquat. Toxicol*. 1:329-342.

Tsai, C. L., Jang, T. H. and Wang, L.H. 1995. Effects of mercury on serotonin concentration in the brain of tilapia, *Oreochromis mossambicus*. Neurosci. Let. 184: 208-211.

Walton, W.E., Hairston, N.G. and Wetterer, J. K. 1992. Growth-related constraints on diet selection by sunfish. *Ecol.* 73: 429-437.

Ware, D. M., De Mendiola, B.R. and Newhouse, D.S. 1981. Behavior of first-feeding Peruvian anchoveta larvae, *Engraulis ringens J.Rapp. P.–v. Reun. Cons. Int Explor. Mer* 178: 467-474.

Weis, J. S., Smith, G., Zhou, T., Santiago-Bass, C. and Weis, P. 2001. Effects of contaminants on behavior: biochemical mechanisms and ecological consequences. *Bioscience* 51:209-217.

Weis, J. S. and Weis, P. 1995a. Effects of embryonic exposure to methylmercury on larval prey-capture ability in the mummichog, *Fundulus heteroclitus*. *Environ. Toxicol. Chem*. 14:153-156.

Weis, J. S. and Weis, P. 1995b. Swimming performance and predator avoidance by mummichog (*Fundulus heteroclitus*) larvae after embryonic or larval exposure to methylmercury. *Can. J. Fish. Aquat. Sci*. 52: 2168-2173.

Westerman, M., and Holt, G. J. 1994. RNA:DNA ratio during the critical period and early larval growth of the red drum *Sciaenops ocellatus*. *Mar. Biol.* 121:1-9.

Wieser, W., Krumschnabel, G. and Ojwang-Okwor J. P. 1992. The energetics of starvation and growth after refeeding in juveniles of three cyprinid species. *Environ. Biol. Fishes.* 33: 63-71.

WHO. Global Assessment of the State-of-the-Science of Endocrine Disruptors. 2002. In Damstra, T, Barlow S, Bergman A, Kavlock R, van der Kraak G, eds. International Programme On Chemical Safety.

Zhou, T. and Weis, J. S. 1998. Swimming behavior and predator avoidance in three populations of *Fundulus heteroclitus* larvae after embryonic and/or larval exposure to methylmercury. *Aquat. Toxicol.* 43:131-148.

CHAPTER 5. ENDOCRINE DISRUPTION IN FISH: PREDICTING POPULATION-LEVEL RESPONSES FROM LABORATORY STUDIES

5.1. Introduction

Endocrine disruption is well documented in fish (Kime, 2001), but linking the effects of endocrine disrupting chemicals to a population response remains an "open challenge" (Mills and Chichester, 2005). Fish responses to the exposure to endocrine disruptors in the natural environment are usually documented as a high occurrence of abnormal gonad development or blood chemistry (e.g., Munkittrick et al., 1994; Lye et al., 1997; Allen et al., 1999). The effect of endocrine disruptors on population abundance is more difficult to ascertain. In many situations, it is likely that the abundance of a fish population would not be obviously affected by exposure to a contaminant because only a portion of the individuals are required to breed successfully. Sometimes, even with little effects on population abundance, too few individuals reproducing can lead to concerns about genetic diversity (Sumpter, 2005), but this is relatively rare in most fishes. Because of the highly variable and stochastic nature of fish population dynamics (Rothchild, 1986; Fogarty et al., 1991), the effects of endocrine disruption on the abundance of natural populations are likely to be only noticed when the effect is dramatic (Sumpter, 2005).

Establishing cause and effect between population decline and exposure to an endocrine disruptor usually involves either a top-down or bottom-up research approach. A top-down approach requires one to use characteristics of the population response to try to figure out the most likely cause from a suite of potential candidate stressors (e.g., contaminants, habitat loss, fishing harvest, exotic species, global climate change – Jaworska et al., 1997). An alternative approach is a bottom-up approach in which population responses to contaminant exposure are predicted from modeling based on

laboratory data (e.g., Rose et al., 2003). The predicted population responses in a bottom-up approach provide information on the likely magnitude, and other characteristics, of the responses to look for in natural populations. Implementing the bottom-up approach is a task that is as equally daunting as the top-down approach, and requires collaboration between fish biologists, hydrologists, engineers, ecologists, population geneticists, and modelers (Rose et al., 2003; Sumpter, 2005). Here, I describe a bottom-up approach that scales the effects of endocrine disruption documented on individual fish in the laboratory to the resulting long-term population response.

The bottom-up approach of linking contaminant effects to population responses has been used by others. Several previous studies have attempted to scale the effects of stress, contaminants, and endocrine disruption up to the population level using mathematical and simulation models, such as matrix projection models and delayed differential equations. Most of these examples in toxicological research have used simplified matrix models with no density dependence or stochastic processes (Forbes et al., 2001; Forbes and Calow, 2002). Matrix models with density dependent and stochastic processes are not amenable to powerful equilibrium analyses, which tend to complicate analysis of the results. Density dependence often dampens the predicted population response to contaminant exposure (Grant, 1998; Forbes et al., 2001). Some examples of these modeling analyses have included realistic exposure scenarios, density dependence, and stochasticity (e.g., Barnthouse et al., 1990, Brown et al., 2003; Rose et al., 2003; Rose 2005, Spromberg and Birge, 2005). However, in these applications the effects of stress are usually explored in the context of the life history of the organism to infer whether responses can be related the life history strategy of the fish (Hansen et al., 1999;

Heppell et al., 2000). In addition, these life history focused applications tend to use general (not site-specific) information on growth, mortality, and reproductive rates and generic stress scenarios (Rose and Cowan, 2000; Rose, 2005).

The bottom-up approach employed here uses a variation of the classical matrix projection model to scale laboratory-derived effects of endocrine disruption on Atlantic croaker to population level responses. Matrix models have been applied to population analyses since the 1940's, and are powerful tools for analyzing population dynamics (Caswell, 2000). The Atlantic croaker matrix model used here simulates two nursery areas for each population, includes site-specific estimates of density dependence and stochasticity, and uses multiple time steps to accommodate the various durations in young of the year (YOY) lifestages. The matrix model was applied to two geographically distinct populations of Atlantic croaker: Mid Atlantic Bight (MAB) and the Gulf of Mexico (GOM). Both populations have been subjected to fishing pressure and have been exploited in different ways. As a result, the populations exhibit differences in their age-structure, growth, mortality rates, and reproductive rates (Diamond et al., 1999; Diamond et al., 2000; Waggy et al., in press).

Atlantic croaker is a good model species upon which to develop matrix projection models of population dynamics. Croaker is common along the eastern shoreline of the US and in the GOM, and exhibit a common life history strategy for species that use estuaries as nursery habitats. Atlantic croaker also have commercial and ecological importance, and are well studied in laboratory and field (Diamond et al., 1999, 2000, in prep; Rose et al., 2003). Because of the croaker's widespread distribution, it is also a good species to study spatial and temporal patterns in contaminant body burdens as

indicators of contaminant hotspot areas. In this study, I focus on populations in the MAB and the GOM. The MAB includes estuaries from Virginia and North Carolina and was the focus of earlier modeling efforts (Rose et al., 2003). The GOM includes estuaries from Louisiana and Texas (Diamond et al., 1999, 2000). Population dynamics of Atlantic croaker in response to contaminants within an individual region may yield important insights into ecosystem health and function, and comparisons between two different populations may also provide insight into how life history and site specific factors influence a population's response to contaminant stress.

Atlantic croaker is iteroparous, highly fecund, and individuals spawn several batches of eggs between August and March. Adults live in the ocean, migrating south during the fall and winter, and return in the spring. Eggs are spawned offshore during the migration. After fertilization, eggs hatch into yolk-sac larvae in two days. After the yolk is absorbed in about 4-5 days, yolk-sac larvae initiate exogenous feeding and become ocean larva. Ocean larvae feed on zooplankton (Govoni et al., 1986; Chapter 4) and depend on passive transport mechanisms to carry them inshore to their estuarine nursery areas (Miller et al., 1984). After 30-60 days, the ocean larvae attain 7 to 12 mm in body length and arrive at the estuary (Warlen, 1982; Nixon and Jones, 1997), where they become estuarine larvae. Estuarine larvae move through the estuaries to reach the primary nursery areas consisting of shallow, brackish creeks, and marshes. At about 20 mm in length, estuarine larvae become early juveniles. Early juveniles become late juveniles at about 40 to 65 mm and move into secondary nursery areas consisting of deeper sounds, bays, and channels. Most late juveniles migrate to the ocean to join the adults during the fall of their first year. About 50% of Atlantic croaker mature at the end

of their first year, and 100% of age-2 and older croaker are mature. Historically, adults lived to about 15 years of age (Hales and Reitz, 1992), but a maximum age of 8 to 12 years is more common now due to environmental conditions and fishing pressure (Rose et al., 2003; Diamond et al., in prep).

Differences in life history characteristics between the MAB and GOM populations are largely driven by different historical exploitation patterns and environmental conditions (Diamond et al., 1999). Adult croaker live to age 12 in the MAB, but only to age 8 in the GOM, and the difference may be attributed to higher exploitation rates in the GOM. Total removals due to harvest of Atlantic croaker in the Gulf were estimated to be three times larger than in the Atlantic. Fishery related mortality also concentrated on different stages in MAB and GOM. In the GOM, fishing mortality was a result of bycatch from shrimping and from industrial fishing focused on age-0 and age-1 croaker. In contrast, a higher proportion of the catch in the MAB was older adults, because Atlantic croaker is fished for food in Virginia and North Carolina. Fisheries in North Carolina estuaries also catch many juveniles as bycatch from adult fisheries. Age 1 and age 2 Atlantic croaker are similar sized between the two populations, but MAB grow faster after age 3. GOM fish reach a slightly smaller age of maturity (140 mm) than fish from the MAB (150-170 mm). Until about age 7, mature females from the GOM tend to have higher fecundities than females of the same age in the MAB. Differences in young-of-the-year growth and survival between the two populations is largely driven by the warmer water temperatures in the GOM, and differences in prey and predator densities between the GOM and MAB. Density dependent mortality of late

juveniles, estimated from long-term field monitoring, also appears to differ in magnitude between the MAB and GOM.

I used the matrix model to predict the population responses of croaker to exposure to polychlorinated biphenyls (PCBs) and methylmercury (MeHg). Analyses were performed for the MAB and GOM versions of matrix model. Two nursery areas were simulated for each population: Virgina and North Carolina estuaries for MAB and Louisiana and Texas estuaries for GOM. Both PCBs and MeHg are found within the estuaries of the US (Summers, 2001). The effects of the contaminants on croaker fecundity and egg mortality were determined directly from laboratory experiments, and the effects on ocean larval stage duration and survival were determined by analysis of laboratory data via statistical methods and an individual-based larval stage model (Chapter 4). Different exposure scenarios were simulated that included different proportions of the population exposed, whether contaminants were eliminated after spawning or persisted for the lifetime of the female, and which nursery habitat area was contaminated.

5.2. Methods

5.2.1. Matrix Model Description

The matrix projection model was a stage-within-age model that represented two nursery areas and used multiple time-steps to represent young-of- the-year (YOY) lifestages (Figs. 5.1 and 5.2). The model was coded in Fortran90. The MAB model has been described previously (Rose et al., 2003). An updated description of the MAB version of the model, and the version used here, is described in Diamond et al. (in prep). The GOM model is very similar in structure to the MAB version, except that the MAB

version simulates two spawning cohorts per year, while the GOM version simulates one spawning cohort per year. The model represented the YOY portion of the life cycle as 6 life stages, which were defined previously by initial and final lengths (Diamond et al., 1999). The numbers of individual in the six YOY life stages were solved using different time steps to accommodate the wide range in durations among stages: daily timestep for egg and yolk-sac stages, biweekly for ocean larval and estuary larval stages, monthly for early and late juveniles, and annual for age 1 and older individuals (Figs. 5.1 and 5.2). Surviving individuals from finer timesteps that were determined to progress into the next lifestage that used a coarser timestep accumulated until the appropriate number of timesteps had passed and were then moved into the next life stage. Individuals that survived to age 1 were passed to the adult portion of the model, which was updated annually.

The geographic region associated with each population consisted of two nursery areas. The MAB nursery areas consisted of estuaries from Virginia (VA) and North Carolina (NC) (Fig. 5.1). Nursery areas in the Atlantic south of North Carolina were not modeled because genetic studies suggested that the entire Atlantic was the same stock and Diamond et al. (2000) were unable to find much data on YOY parameter values. Estuaries from Louisiana (LA) and Texas (TX) comprised the nursery areas for the GOM population (Fig. 5.2). Two pulses of egg production (cohorts), occurring in the Spring and Fall, were simulated for the MAB, while only one pulse of egg production in the Fall was simulated for the GOM. Model simulations started each 360-day year on July 1.

5.2.2. Matrix Elements

Stage-based matrix projection models require the estimation of two elements for each life stage: the diagonal element (P) and the sub-diagonal element (G). P is the probability of surviving a timestep and remaining in the same life stage, whereas G is the probability of surviving a timestep and moving to the next life stage (Caswell, 2000). P and G are estimated from the instantaneous mortality rate (Z) and stage duration (D):

$$P_i = \sigma * (1 - \rho) \quad (5.1)$$

$$G_i = \sigma * \rho \quad (5.2)$$

$$\rho = \frac{\sigma^D - \sigma^{D-1}}{\sigma^D - 1} \quad (5.3)$$

where D is the stage duration in timesteps and σ is the fraction surviving a timestep ($\sigma = \exp^{-Z}$). To adjust the mortality and stage duration of lifestages that were operating on 15 and 30 day timesteps, Z was multiplied by the number of days in the timestep, and D was divided by the number of days in the timestep. The age-based matrix for age-1 and older individuals simply used the annual mortality rate to determine the annual survival fraction (i.e., G is annual survival and P=0).

5.2.3. Reproduction

Annual reproduction was simulated with proportions of the total eggs produced each year divided among the two nursery areas for each of the populations, and further divided between the two spawning cohorts for the MAB population (Diamond et al., in prep). Field data showed that estuarine larvae abundance peaked in late summer to

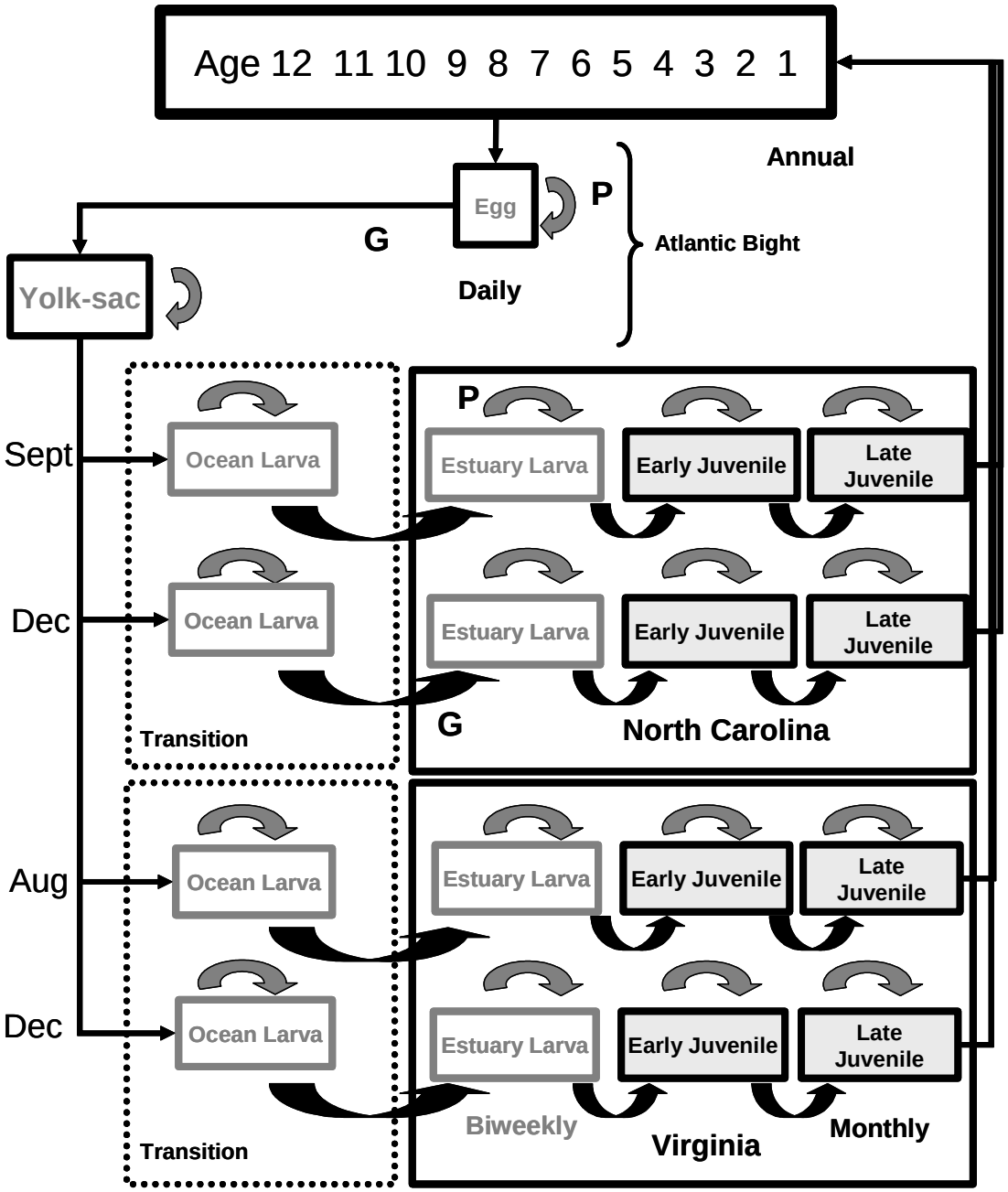

Figure 5.1. Movement diagram of the matrix projection model for the Mid-Atlantic Bight (MAB). Adults spawn eggs in the open ocean, and have two spawning cohorts per year. Adults, eggs, and yolk-sac larvae reside in the open ocean. Ocean larvae drift in ocean currents to estuarine nursery areas and become estuarine larvae. Estuarine larvae, ocean larva, early juveniles, and late juveniles reside in North Carolina and Virginia nursery areas. Eggs and yolk sac dynamics are simulated using a daily timestep; ocean larvae and estuary larva use a 15 day timestep; early and Late juveniles use a 30 day timestep; adults use an annual timestep. P is the probability of surviving and staying in the lifestage, G is the probability of surviving and moving to the next lifestage (after Rose et al., 2003).

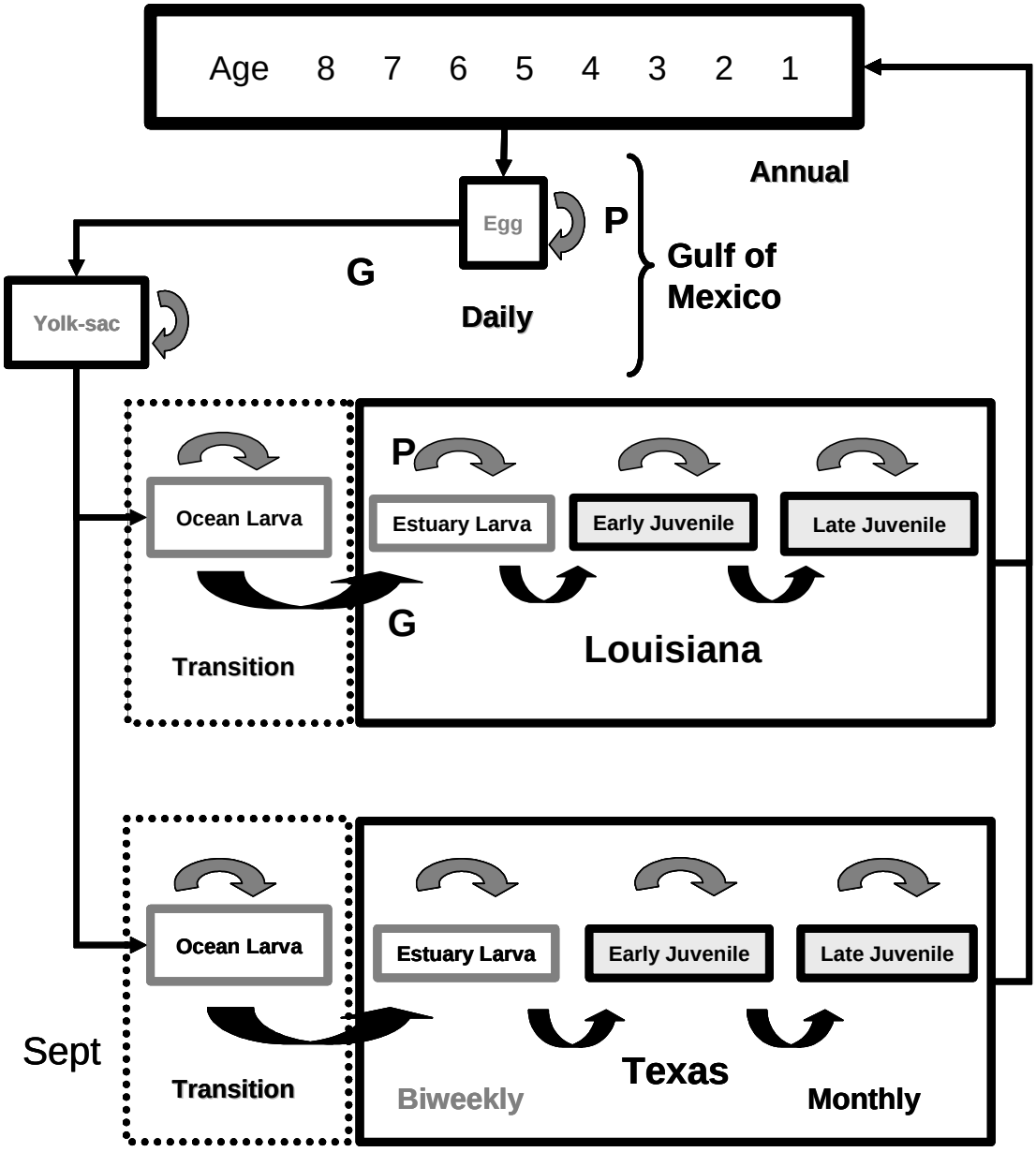

Figure 5.2. Movement diagram of the matrix projection model for the Gulf of Mexico (GOM). Adults spawn eggs in the open ocean and have a single spawning cohort per year. Adults, eggs, and yolk-sac reside in the open ocean. Ocean larvae drift in ocean currents to estuarine nursery areas and become estuarine larvae. Estuarine larvae, ocean larvae, early juveniles, and late juveniles reside in Louisiana and Texas nursery areas. Eggs and yolk sac dynamics are simulated using a daily timestep; ocean larvae and estuary larva use a 15 day timestep; early and Late juveniles use a 30 day timestep; adults use an annual timestep. P is the probability of surviving and staying in the lifestage, G is the probability of surviving and moving to the next lifestage

early fall (cohort 1) and also in the winter (cohort 2) in both VA and NC estuaries, while estuarine larvae abundance only peaked in the winter for both LA and TX estuaries. At the beginning of each year, total annual egg production ($\frac{1}{2}*\sum N_i*m_i*f_i$) was calculated, where N_i is the number of individuals (males and females) in age-class i, m_i is the fraction mature for age-class i, and f_i is the number of eggs per female of age-class i (Table 5.1). For the MAB population, 70% of the total annual number of eggs produced were allocated to cohort 1 and 30% were allocated to cohort 2. Within each cohort, 60% of the eggs drifted to NC, while 40% drifted to VA. In the GOM, there was only one cohort, and 60% of the eggs drifted to LA, and the remaining 40% drifted to TX. For the MAB version, cohort 1 eggs that were destined for VA were added to the simulated population on the midpoints of months as: 15% in August, 35% in September, 35% in October, and 15% in November. For the NC nursery region, cohort 1 eggs were added on the midpoints of months as 20% in September, 30% in October, 30% in November, and 20% in December. Cohort 2 eggs in the MAB version were added to both VA and NC as 20% in December, 40% in January, 30% in February, and 10% in March. The GOM version had one spawning cohort, and eggs that were bound for both LA and TX were added at the same time on the midpoints of months as 20% in September, 40% in October, 20% in November, and 20% in December.

5.2.4. Estimation of Baseline Model Parameters

Values of P and G for the six YOY stages by cohort, nursery area, and population were calculated from stage duration and mortality estimates using equations (5.1)-(5.3).

Table 5.1. Adult mortality rate and fecundity (eggs/female) fraction for reproductively mature individuals per age class for the MAB and GOM populations (Diamond et al., in prep, Diamond et al., 1999).

Variable	MAB	GOM
Adult mortality (yr^{-1})	0.66	0.45
Age 1 fecundity	15313.9	27204.9
Age 2 fecundity	187486.6	278813.5
Age 3 fecundity	296823.9	356449.7
Age 4 fecundity	397520.4	437324.1
Age 5 fecundity	482228.3	498877.1
Age 6 fecundity	549632.9	545724.6
Age 7 fecundity	601381.9	581379.9
Age 8 fecundity	640175.7	608516.8
Age 9 fecundity	668792.1	-
Age 10 fecundity	689667.5	-
Age 11 fecundity	704778.6	-
Age 12 fecundity	715658.2	-

Estimates of mortality rates and stage durations were for present day conditions (Table 5.2). Stage durations and mortality rates by life stage were determined from information reported in the literature, and by statistical analysis of long-term monitoring data for each of the four nursery areas (described in detail in Diamond et al., in prep). The stage durations and mortality rates used to estimate P and G values were developed first for the better studied MAB (Diamond et al., 1999, 2000), and then modified to reflect conditions in the GOM. Modifications to MAB values were based on information reported for croaker [or the related weakfish (*Cynoscion regalis*) and red snapper (*Lutjanus campechanus*)] in the Gulf of Mexico, and based upon statistical analysis of long-term monitoring data for LA and TX.

Estimation of the P and G elements of the projection matrix for YOY stages (equations 5.1-5.3) required values of instantaneous mortality rate (Z), which provides an estimate of σ, and of stage duration (D) (Table 5.2; Diamond et al., in prep). Duration of the egg and the yolk-sac larva stages by cohort and nursery area were based on

laboratory-derived relationships that were then adjusted for average water temperatures from monitored values in areas inhabited by the life stage. Mortality rates of eggs were calculated from an equation that related mortality rates to fish egg size. Mortality rate of yolk-sac larvae was calculated by cohort and nursery area by using a regression relationship between growth rate and mortality rate. Stage durations of ocean larvae, estuary larvae, early juveniles, and late juveniles were calculated using the entering and exiting lengths that define each stage and average growth rate as estimated from otolith analysis of croaker. Mortality rates of ocean larvae, estuary larvae, early juveniles, and late juveniles were estimated from growth-based relationships or from catch-curve analysis of field data.

Adult annual survival probabilities, fraction mature, and fecundity for ages 1 to 12 for MAB and for ages 1 to 8 for the GOM were specified from reported values in the literature (Table 5.1; Diamond et al., in prep). Many of the adult parameters depended on mean length with age, which were estimated using von Bertalanffy growth equations. Data on length-at-age were those reported from commercial fisheries (catch) and from fishery-independent monitoring. For the GOM and MAB, adult annual natural mortality rate of 0.37/year was estimated using previously estimated coefficients for the von Bertalanffy growth equation and assumed water temperatures that the adults would experience (Diamond et al., 1999). For the MAB population, fishing mortality rate as a result of bycatch from shrimp harvesting was added to the late juvenile stage in the NC nursery habitat. A fishing mortality rate of 0.29/year was imposed on age 1 and older adults; this rate has been identified as the target by recent fisheries management plans

Table 5.2. Estimated mortality rates and stage durations for the six YOY stages in each of the two nursery areas and spawning cohorts of the MAB (Virginia and North Carolina) and GOM (Louisiana and Texas) populations. The MAB population has two spawning cohorts per year while the GOM has a single spawning cohort per year. The mortality and duration values were obtained from information reported in the literature and analysis of long-term field monitoring data and the mortality rates of the EJ and LJ lifestages were adjusted by equal amounts for each region to stabilize model predictions of total population abundance over time (Diamond et al., in prep, Diamond et al., 1999).

Mid Atlantic Bight								
Nursery Area	Virginia				North Carolina			
Cohort	1		2		1		2	
	Mortality (d^{-1})	Stage Duration (d)	Mortality (d^{-1})	Stage Duration(d)	Mortality (d^{-1})	Stage Duration(d)	Mortality (d^{-1})	Stage Duration (d)
Egg	0.3579	1.28	0.3579	1.94	0.3168	1.00	0.3579	1.36
Yolk-sac	0.1450	5.31	0.0714	10.73	0.2193	3.52	0.1331	5.79
Ocean Larva	0.1521	30.85	0.1075	43.55	0.1341	34.95	0.1269	36.94
Estuary Larva	0.0706	24.37	0.0467	36.66	0.0542	31.66	0.0384	44.45
Early Juvenile	0.0153	138.72	0.0153	122.91	0.0153	148.02	0.0153	156.64
Late Juvenile	0.0113	159.46	0.0242	144.20	0.0344	140.85	0.0503	114.83
Gulf of Mexico								
Nursery Area	Louisiana				Texas			
	Mortality (d^{-1})	Stage Duration (d)			Mortality (d^{-1})	Stage Duration (d)		
Egg	0.4984	2.00			0.4984	2.00		
Yolk-sac	0.1645	4.00			0.1645	4.00		
Ocean Larva	0.0900	45.50			0.0900	45.50		
Estuary Larva	0.0387	53.50			0.0414	53.50		
Early Juvenile	0.0233	75.00			0.0412	75.00		
Late Juvenile	0.0185	180.00			0.0305	180.00		

(ASMFC, 2004). Natural and fishing mortality rate was combined for late juveniles in the GOM population and was set to 0.036 (TX) and 0.022(LA) based on the draft fishery management plan for groundfish (GMFMC, 1980). The fishing mortality for adults was set to 0.07/year to relect harvest from other fisheries; there is no official fishery for adult croaker in the GOM. The fraction of mature fish at age was 0.5 of age 1 and 1.0 for age 2 and older, and fecundity (eggs/mature female) was estimated from averaged length at age data (Table 5.1).

5.2.5. Stochasticity: Egg Production and Winterkills

Interannual stochasticity was imposed in both populations by applying a multiplier to annual egg production each year. Annual egg production was randomly varied around the computed expected value each year by multiplying egg production with a deviate derived from a lognormal distribution with a mean of 1 and standard deviation of 0.6 for the MAB, and a mean of 1 and standard deviation of 0.5 for the GOM. Standard deviations were chosen so that the predicted CV of interannual abundances of late juveniles matched the CVs computed from long-term, field-sampling data.

A second source of stochasticity was episodic mortality imposed on estuarine larvae and early juveniles in the MAB population only in order to represent the effects of harsh winters (Lankford and Targett, 2001). Years for which winterkill mortality was applied were randomly selected with probability of 0.6 in the VA and 0.2 in the NC nursery areas. Probabilities of winterkill were based on the average frequency that historically monitored water temperatures in each year included at least one winter month with an average temperature colder than $3^{o}C$. In years with harsh winter, stage survivals of estuarine larvae and early juveniles were each reduced by 1%.

5.2.6. Density Dependence

Late juvenile stage mortality rate was specified as density-dependent for both the MAB and GOM versions of the model (Diamond et al., in prep). The density dependent relationship for the MAB was based on regression analysis of catch curves from 20 years of monthly sampling of YOY croaker at about 200 stations in Virginia estuaries and at about 100 stations in North Carolina estuaries. Both nursery areas exhibited similar relationships between annual loss rates and average abundance; therefore data from both areas were pooled into a single density-dependent relationship. The GOM density dependent relationship for late juveniles was estimated from 30 years of monthly sampling of YOY croaker from random locations from nine bays in Texas. Data collected from stations in Louisiana was also analyzed, but there was no relationship between loss rate and average abundance so the Texas relationship was used in the model for both the LA and TX nursery areas.

The relationship between annual apparent loss rates (mortality plus surviving to the next life stage) and average abundance was linear with a positive, shallow slope for both populations. Loss rates and average abundance were standardized by dividing by the mean loss rate and mean average abundance. A linear relationship was fit to standardized loss rate plotted against standardized abundance for both GOM and MAB (Fig. 5.3). For the MAB, the relationship between standardized loss rate (SdLR) and standardized abundance (SdAb) was SdLR = 0.0516(SdAb) + 0.9481 (R^2=0.01) and for the GOM was SdLR = 0.1239(SdAb) + 0.876 (R^2=0.322).

The linear relationships between standardized mean loss rate and standardized abundance were used to create density dependence multipliers that were then applied to

late juvenile stage mortality rate every month of the simulation. I used a mini version of the model that simulated a single cohort of late juveniles for 6 months to determine multipliers of late juvenile stage mortality rate that resulted in relationships between apparent loss rate (those that died plus those progressed to age 1) and standardized abundance similar to those derived from the field data (see Fig 5.6A). The linear relationship between multiplier of mortality rate and standardized abundance derived for the MAB and GOM were very similar to the original relationships between standardized loss rate and standardized abundance estimated from the field data. For simplicity, I used the linear relationships originally derived for the field data in the model to determine multipliers of late juvenile mortality rates.

In full model simulations, the multiplier of late juvenile stage mortality rate was applied monthly to generate new values of P and G. The normalizing abundance was estimated for each nursery area in each population to be roughly the average late juvenile abundance under stabilized baseline simulation conditions (i.e., no density dependence or stochasticity). Each monthly time step for late juveniles, the simulated abundance of late juveniles predicted in each nursery area was divided by the appropriate normalizing abundance, a multiplier of mortality rate was calculated and applied to the baseline mortality rate, and then new values of P and G for the late juvenile stage were computed. This was repeated for each month that late juveniles were present.

5.3. Model Simulations

5.3.1. Stabilization of Baseline Conditions

The GOM and MAB baseline versions of the model (without stochasticity and density-dependence) were adjusted to obtain similar total annual abundances and stable

population trajectories. The actual absolute numbers in each population was arbitrarily set to be one million adults. Putting both populations on the same absolute scale helped in the comparisons of their responses to contaminant exposure. The growth, mortality, reproductive rates, and other population characteristics still differed between populations, and density-dependence (described below) was benchmarked to the simulated population abundances in each population. The simulated populations were stabilized to 1 million adults by adjusting the mortality rates of early and late juvenile stages. The mortality rates of early and late juveniles were adjusted because estimation of these parameters involved a high measure of uncertainty (Diamond et al., in prep). The same multiplier of mortality rate was applied to both nursery regions in each population but differed between populations. Subsequent baseline simulations were then performed that included stochasticity and density-dependent mortality.

5.3.2. PCB and MeHg Effects

Effects of PCBs and MeHg included reduced fecundities and egg survival that were measured directly in the laboratory, and changes in ocean larva stage duration and survival that were predicted from a larval cohort individual-based model applied to behavioral toxicological laboratory studies (Chapter 4).

Contaminant effects were imposed by creating new contaminant matrices for PCBs and MeHg exposed fish, and the contaminant matrices used altered elements of the baseline matrix. New fecundity estimates due to PCBs or MeHg were calculated by taking the percent reduction in fecundity observed in the laboratory (65% for PCBs and 33% for MeHg based on measured GSIs; Peter Thomas, unpublished data), and applying the same reduction to baseline fecundity values in the matrices. To impose the change in

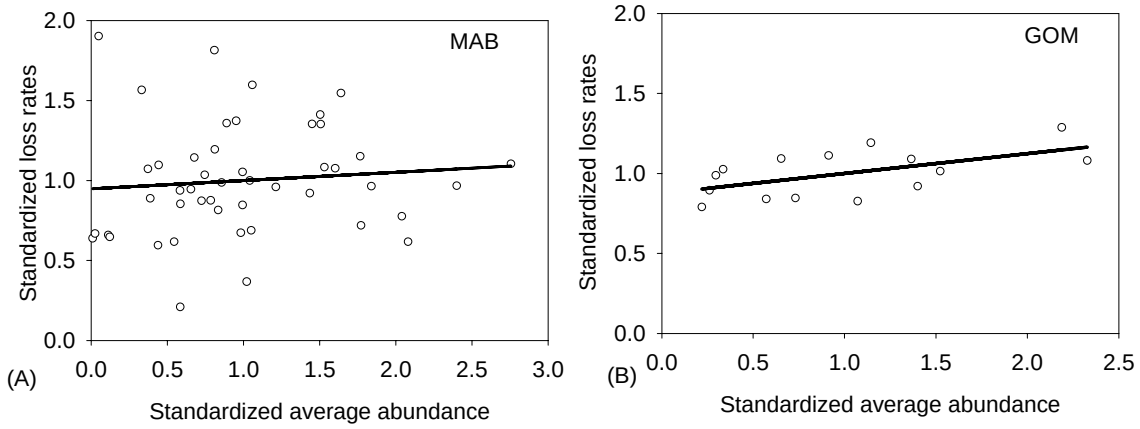

Figure 5.3. Linear relationships and observed values (from field data) between standardized loss rates and standardized average abundance for the (A) MAB (R^2=0.01) and (B) GOM (R^2=0.322) populations. The MAB function used pooled data sampled from Virginia and North Carolina, whereas the GOM function used data sampled from Texas only.

survival of eggs that was due to the effects of contaminants, egg survival was first estimated from baseline parameters ($\sigma = \exp^{-Z*D}$). Then, the percent reduction in survival due to contaminant exposure (81% for PCBs and 45% for MeHg; Thomas, unpublished data) was applied to the baseline survival. Finally, a new mortality (Z) was calculated, using the same stage duration as baseline, which resulted in new values of P and G for the egg stage.

Ocean larval stage duration and survival was altered in a similar way to egg survival but duration was also affected by contaminant exposure. I used the results from Chapter 4 that scaled the low dose PCB and low dose MeHg effects on larval behavior (swimming speeds and probability of escaping a predator) to stage duration and survival using statistical and individual-based models. Specifically, I used the results based on the linear regression using logits, and the PCB simulations were also assumed to have an

effect on larval growth via metabolism (Fig. 4.8 in Chapter 4). Ocean larval survival in the model was first calculated from baseline parameters. Then, the percent reductions in stage survival (47% for PCBs and 86% for MeHg) and stage duration (18.7% for PCB and 3.9% for MeHg) due to contaminants was applied to baseline parameters, and a new mortality rate (Z) was calculated using the changed survival and the new stage duration. New P and G values for the ocean larva stage were computed from the adjusted mortality rate and new stage duration.

I assumed some percent of individuals were affected in a specified nursery habitat area and that affected percent were moved into the contaminant matrices and tracked (Fig. 5.4). It was assumed that individuals would accumulate contaminants in the estuaries during their first year of life. After late juveniles left contaminated estuaries at age 1, they were moved to adult contaminant matrices. Adults in the contaminant matrices had reduced fecundities due to the effects of PCBs or MeHg. The eggs spawned from contaminant affected adults, were randomly distributed between the two nursery areas and were placed into contaminant matrices until estuarine larva stage. When the contaminant-affected individual reached the estuarine larval stage it was moved to the baseline matrix because contaminant effects no longer applied (Fig. 5.4).

5.3.3. Contaminant Exposure Scenarios

One-hundred year model simulations under different degrees of exposure of PCBs and MeHg in each nursery habitat were performed. PCB effects were simulated under two alternatives: first-time spawning and lifetime spawning. First-time spawning assumed that PCBs would accumulate in the ovaries of mature adult females because PCBs are lipophilic (Menone et al., 2000). Once the PCB-exposed females spawned for

the first time, the effects of the PCBs were removed under the assumption that female's body burden of PCBs was released with the eggs. The lifetime PCB effects alternative assumed that the effects of PCBs would last the lifetime of that female (i.e., spawned eggs at all ages). MeHg effects were simulated under the lifetime alternative only.

Contaminant scenarios were defined based on exposure occurring in a single nursery area with 10, 25, 50 or 100% of the individuals in that nursery area being exposed (Fig. 5.4). Analyses were performed for the MAB and GOM populations. Each year, the assumed percent of contaminant-exposed fish was applied to the number of age 1 survivors as they exited from their nursery area and they were moved to the contaminant adult matrix (i.e., reduced fecundity). The remaining percentage of age 1 survivors, assumed unexposed, were moved to the baseline adult matrix. Eggs that were produced from the contaminant adult matrix were randomly distributed between nursery areas (and spawning cohorts for MAB), and entered the contaminant YOY matrices (altered P and G values of eggs and ocean larva). Upon reaching the estuarine larval stage, exposed individuals were shunted to the baseline matrices for the remainder of the YOY stages (estuarine larvae, early juvenile, and late juvenile). Under first-time effects of PCBs, adults got moved to the baseline adult matrix after spawning for the first time, while for the life time effects for PCBs and MeHg exposed adults stayed in the contaminant matrix throughout their life. The assumption was that young got their PCBs and MeHg from their parents, who were exposed while the parents were themselvesYOY in the nursery habitats. The young then exhibited the contaminant effects but then, once reaching the estuarine larval stage, young became like unexposed individuals for the rest

of their lives. Young did not pass their contaminant burden onto their young, unless they themselves were also exposed while they were in their nursery habitat.

5.3.4. Model Predictions

Models predictions of population-related variables were compared among the baseline, first-time PCBs, lifetime PCBs, and lifetime MeHg exposure scenarios. Population-related variables examined were: annual number of adults (age 1 and older), annual numbers by age-class (age-structure), numbers entering the late juvenile stage each year, annual total egg production and by age-class (reproductive output), recruits versus spawners (i.e., number surviving to age 1 versus total eggs produced), and population growth rates (r). I reported numbers entering both the late juvenile stage and age-1 to examine annual dynamics prior to and after density-dependent mortality occurred. Population growth rates were calculated as the slope of the regression of $\ln(N_t)$ against year where where N is the number of adults each year. All outputs were based on years 20 through 100 in the simulation; the first 20 years were ignored to minimize any effects of initial conditions and to allow any imposed effects to manifest themselves. Coefficient of variation (CV=100*mean/sd) were computed for each replicate simulation, and then averaged over replicate simulations to obtain a single value of the CV. I ran ten replicate 100-year simulations for each condition. For clarity, I show the results of one replicate or three replicates simulations on some plots. The overall effects of PCBs and MeHg, in terms of changes in average adult abundance and population growth rates, were based on all 10 replicate simulations.

5.4. Results

5.4.1. Baseline Simulations

Total annual abundance of adult and late juveniles exhibited different dynamics between the baseline simulations of the MAB and GOM populations (Fig. 5.5). CV of adult abundance, averaged over three replicates, was 40.9% for the MAB population (Fig. 5.5A), compared to an average CV of 20.0% for the GOM population (Fig. 5.5B). The MAB population showed larger fluctuations in adult abundance than the GOM; Lankford and Targett (2001) reported large interannual fluctuations in Atlantic croaker population abundance in the MAB. As expected because I stabilized the density-independent, deterministic versions of the model, both populations showed population growth rates close to zero (Table 5.3). For the MAB population, both nursery areas and spawning cohorts contributed to the total number of individuals entering the late juvenile stage each year (Fig. 5.5C). For the GOM population, the number of individuals entering the late juvenile stage was much higher for the LA nursery area than for the TX area (Fig. 5.5D).

Predicted CVs of annual numbers of entering late juveniles were roughly in the same range as observed values derived from long-term field monitoring. The observed CVs were calculated by computing the summed sampling catch of late juveniles for each year of field sampling, and then calculating the CV over years (Diamond et al., in prep). The predicted CVs for late juvenile abundance were calculated from the total number entering each life stage by cohort and area for each year of the simulation. Model predicted CVs of late juveniles from MAB population ranged from 54 to 64% over replicates versus the observed CV values of 74% in Virginia estuaries and 54% in North

Carolina estuaries. Predicted CVs of late juveniles for the GOM population were about 60%, which is just slightly higher than observed values of 45% to 55%.

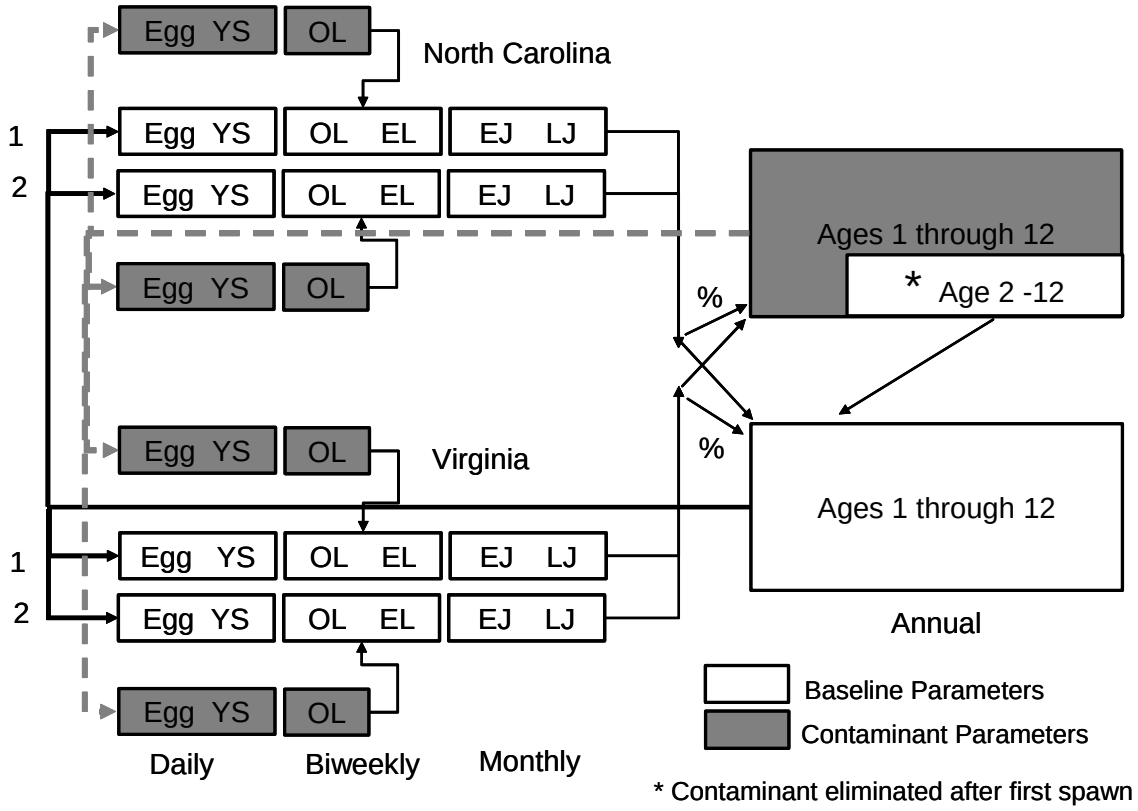

Figure 5.4. Schematic showing how contaminant exposed individuals were moved through baseline and contaminant-adjusted matrices in the MAB. Contaminant effects are imposed in a similar way for the GOM except that there is only one spawning cohort per year for each nursery area. Egg = egg lifestage, YS = yolk sac, OL = ocean larva, EL = estuary larva, EJ = early juvenile, LJ = late juvenile. Numbers 1 and 2 refer to spawning cohorts per year.

The number of individuals surviving to age 1 mimicked the number of individuals entering the late juvenile stage for the MAB population (Fig. 5.5E) but not for the GOM population (Fig. 5.5F). For the MAB population, the numbers of individuals surviving to age 1 was an order of magnitude smaller than the number of late juveniles, but the temporal patterns were very similar (Fig. 5.5E). For the GOM population, the numbers surviving to age 1 were also about an order of magnitude smaller than the numbers entering the late juvenile stage, but the annual numbers of age 1 were much more dampened than the late juveniles; large spikes in late juvenile abundance were not mirrored in numbers of age 1 (Fig. 5.5F).

Dampened numbers surviving to age 1 in the GOM was likely due to more individuals experiencing a strong density-dependent mortality during the late juvenile stage. The multiplier function of late juvenile mortality rate for the GOM had a slightly steeper slope than the function for the MAB (Fig. 5.6B). This resulted in a stronger compensatory relationship between annual spawners (total eggs) and recruits (number surviving to age 1) for the two GOM nursery areas (Fig. 5.6D) compared to the VA and NC nursery areas of the MAB (Fig. 5.6C). The relationship between recruits and spawners showed more leveling off at high egg production for LA and TX. While TX had the strongest density dependent relationship of all of the nursery areas, relatively few individuals came through the TX nursery area compared to the LA area.

Simulated age-structure differed between the MAB and GOM populations (Fig. 5.7). Both populations averaged about one million total adults. Individuals lived to age 12 in the MAB and to age 8 in the GOM. Age 1 and age 2 individuals contributed

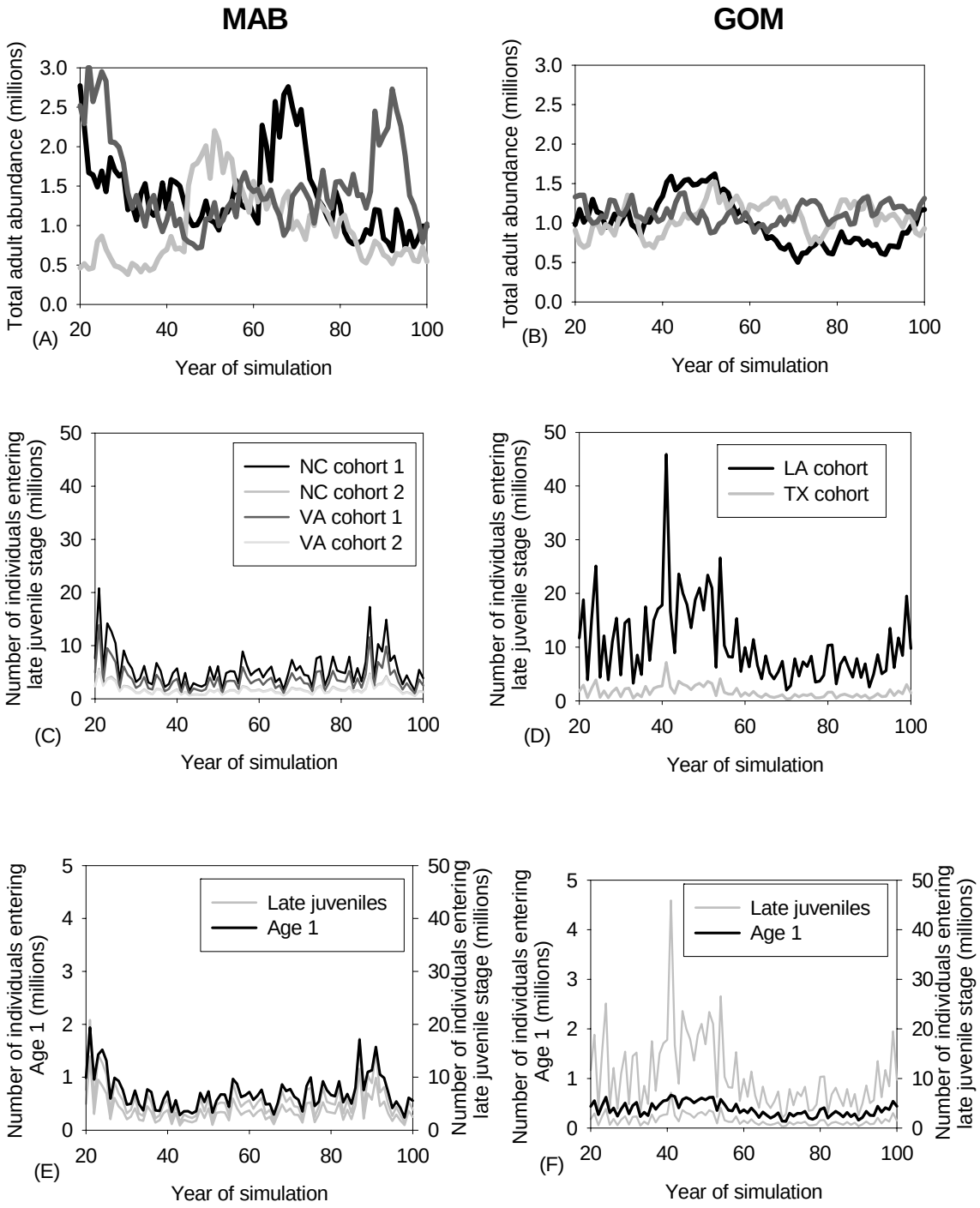

Figure 5.5. Predicted annual abundances of adults (A and B), number entering the late juvenile stage by nursery and cohort (C and D), and number surviving to age 1 (E and F) from replicate simulations of the MAB and GOM populations Three representative replicate simulations are shown in the top row, and one replicate simulation is shown in the middle and bottom rows. Note the scale difference for age 1 survivors on the left side y-axis and number entering late juvenile stage on the right side y-axis of panels (E) and (F).

proportionately more to the MAB population (Fig. 5.7A) than they did to the GOM population (Fig. 5.7B). Age frequency histograms (vertical slices through Fig. 5.7) were more peaked and showed a steeper decline with age for the MAB, while they were flatter with age for the GOM.

Differences in age structure between the MAB and GOM were also reflected in reproductive output (annual total eggs) by age (Fig. 5.8). In the MAB, which was more dominated by younger adults, age 2 and age 3 individuals produced the most eggs (30% and 25% of the total). In the GOM population, young age classes were also important but the more even age-structure resulted in young ages being somewhat less important to the total (26% for age 2 and 21% for age 3). Ages 1 through 3 combined contributed an average of 59% of the total eggs each year for the MAB versus 52% for the GOM.

5.4.2. PCB and MeHg Simulations

Simulated population responses to PCBs and MeHg differed somewhat between the MAB and GOM populations, and were affected by the nursery habitat of exposure, percent of individuals exposed, and first time versus lifetime effects (Fig. 5.9). In both the MAB and GOM, simulated populations exhibited the greatest declines with increasing percent exposure for only one of the two nursery areas (VA for MAB and LA for GOM). Exposure to PCBs or MeHg in the NC nursery area resulted in a lowered population abundance with increasing percent exposed, but the effect was smaller than for exposure in VA. Exposure of up to 100% of the individuals in the TX nursery area resulted in almost no decrease in average population abundance.

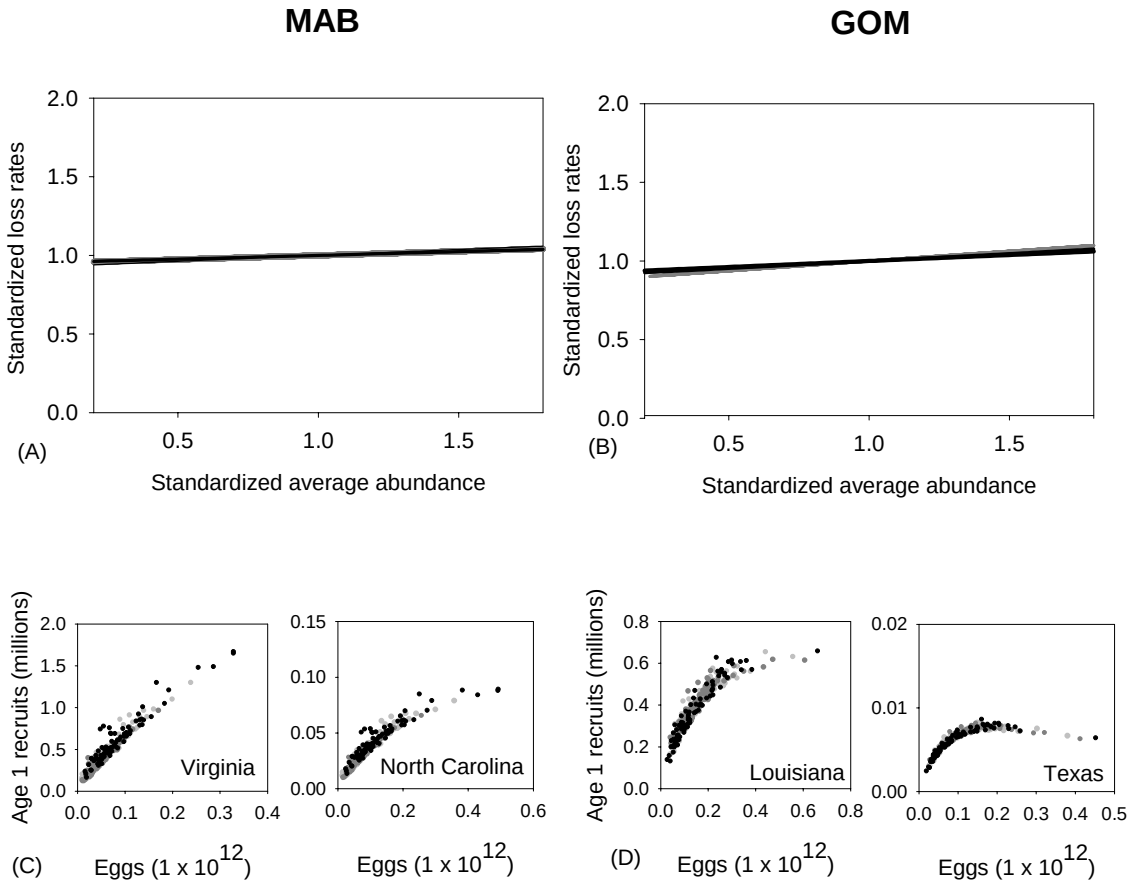

Figure 5.6. Simulated (black line) and fitted to field data (grey line) relationships between standardized loss rates and standardized average abundance for the (A) MAB and (B) GOM. Panels (C) and (D) show the spawner-recruit relationships for MAB and GOM that result from the same relationships for density dependent late juvenile mortality as used in (A) and (B) but imposed in the baseline simulation of the full model. Density-dependent mortality of late juveniles was simulated by deriving a linear function between the multiplier and standardized abundance, that when applied every month in a mini version of the matrix model (single cohort of late juveniles), resulted in the simulated relationship between standardized loss rate and standardized average abundance similar to field data (A and B). This linear function was then incorporated into the full matrix model and the spawner-recruit relationships shown in (C) and (D) resulted.

Changes in population growth rates (Table 5.3), computed from the predicted time series of annual adult abundances, generally reflected the responses predicted in mean population abundances (Fig. 5.9). Population growth rates declined relative to baseline the most with increasing percent exposure when individuals were exposed in the VA or LA nursery areas, declined only moderately for NC exposure, and changed very little from the baseline value for TX exposure.

First time versus lifetime effects of PCBs had the expected consequence of resulting in relatively smaller decreased populations for first time effects, especially for VA and LA exposures where responses to exposure were very clear (Fig. 5.9). Predicted reductions in population abundance with increasing percent exposure were less dramatic for VA and LA exposures when PCB effects were first time only as compared to PCB effects assumed to operate over the entire lifetime (black circles decreased less with increasing percent exposure in top PCB panel versus in the middle PCB panel of Fig. 5.9). The same lessening of response for first time effects versus lifetime effects was predicted for the NC exposure, although the decline in both cases was less severe than for the VA or LA exposures.

The effects of PCBs and MeHg differed between the MAB and GOM populations, with the GOM population appearing to be more resilient than the MAB population (Fig. 5.9; Table 5.3) In the MAB, PCBs and MeHg affected population abundance when only 10% of individuals from the VA nursery area were exposed. In contrast, the GOM population did not show clear negative responses until 25% of the individuals were exposed. For the 25% and 50% exposures of individuals in VA or in LA

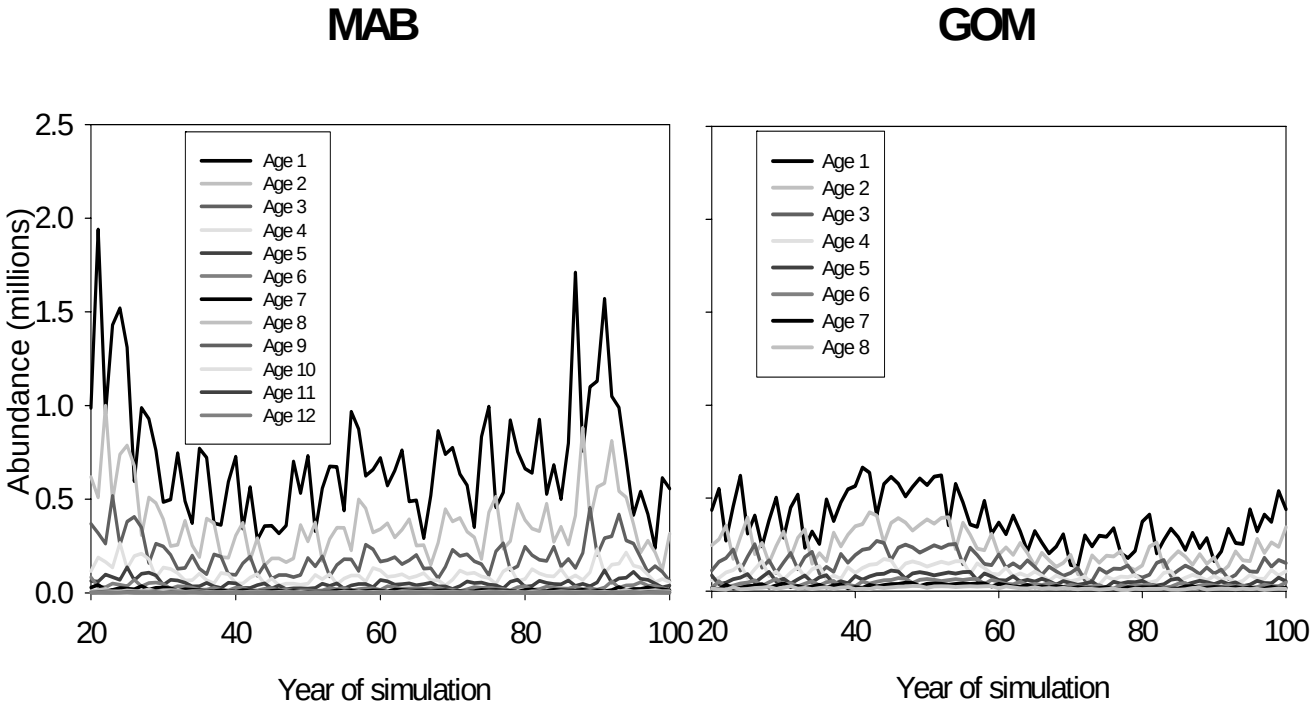

Figure 5.7. Predicted age structure from a representative replicate simulation under baseline conditions for the MAB and GOM populations.

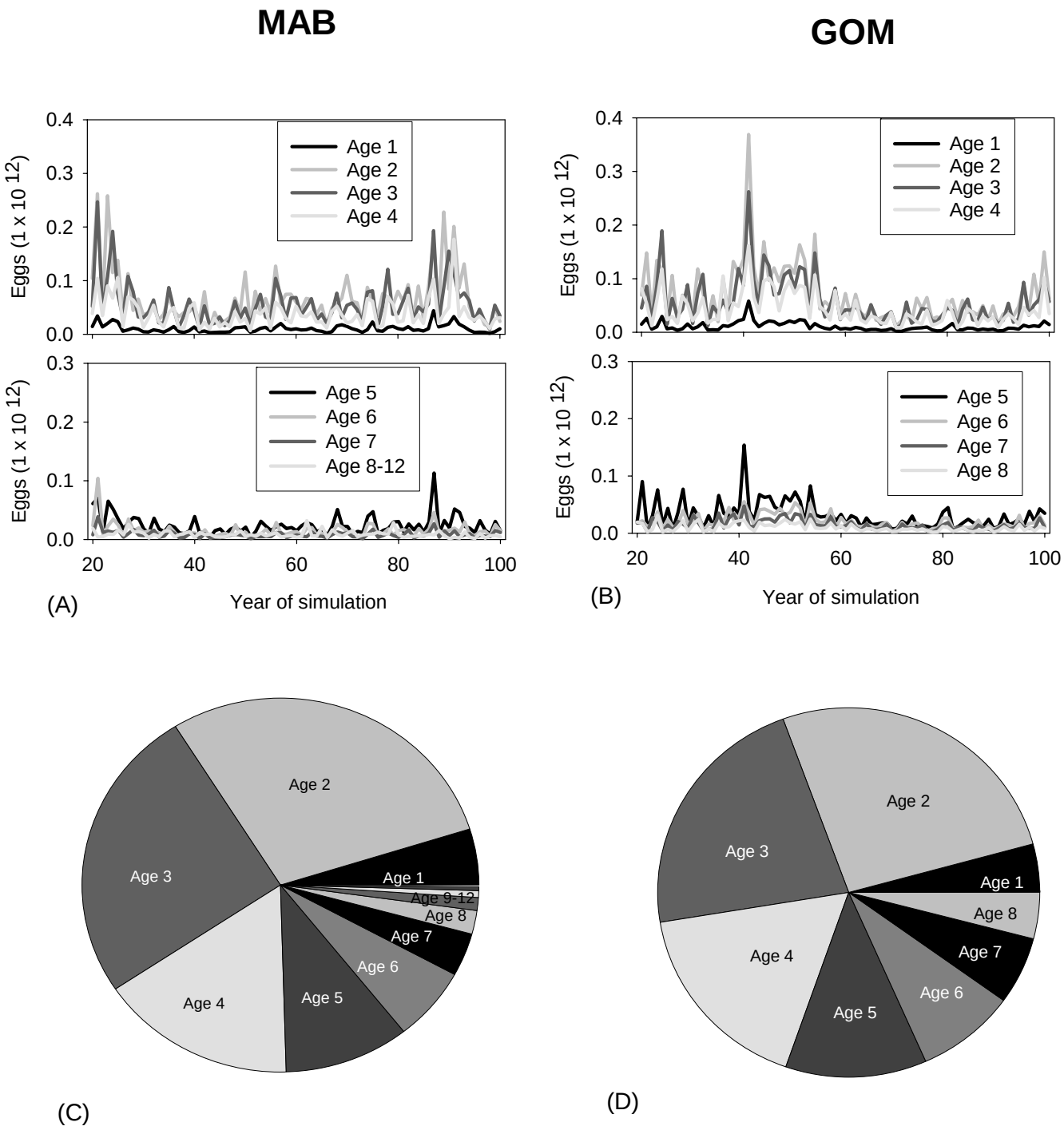

Figure 5.8. Predicted reproductive output (percent of annual eggs) by age for the MAB and GOM, shown as time series plots of a single replicate simulation (A) and (B) and as a pie chart based on averaging over years and three replicate simulations (C and D) .

Figure 5.9. Predicted average annual adult abundance for baseline, first time PCB effects, lifetime PCB effects, and lifetime MeHg effects for the MAB and GOM under 10, 25, 50, and 100% of the individuals exposed in each of the nursery areas. Open bars represent mean and standard error of total population abundance based on ten replicate simulations. Circles represent the mean total abundance over years from each replicate simulation.

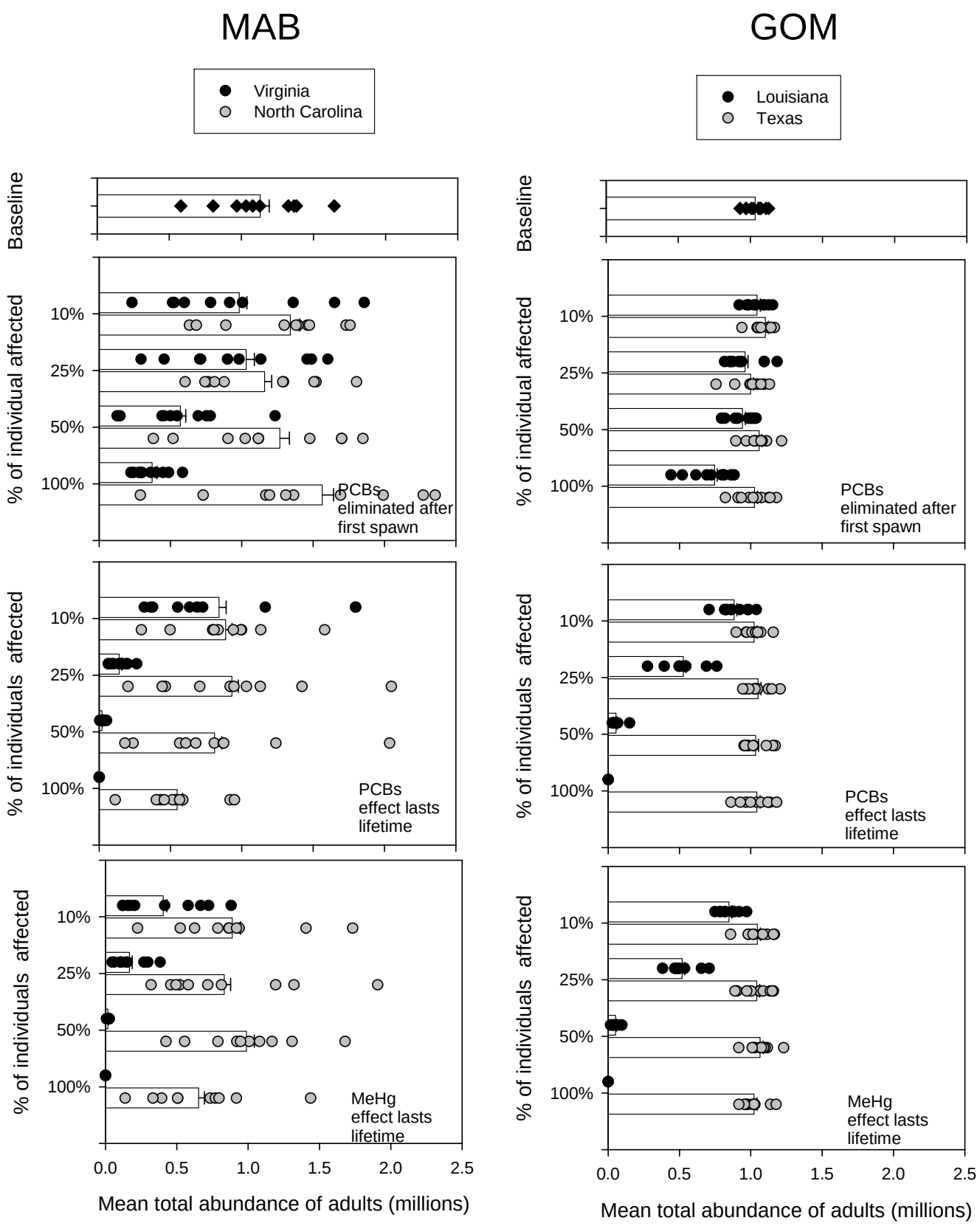
MAB
GOM
Virginia
North Carolina
Louisiana
Texas
Baseline
% of individual affected
% of individuals affected
10%
25%
50%
100%
PCBs eliminated after first spawn
PCBs effect lasts lifetime
MeHg effect lasts lifetime
0.0
0.5
1.0
1.5
2.0
2.5
Mean total abundance of adults (millions)

Table 5.3. Estimated population growth rates (r) from simulated annual adult abundances for baseline, first time PCB effects, lifetime PCB effects, and lifetime MeHg effects for the MAB and GOM under 10, 25, 50, and 100% of the individuals exposed in each of the nursery areas.

Region	MAB		GOM	
Baseline	-0.0014		0.0002	
Nursery Area	VA	NC	LA	TX
PCBs eliminated after first spawn				
10 % affected	-0.0100	-0.0093	-0.0004	0.0015
25 % affected	-0.0074	-0.0081	-0.0012	-0.0007
50 % affected	-0.0190	-0.0123	0.0009	-0.0010
100% affected	-0.0310	-0.0030	-0.0006	-0.001
PCBs effect last lifetime				
10 % affected	-0.0189	-0.0022	-0.0027	-0.0009
25 % affected	-0.0478	-0.0076	-0.0090	-0.0023
50 % affected	-0.1249	-0.0162	-0.0605	0.0029
100% affected	-0.4488	-0.0111	-0.5202	-0.0006
MeHg effect last lifetime				
10 % affected	-0.0202	-0.0151	0.0015	-0.0001
25 % affected	-0.0640	0.0009	-0.0101	0.0020
50 % affected	-0.1246	-0.0152	-0.0542	-0.0015
100% affected	-0.4249	-0.0167	-0.4483	0.0012

to both PCB scenarios and to MeHg, the MAB population abundance declined more than the GOM abundance.

The greater resilience of the GOM population to contaminant effects can be explained, in part, by differences between the GOM and MAB age structure and degree of density-dependent mortality. First time effects of PCBs illustrated how age structure could influence population responses. Baseline simulations demonstrated that older individuals contributed more to eggs production in the GOM than in the MAB, and that age-2 individuals dominated reproductive output in the MAB (Fig. 5.8). First time effects of PCBs only affected the fecundity of adults while they were age 1 or age 2 individuals, after which all have matured and so subsequent spawning was not longer affected by PCBs. Both the MAB and GOM populations used the same maturity schedule with age. The MAB population showed greater declines to increasing exposures with first time effects because reduced fecundity affected more of the spawning population. For example, under 50% exposure the contribution to annual egg production in VA from age 1 individuals was reduced by 1.3% and from age 2 individuals by 5% with little shifts in age-specific contributions for LA (Fig. 5.10).

Greater resilience of the GOM population was also due to stronger density dependent mortality of late juveniles. Spawner-recruit relationships for each nursery habitat (Fig. 5.11) were plotted for the exposures that showed the greatest difference between the two populations (i.e., 50% exposure in VA and LA for first time PCB effects, and 25% exposure for VA and LA for lifetime PCB and MeHg exposures).

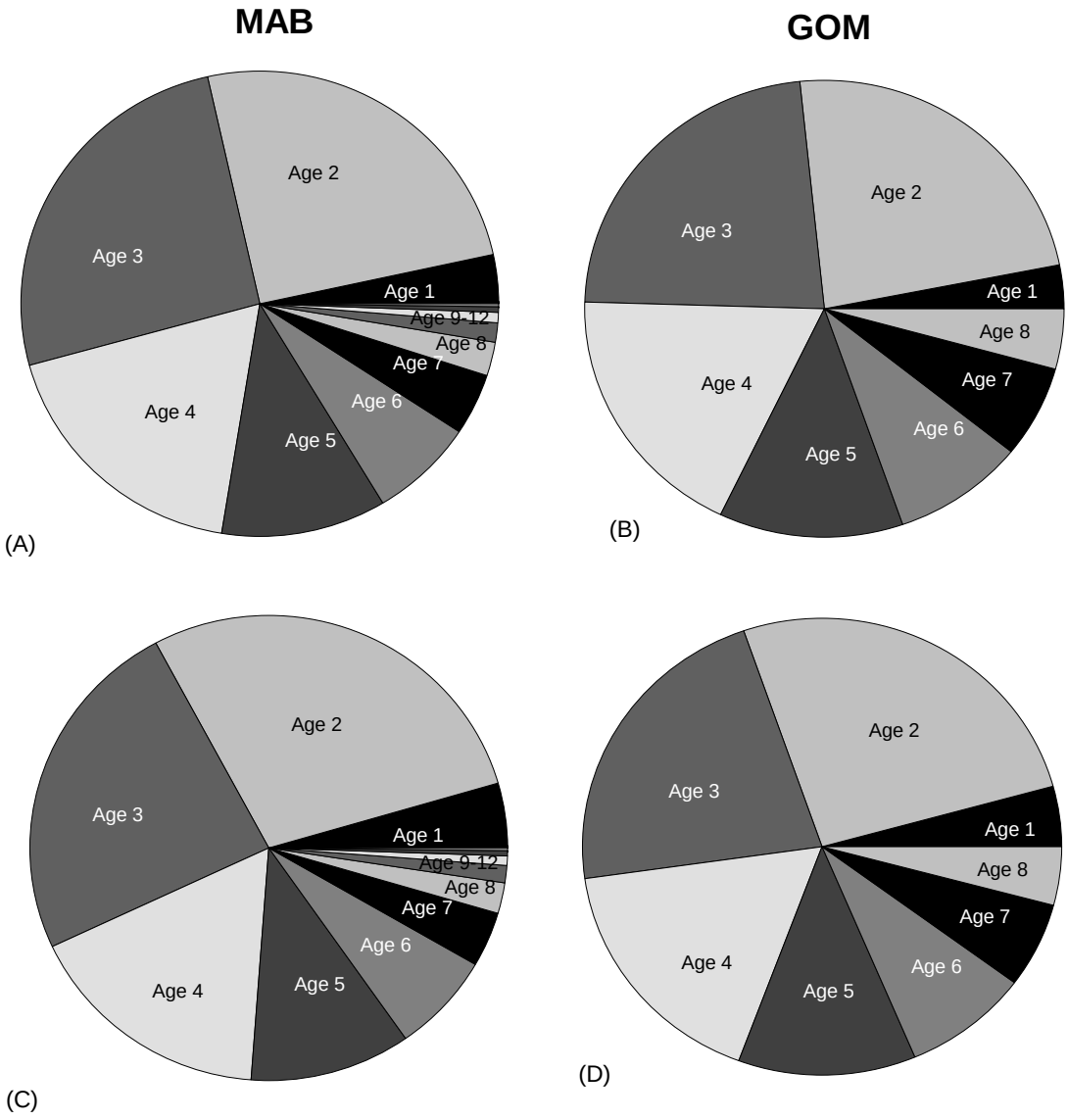

Figure 5.10. Mean reproductive output (percent of annual egg production) by age class for a 50% exposure level of PCBs assumed to have first time effects for exposure occurring in (A) Virginia, (B) Louisiana, (C) North Carolina, (D) Texas. Averaged contributions by age were based on averages computed over years in each of three replicate simulations, and then averaged over replicates.

For the first time PCB effects under 50% exposure in VA, the spawner recruit relationships in both VA and NC were both nearly linear and showed little compensation (Fig. 5.11A). In contrast, the spawner-recruit relationships in LA and TX under the 50% LA exposure showed a wider range of egg production values and a leveling off at recruitment at very high values of egg production (Fig. 5.11A). For the lifetime PCB and MeHg effects with 25% exposure in VA, the spawner-recruit relationships for VA and NC were condensed near the origin at low egg production and where little density-dependence occurs (Fig. 5.11B and C). The spawner-recruit relationships in LA and TX under 25% exposure in LA showed that density-dependent survival was important for the late juvenile stage, as recruitment leveled off at high egg production values (Fig. 5.11 B and C).

5.5. Discussion

Using a bottom-up approach to scale the laboratory results on Atlantic croaker to the population level suggests that, under high enough exposure levels, PCBs and MeHg could induce significant changes in population dynamics (Fig. 5.9). When PCBs and MeHg were assumed to affect adults and their offspring throughout their lifetime, both resulted in similar responses, despite the fact that each contaminant imposed different effects on lifestages (Table 5.3). Based on the laboratory experiments used to define effects, PCBs had a much larger effect on egg survival and fecundity than MeHg, whereas MeHg imposed a greater reduction in the survival of ocean larvae. However, the mechanistic differences in contaminant effects showed very little resolution at the population level. A much larger effect was whether the contaminant effects were

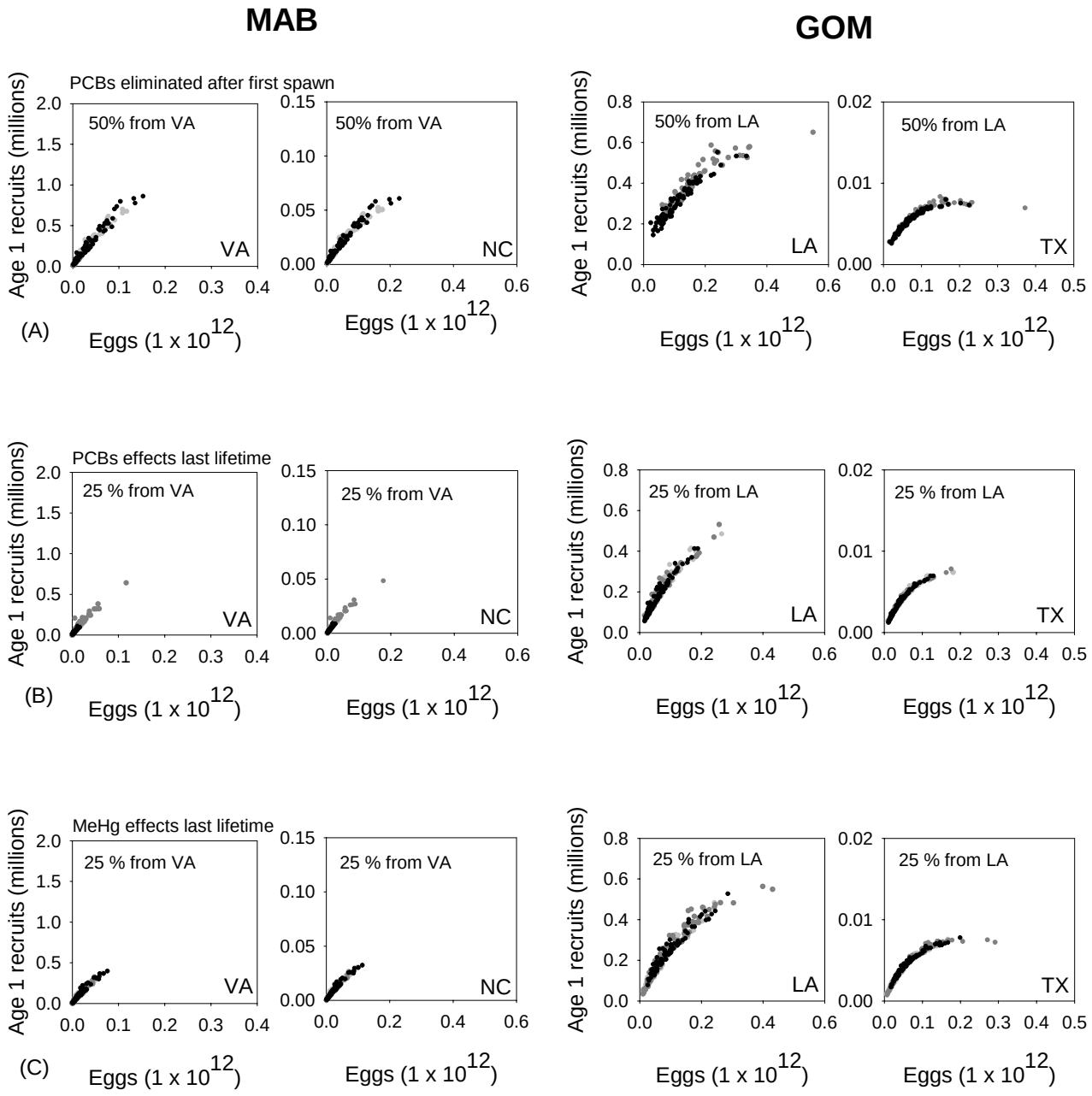

Figure 5.11. Predicted spawner-recruit relationships by nursery area for the MAB and GOM populations for 50% exposure level with first time PCB exposure, and for 25% exposure levels for the lifetime PCB and lifetime MeHg exposures. MAB exposure occurred in the VA nursery area and GOM exposure occurred in the LA nursery area.

eliminated with the eggs (first time effects) or maintained throughout the lifetime of the adult. With everything else equal, predicted responses to PCB exposure were consistently smaller under first time effects than under lifetime effects, and these differences were much larger than the differences between comparable PCB and MeHg exposures. One interesting question that deserves further exploration is whether first time or lifetime effects are more realistic for PCBs, and whether it also applies to MeHg.

The effects of contaminants on simulated Atlantic croaker populations in MAB and GOM depended were dominated by exposure in one of the two nursery areas. Predicted population responses were greatest for VA and LA exposures, with only moderate response predicted for NC exposure and no response predicted for TX exposures (Fig. 5.9; Table 5.3). In the MAB, more eggs entered the NC estuaries (60%) than the VA estuaries (Fig. 5.5), but the high mortality experienced by late juveniles in NC due to bycatch (Table 5.2) meant that NC was not contributing many individuals to the total population abundance. In the GOM, not only did more eggs enter the LA nursery habitat (60%) than the TX habitat, but TX also included a high late juvenile mortality rate due to bycatch.

For a given percent exposed, predicted population declines to VA and LA exposures were consistently greater in the MAB than in the GOM (Fig. 5.9). The first time effects results clearly demonstrated the greater resilience of the GOM population. Predicted decreases in mean population abundance occurred in the MAB at the 50% and 100% exposures for VA exposure, whereas the predicted decrease in the GOM was still small even at the 100% exposure in LA (Fig. 5.9). Greater resilience of the GOM population was also seen in the lifetime exposure simulations, as the decrease in mean

abundance of the MAB population with increasing percent exposed in VA was more dramatic than the decline predicted for the GOM with increasing exposure in LA.

The differences in population responses between the MAB and GOM can, in part, be explained by life history and different fishing pressures on Atlantic croaker between the MAB and GOM populations. Adult mortality rates differed between the MAB and GOM (Tables 5.1 and 5.2), and this resulted in different age structures (Fig. 5.7) and slightly different reproductive output by age (Fig. 5.8). In the MAB older croaker are caught for a food fishery, which allows for increased numbers of younger age classes to persist relative to older age classes, therefore the younger age classes contribute more eggs. In contrast, in the GOM, all ages appear to be equally likely to be fished (Diamond et al., 1999). In the MAB, age 2 and age 3 croaker contributed proportionately more eggs than in the GOM. In the GOM, the age class contributions for age 5 and older decreased slightly with age, whereas in the MAB age 5 and older individuals contributed much less eggs.

Site specific factors may also contribute to the differences observed between the MAB and GOM population responses to contaminants. The MAB experienced additional stress in the form of winterkill, whereas populations in the GOM were not exposed to such cold conditions. The density dependence of the late juvenile mortality rate appeared to be stronger in GOM, which was likely due to the application of a different linear function with a slightly steeper slope (Fig. 5.6). Density dependent mortality relationships have been shown to be site specific and to vary between populations of other species of fish, implying that the degree of density dependence may be shaped by local available habitat and environmental conditions (Rose and Cowan, 2000).

Differences in density dependent relationships between populations can play an important role in how populations respond to contaminant stress. Because the GOM population exhibited a stronger density-dependent relationship between recruits (age 1 survivors) and spawners (egg production) (Fig. 5.11), the GOM population was more resilient than the MAB population to changes induced by contaminant stress.

Simulation results from this study are somewhat consistent with previous elasticity analyses that were done on the MAB and GOM populations using matrix models that did not include stochasticity or density dependence (Diamond et al., 2000). Prior elasticity analyses suggested that the MAB population was more sensitive than the GOM population to fecundity. In the simulations presented here, the MAB population was predicted to decline more than the GOM population with increasing levels of exposure (Fig. 5.9). However, prior sensitivity analyses also suggested that both MAB and GOM populations were more sensitive to mortality in ocean larva stage than to any other lifestage. While PCBs and MeHg had different effects on fecundity, egg survival, and ocean larval stage duration and survival in my model simulations, the predicted population responses at comparable exposure levels were relatively similar. The relative insensitivity of the model to different magnitudes of effects among fecundity, egg survival, and ocean larval survival, was likely due to the sequential nature of the effects affecting YOY life stages and the application of a density dependent mortality function in the latest YOY stage (late juveniles). Other analyses of population models also have shown how it is difficult to track the effects of changes to vital rates after they are compensated for by density dependence in later stages (Grant, 1998). The relative importance of changes to the ocean larval stage, relative to other effects, was therefore

unclear from simulations. If PCBs and MeHg, with their different mixes of effects, had resulted in different population responses, perhaps the relative importance of the changes in the ocean larval stage in the model simulations could have been inferred.

My simulations of PCB and MeHg effects are within the realm of possibility as both PCBs and MeHg are found in the sediments of estuaries in the MAB and GOM (Summers, 2001). The US Environmental Protection Agency (EPA) set up the Environmental Monitoring and Assessment Program (EMAP) in which estuarine conditions were survey in 87% of estuaries in the continental US. From 1991 to 1997, EMAP surveyed 190 stations along the east coast of the U.S (http://www.epa.gov/emap), and divided the stations into provinces: Louisiana province included estuaries from LA and TX, Carolina province included estuaries from NC, and Virginia province included estuaries from VA. About 1-2% of the estuarine sediments in the entire US exceeded concentrations of contaminants that were above what EMAP termed ER-M guidelines (i.e., contaminant concentrations high enough to be associated with adverse effects on estuarine organisms in the field and laboratory). Around 10-29% of the estuaries in the entire US contained sediments with contaminant concentrations that exceeded ER-L guidelines (i.e., contaminant concentrations with a low, but a non-zero probability of affecting an organism adversely).

Contaminants in the sediments varied between the MAB and GOM geographic regions (Summers, 2001). In the MAB, 46% of the estuarine sediments were enriched with metals, such as methylmercury, and 63% of the sediments were enriched with PCBs. The GOM had generally lower occurrences of contaminants, with 29% of sediments enriched by metals and 28% enriched with PCBs. Most locations exceeding ER-M

guidelines were located in the MAB, while the GOM contained many locations with contaminant concentrations in excess of the ER-L guidelines. Thus, it is likely that croaker in these nursery habitats are exposed to some levels of PCBs and MeHg.

I attempted to relate the low dose experimental results used to define the effects of PCBs and MeHg in simulations to body burdens measured in field-caught croaker. During sampling for EMAP, a trawl was done at each station and the organisms caught in the trawl were homogenized by species and analyzed for body burdens of contaminants (http://www.epa.gov/emap). I used data from the last year of sampling for each province and computed average body burdens of mercury and PCBs in Atlantic croaker for the east coast, and the Carolina, Louisiana, and Virginia sampling provinces (Table 5.4). The low dose of PCBs used in the laboratory was calculated to be approximately 3.3 µg/g of dry weight of ovary which translates roughly to a concentration of 0.66µg/g dry weight of muscle tissue (2.5:0.5 = ratio of contaminant in ovary:muscle therefore 3.3 µg/g ovary = 0.66 µg/g of muscle; Rose et al., 2003). The MeHg concentration used in the laboratory experiment was measured in the eggs to be 0.3 to 1 ng/g of fish egg (Alvarez, 2005). Assuming a 2% transfer of MeHg to the egg (Alvarez, 2005), results in an adult body burden of 0.015 to 0.05 µg/g fish.

The low dose PCB concentrations used in the laboratory experiments were high relative to EMAP field- measured concentrations (0.66 µg/g versus about 0.01 to 0.1 µg/g). The low dose concentrations are possible, as concentrations similar to those that resulted from the low dose have been reported in other field-caught fish species, albeit in highly contaminated areas (Rose et al., 2003). The low dose of MeHg used in the

Table 5.4. PCB and MeHg concentrations in field-caught Atlantic croaker tissue collected as part of the EMAP.

	N stations	N croaker	Contaminant	Mean concentration (µg/g fish)	Std Error	Lower CL (95%)	Upper CL (95 %)
Entire East Coast	190	69	Hg	0.07880	0.01093	0.05698	0.10061
		79	PCB	0.03132	0.00627	0.01883	0.04380
Carolina	24	16	Hg	0.15475	0.03310	0.08419	0.22531
		16	PCB	0.09802	0.02293	0.04915	0.14690
Louisiana	89	43	Hg	0.06653	0.00915	0.04806	0.08500
		50	PCB	0.01423	0.00201	0.00376	0.01184
Virginia	77	10	Hg	0.01000	0.00211	0.00523	0.01477
		13	PCB	0.03965	0.00634	0.02582	0.05348

laboratory experiments was within the range of values reported in field-caught croaker (0.015 to 0.5 µg/g versus about 0.01 to 0.15 µg/g).

While I tried to incorporate a high degree of biological realism in the croaker population model (e.g., nursery-specific density dependence and YOY stage durations and survival rates), the model had some limitations. First, the model was stabilized to ease analysis and comparisons between populations. Atlantic croaker populations could already be in a state of decline and experiencing stress from a variety of other sources (Diamond et al., 2000); in a declining population, the added effects of contaminant stress could exacerbate population decline. Second, the model was stabilized with fishing in the baseline model set to projected harvesting goals. It is likely that fishing pressure will fluctuate over the next 100 years and, to date, the target management fishing mortality rates have not been achieved in all areas. Third, because I incorporated density dependence and stochasticity, model analyses required simulation. I could not calculate population growth rate using equilibrium analysis, as such analyses are only possible for very specific versions of stochastic and density dependent matrices (Caswell, 2000).

Finally, the effects of PCBs and MeHg on Atlantic croaker included in this model are likely not the only effects induced by these contaminants. Effects on egg survival, fecundity, and ocean larval stage duration and survival were the effects measured consistently in the laboratory experiments. The matrix model structure is very flexible, and as additional effects of PCBs and MeHg on croaker become available, they can be incorporated into model simulations.

My analysis is an example of using empirically grounded models in a way that allows for comparison of long-term responses of two different populations to exposure to two different contaminants. Others have used realistic site-specific models but examined single contaminants (e.g., Jaworska et al., 1996; Rose et al., 2003), or have used theoretical models to compare contaminants as idealized stressors (e.g., Schaaf et al., 1993; Spromberg and Birge 2005). There are very few studies that examine the effect of an interaction between toxicant effects and organism density on population dynamics (Forbes et al., 2001). Conservation biologists have expressed concern over the omission of density dependence in the study of most field populations (Grant and Benton, 2000). Extensive use of literature information and analysis of long-term field data (Diamond et al., in prep) enabled specification of differences between the MAB and GOM populations, and differences between nursery areas within each population. Coordination with toxicologists and ecologists enabled laboratory experiments that documented PCB and MeHg effects on fecundity and egg survival that could be used directly to change matrix model parameters, and documented behavioral effects on larvae that then could be scaled using statistical and individual-based modeling (Chapter 4) to changes in matrix model parameters.

My analysis demonstrates that with careful analysis of literature studies and field data, and coordinated laboratory studies, subtle and behavioral effects of endocrine disruptors can be scaled to long-term population responses. My analyses also illustrate why it can be difficult to document a population decline in response to an endocrine disrupting chemical in an oceanic species. When the species under investigation has a dispersal phase in its life history and exhibits no site fidelity, it is difficult to relate local contamination to overall population abundance (Schaaf et al., 1987). The extreme situation was illustrated in this analysis. Model results showed that it was possible for an entire estuarine habitat area (TX in the GOM model) to be heavily impacted by contaminants (100% exposure) and not cause a detectable population decline. Model analyses were set up in an ideal situation to be able to detect responses; the only difference between baseline and exposed simulations was the effects of the contaminant. In nature, we do not have luxury of repeating history without and with a stressor, and other factors (e.g., water temperature, prey and predator dynamics, fishing pressure) that vary within and between were treated as invariant in model simulations.

Pollution has been defined as one of three leading causes of extinction in marine species (Reynolds et al., 2005). Generally, over-exploitation is considered the first major cause of extinction, and habitat loss is a close second. More often than not, a fish population is exposed to multiple stressors in the natural environment, and the effects are not always additive or predictable (Power, 1997). While contaminants may not exert as noticeable dramatic effect on fish populations, except in certain highly-contaminated situations, the stress imposed by contaminants may make a population more susceptible to other perturbations such as fishing, hypoxia, climate change, and exotic species

alterations of community structure (Forbes et al., 2003). The model presented here shows good potential as a tool for interpreting the population responses to contaminant stress in complicated systems. With further refinements that include varying the effects of other stressors and generating estimates of uncertainty, my modeling approach should have utility in teasing out how multiple natural factors and anthropogenic stressors affect fish population dynamics.

5.6. References

Allen, Y., Scott, A.P., Matthiessen, P., Haworth, S., Thain, J.E. and Feist, S. 1999. Survey of estrogenic activity in United Kingdom estuarine and coastal waters and its effect of gonadal development of the flounder *Platichthys flesus*. *Environ. Toxicol. Chem*.18: 1791-1800.

Alvarez, M. C. 2005. Significance of environmentally realistic levels of selected contaminants to ecological performance of fish larvae: effects of atrazine, malathion, and methylmercury. PhD Dissertation. University of Texas, Austin, Texas.

Barnthouse, L. W., Suter, G. W.I. and Rosen, A. E. 1990. Risks of toxic contaminants to exploited fish populations: influence of life history, data uncertainty and exploitation intensity. *Environ. Toxicol. Chem.* 9:287-311.

Brown, A. R., Riddle, A. M., Cunningham, N. L., Kedwards, T. J., Shillabeer, N. and Hutchinson T. H. 2003. Predicting the effects of endocrine disrupting chemicals on fish populations. *Hum. Ecol. Risk Assess.* 9:761-788.

Caswell, H. 2000. Matrix population models. Sinauer Associates Inc., Sunderland, Massachusetts.

Diamond, S. L., Cowell, L.G. and Crowder, L. B. 2000. Population effects of shrimp trawl bycatch on Atlantic croaker. *Can. J. Fish. Aquat. Sci.* 57:2010-2021.

Diamond, S. L., Crowder, L.B. and Cowell, L. G. 1999. Catch and bycatch: the qualitative effects of fisheries on population vital rates of Atlantic croaker. *Trans. Am. Fish. Soc.* 128:1085-1105.

Diamond, S.L., Murphy, C.A and Rose, K.A. (in prep). Simulating the effects of global warming on Atlantic croaker population dynamics in the Mid-Atlantic region: pushing the limits on what we know. To be submitted to *Global Change Biology.*

Fogarty, M. J., Sissenwine, M. P. and Cohen, E.B. 1991. Recruitment variability and the dynamics of exploited marine populations. *TREE* 6: 241-246.

Forbes, V. E., and Calow, P. 2002. Extrapolation in ecological risk assessment: balancing pragmatism and precaution in chemical controls legislation. *Bioscience* 52:249-257.

Forbes, V. E., Sibly, R. M. and Calow, P. 2001. Toxicant impacts on density-limited populations: a critical review of theory, practice and results. *Ecological Applications* 11:1249-1257.

Forbes, V. E., Sibly, R.M. and Linke-Gamenick, I. 2003. Joint effects of population density and toxicant exposure on population dynamics of Capitella sp. I. *Ecological Applications* 13:1094-1103.

Govoni, J. J., Ortner, P. B., Al-Yimani, F and Hill, L.C. 1986. Selective feeding of spot, *Leistomus xanthurus* and Atlantic croaker, *Micropogonias undulatus*, larvae in the Northern Gulf of Mexico. *Mar. Ecol. Prog. Ser*. 28: 175-183.

Grant, A. 1998. Population consequences of chronic toxicity: incorporating density dependence into the analysis of life table response experiments. *Ecol. Model.* 105:325-335.

Grant, A. and Benton, T. G. 2000. Elasticity analysis for density-dependent populations in stochastic environments. *Ecology* 81:680-693.

Hales, L.S. Jr. and Reitz, E. J. 1992. Historical changes in age and growth of Atlantic croaker, *Micropogonias undulatus* (Perciformes: Sciaenidae). *J. Archaeol. Sci.* 19:73-99.

Hansen, F., Forbes, V.E. and Forbes, T. L. 1999. Using elasticity analysis of demographic models to link toxicant effects on individuals to the population level: an example. *Funct. Ecol.* 13:157-162.

Heppell, S., Caswell, H. and Crowder, L.B. 2000. Life histories and elasticity patterns: perturbation analysis for species with minimal demographic data. *Ecology* 81: 654-665.

Jaworska, J.S., Rose, K. A., and Barnthouse, L. W. 1997. General response patterns of fish populations to stress: an evaluation using an individual-based simulation model. *J. Aquat. Ecosys. Stress Recov*. 6:15-31.

Jaworska, J.S, Rose, K. A and Brenkert, A. L. 1997. Individual-based modeling of PCBs effects on young-of-the-year largemouth bass in southeastern USA reservoir. *Ecol. Model.* 99:113-135.

Kime D.E. 2001. Endocrine disruption in fish. Norwell, Massachussets: Kluwer Academic Publishers.

Lankford, T. E. J. and Targett, T. E. 2001. Low-temperature tolerance of age-0 Atlantic croakers: recruitment implications for U.S. Mid-Atlantic estuaries. *Trans. Am. Fish. Soc.* 130:236-249.

Lye, C. M., Frid, C. L. J, Gill, M. E. and McCormick, D. 1997. Abnormalities in the reproductive health of flounder *Platichthys flesus* exposed to effluent from a sewage treatment works. *Mar. Pollut. Bull*. 34: 34-41.

McCarthy, I. D., Fuiman, L.A. and Alvarez, M. C. 2003. Aroclor 1254 affects growth and survival skills of Atlantic croaker *Micropogonias undulatus* larvae. *Mar. Ecol. Prog. Ser*. 252:295-301.

Menone, M. L., Aizpun de Moreno, J. E., Moreno, V. J., Lanfranchi, A, L, Metcalfe, T. L. and Metcalfe, C. D. 2000. PCBs and organochlorines in tissues of silversides (*Odontesthes bonariensis*) from a coastal lagoon in Argentina. Arch. Environ. Contam. Toxicol. 38:202-208.

Miller, J. M., Reed, J. P. and Pietrafesa, L. J. 1984. Patterns, mechanisms and approaches to the study of migrations of estuarine-dependent fish larvae and juveniles. In: McCleave, J.GG, G.P. Arnold, J. J. Dodson, and W. H Neill (eds), Mechanisms of Migration in Fishes, Plenum Press, NY, NY, USA .pp. 209-225.

Mills, L. J., and Chichester, C. 2005. Review of evidence: are endocrine-disrupting chemicals in the aquatic environment impacting fish populations? *Sci. Tot. Environ.* 343:1-34.

Munkittrick, K. R., Van Der Kraak, G.J. ,McMaster, M.E., Portt, C. B., van den Heuvel, M.R. and Servos M. R. 1994. Survey of receiving-water environmental impacts associated with discharges from pulp mills: 2. Gonad size, liver size, hepatic EROD activity and plasma sex steroid levels in white sucker. *Environ. Toxicol. Chem*. 13: 1089-1101.

Nixon, S. W. and Jones, C.M. 1997. Age and growth of larval and juvenile Atlantic croaker, *Micropogonias undulatus*, from the Middle Atlantic Bight and estuarine waters of Virginia. *Fish. Bull*. 95:773-784.

Power, M. 1997. Assessing the effects of environmental stressors on fish populations. *Aquat. Toxicol*. 39:151-169.

Reynolds, J. D., Dulvy, N. K., Goodwin, N. B. and Hutchings, J. A. 2005. Biology of extinction risk in marine fishes. *Proc. Royal Soc. B.* 272:2337-2344.

Rose, K. A., 2000. Why are quantitative relationships between environmental quality and fish populations so elusive? *Ecol. Appl*. 10: 367-385.

Rose, K. A. 2005. Lack of relationship between simulated fish population responses and their life history traits: inadequate models, incorrect analysis, or site-specific factors? *Can. J. Fish. Aquat. Sci*. 62:886-902.

Rose, K. A., and Cowan, J. H. Jr. 2000. Predicting fish population dynamics: compensation and the importance of site-specific considerations. *Environ. Sci. Policy* 3:S433-S443.

Rose, K. A., Murphy, C. A., Diamond, S. L., Fuiman, L. A. and Thomas, P. 2003. Using nested models and laboratory data for predicting population effects of contaminants on fish: a step toward a bottom-up approach for establishing causality in field studies. *Hum. Ecol. Risk Assess*. 9:231-257.

Rothchild, B. J. 1986. Dynamics of marine fish populations. Harvard University Press, Cambridge, MA, USA

Schaaf, W. E., Peters, D. S.,Coston-Clements, L, Vaughan, D.S. and Krouse, C. W. 1993. A simulation model of how life history strategies mediate pollution effects on fish populations. *Estuaries* 16:697-702.

Schaaf, W. E., Peters, D. S., Vaughan, D. S., Coston-Clements, L. and Krouse, C. W. 1987. Fish population responses to chronic and acute pollution: the influence of life history strategies. *Estuaries* 10:267-275.

Spromberg, J. A. and Birge, W. J. 2005. Modeling the effects of chronic toxicity on fish populations: the influence of life-history strategies. *Environ. Toxicol. Chem*. 24:1532-1540.

Summers, J. K. 2001. Ecological condition of the estuaries of the Atlantic and Gulf coasts of the United States. *Environ. Toxicol. Chem.* 20:99-106.

Sumpter, J. P. 2005. Endocrine disrupters in the aquatic environment: an overview. *Acta. hydrochim. hydrobiol*. 33:9-16.

Waggy, G. L., Brown-Peterson, N. J. and Peterson, M.S.(in press) Evaluation of the reproductive life history of the Sciaenidae in the Gulf of Mexico and Caribbean Sea: "greater" versus "lesser" strategies? *Proc. Gulf. Carib. Fish. Inst*. 57.

Warlen, S.M. 1982. Age and growth of larvae and spawning time of Atlantic croaker in North Carolina. *Proc. Ann. Conf. S.E. Assoc. Fish. & Wildl. Agencies* 34:204-214.

CHAPTER 6. GENERAL CONCLUSIONS

The issue of scale is a well-discussed theme in the field of ecotoxicology. To determine the effects of a contaminant on a population of organisms usually proceeds by first identifying the effect of a contaminant on an individual and then scaling these individual effects to the population level. The bottom-up approach used here is the most amenable approach to establish causality because the mechanisms underlying the adverse effect of a contaminant are usually determined first within an individual organism. Less frequently addressed is how contaminants affect how an organism interacts with other organisms within and between species. Thus, starting with the laboratory results on individuals, and using models to determine how those effects would affect their performance in the ecosystem, is a logical approach to scaling to the population level. In ecotoxicology, there is a need to determine how these individual effects affect natural patterns and how such perturbations scale up to the population. The predictive ability of the bottom-up approach lies in method of scale (Levin, 1992).

In this study, predictions were made on three levels of biological organization and modeling was used to scale one level of organization to another to make predictions. The three types of biological organization studied here were the processes occurring within an individual, the whole individual and how it interacts with its environment, and the behavior of an entire collection of organism (cohort and population). A single model of a single type could not handle all the scaling issues, and in this study I used four different types of models. A physiologically-based, ordinary differential equation model dealt with the processes occurring within an organism and scaled the effects of endocrine disruptors on hormones and biochemical processes to estimates of fecundity. A statistical model

related the behavior of endocrine disrupted larval fish to the probability of escaping a predator. An individual-based model scaled the effects of endocrine disruptors on the probability of escaping a predator, swimming speed, and metabolism to cohort survival and growth. Finally, a matrix projection model predicted the effects of endocrine disruptors on populations of Atlantic croaker located in the Mid-Atlantic Bight and the Gulf of Mexico.

The physiologically-based ordinary differential equation model, described in Chapter 2, placed commonly measured biomarkers into the context of a dynamic system to predict effects on vitellogenesis. Model simulations demonstrated that it was possible to make crude predictions of fecundity changes, through changes in vitellogenin production, and these predictions were based on contaminant-induced changes in hormone concentrations which are commonly measured biomarkers. Model simulations suggested that estradiol was a more sensitive biomarker than testosterone. Model simulations also demonstrated that the timing of biomarker measurement is critical to making accurate predictions on fecundity. According to my model simulations, measurements of steroid levels from contaminant exposed sciaenid fish that were taken during the first 2 months of gonadal recrudescence would show the greatest difference from control fish. The simulation of cadmium effects demonstrated how the model could be used to make predictions of vitellogenesis when an endocrine disruptor affects multiple sites on the hypothalamus-pituitary-gonad-liver axis. I simultaneously simulated two effects for cadmium; the first was how cadmium stimulates the release of luteinizing hormone, and the second was the enhancement of ovarian steroidogenesis. During the course of model development, I also determined that experiments on the rates of

synthesis of testosterone and estradiol in vitellogenic follicles *in vivo* would be useful for model refinement.

Chapter 3 further explored the vitellogenesis model, including simulation of laboratory and field exposures of croaker to hypoxia and the application of Monte Carlo uncertainty analysis. The vitellogenesis model was able to capture the predicted declines in vitellogenin production explored under controlled laboratory experiments of two concentrations of low dissolved oxygen. However, to obtain the expected declines in vitellogenin, the model had to incorporate both an observed effect (gonadotropin suppression), and an hypothesized effect (aromatase impairment), suggesting that the model had potential for identifying uncertain mechanisms of endocrine disruption. The model also predicted a non-linear response between reduced levels of estradiol and cumulative vitellogenin production. The model was applied to field-measured biomarkers and showed excellent potential as an aid in interpreting the likely causes of biomarker results and the potential for expressing the measured biomarkers as reduced fecundity. Model simulations demonstrated that the predicted non-linear responses have implications for the interpretation and analyses of multiple stressors on fish reproduction. Uncertainty analyses showed that the model is well-behaved under parameter variability and that the V_{IT} parameter consistently played a major role in affecting the variance of predicted vitellogenin production under various assumptions about parameter variability and under normoxic and hypoxic conditions. The parameter V_{IT} is used in the Hill function to describe maximum rate of free testosterone production.

In chapter 4, the statistical and individual-based models scaled the effects of contaminants on fish behavior to the population-relevant metrics of larval stage survival

and duration. Model simulations demonstrated that relatively high but possible exposures to contaminants can have significant effects on the survival of larval fish. Whether contaminant effects on predator escape were derived from linear regression using logits or regression tree analyses, or included a metabolic cost, had little affect on predicted stage duration and survival for control and contaminant exposure simulations. Model results showed that contaminants can act differently on individuals, which then manifested themselves at the cohort-level. Both PCBs and MeHg exposures resulted in reduced larval stage survival, but had different effects on stage duration. The opposite effects of PCBs and high-dose MeHg on predicted stage duration was due to differences in their effect by age of the larvae. PCBs affected swim speeds of older larvae, and MeHg affected swim speeds at every age. The predicted results from the model simulations suggested that growth processes (i.e., foraging abilities) were the principle driving force behind ocean larva cohort dynamics. The effects of PCBs and MeHg on stage survival and duration were almost entirely due to swim speed effects on prey encounters and resulting growth rates; the effects of contaminants on swim speed effects on predator encounters and probability of escape had little effects on predation because of assumptions about predator densities and sizes. In other situations, the role of contaminant effects on predation may become more important.

In Chapter 5, the matrix projection model incorporated changes in population-level metrics estimated from the other models, or directly from laboratory studies, to predict the effects of endocrine disruptors on population dynamics of two distinct Atlantic croaker populations. The population models incorporated some realism by including site-specific parameters and processes. Predictions generated from the matrix

model simulations suggested that, if all else was equal, contaminants have potential to impact a population, but there is not much resolution between the two contaminants. The application of PCBs and MeHg effects throughout the lifetime of the fish yielded similar reductions in population abundance. If the contaminant was eliminated after first spawning, as explored for PCBs, the population effect was not as severe. The number of individuals exposed from specific nursery areas also had different effects at the population due to site-specific parameter estimates and mortality differences related to harvest from shrimp bycatch. In the MAB, increasing the amount of individuals exposed to contaminants in NC had a small effect on the population, while increasing the exposure in VA had a large effect on the population. In the GOM, increasing the contaminant-exposed individuals in LA also had a large effect on the population, but a TX-exposure had virtually no effect on population abundance. The GOM appeared to be more resilient to contaminant effects than the MAB and this resilience was attributed to different life-history traits that were driven by different exploitation histories and environments.

Each of the models used in this analysis would benefit from further analyses and from additional empirical studies. My comparison of the physiological model to the laboratory data and the results of the uncertainty analysis suggested that the physiological model would benefit from more detailed information on the processes involved in steroidogenesis, estrogen receptor dynamics, steroid feedback mechanisms, and gonadotropin secretion. The hypoxia simulations highlighted the need for detailed experiments designed to determine the exact mechanism by which hypoxia disrupts the hypothalamus-pituitary-gonad-liver axis.

The probability of escape statistical models and the IBM could also be improved by additional experiments and further synthesis of existing data. Behavioral experiments that involve real predators eating Atlantic croaker larvae, and that are repeated enough times to make reliable statistical predictions, would avoid the extensive standardization that was needed to use red drum experimental results for croaker. Modeling efforts could also be improved by determination of the starvation potential of croaker ocean larvae, and field measurement of the types and densities of predators that prey on croaker larvae. The effects of realistic zooplankton patchiness should be examined using the IBM, and additional laboratory experiments and statistical and IBM simulations should be performed using other contaminants at realistic doses.

The matrix projection population model would benefit from additional field data and better information on contaminant dynamics and exposure. Presently, there is little information on growth and survival of croaker in the South Atlantic Bight and the eastern Gulf of Mexico. Both of these areas are potentially important areas for croaker, and could have survival and growth rates that differ from the mid-Atlantic and other parts of the Gulf of Mexico. The matrix model could be expanded to include the influence of ocean currents and how they affect within-year and interannual variation in the rate and destination of larvae entering the different estuarine nursery areas. More detailed information on the dynamics of the contaminant within an organism (e.g., residency times) and on exposure levels in nature would allow for refinement of exposure scenarios. Finally, the matrix model can be modified to simulate other scenarios, such as different contaminants, multiple stressors (e.g., contaminant exposure with increased

fishing and reduced habitat), contaminant exposures varying over time due to changes in regulations, and different contaminant bioaccumulation patterns in individuals.

The models used in this study effectively scaled three levels of biological organization. However, endocrine disruptors also affect other levels of biological organization beyond the three presented here. Many toxicological studies assess the impact of endocrine disruptors on molecular processes, which is a finer scale than presented here. Increasingly, regulatory agencies require information on how communities of organisms are affected by endocrine disruptors, which is a coarser scale than presented here. Models can be developed to scale the effects observed on the finer molecular scale up to the individual, and different models can be developed to scale the effects on a population to community wide effects. Future studies should also address how error and uncertainty are propagated through the linked models. Information apparently important for one model may become secondary when viewed in the context of all of the models.

In summary, this study demonstrates that it is possible to scale the sublethal effects of endocrine disruptors to the population using a bottom-up approach, and this approach required several different quantitative techniques and a vast amount of empirically derived and synthesized data. This study employed a number of different modeling techniques including ordinary differential equation models, statistical techniques such as linear regression using logits and regression trees, individual-based foraging and predation models, and matrix projection models expanded to use stage-within age on multiple timesteps in multiple spatial areas. In efforts to ground the models in realistic scenarios, the models described here also benefited from the collaboration

between field biologists, biologists, physiologists, and population biologists to provide sources of data. Overall, the combination of using several different modeling techniques, collaboration, and empirical and synthesized data made predictions that bridged several scales. Temporally, I scaled the effects observed in laboratory that are measured in hundreds of seconds, such as endocrine processes and behavioral processes, to long-term population abundances that occur over a hundred years. Mass was scaled from effects occurring at ng of steroid or μg of larvae to tons of adult fish. Spatially, I extrapolated contaminant effects observed in the laboratory to estimations of effects over two large geographic areas encompassing the MAB and GOM.

6.1. References

Levin, S. A. 1992. The problem of pattern and scale in ecology. *Ecology* 73: 1943-1967.

APPENDIX. PERMISSION TO USE COPYRIGHTED MATERIAL

1 February 2005 Our ref: HG/smc/Feb.2005.jl076

Ms Cheryl A Murphy

Cmurph4@lsu.edu

Dear Ms Murphy

REPRODUCTIVE TOXICOLOGY, Vol 19, No 3, 2004, Pages 395-409, Murphy et al, 'Modeling vitellogenesis in …'

As per your letter dated 20 January 2005, we hereby grant you permission to reprint the aforementioned material at no charge **in your thesis** subject to the following conditions:

1. If any part of the material to be used (for example, figures) has appeared in our publication with credit or acknowledgement to another source, permission must also be sought from that source. If such permission is not obtained then that material may not be included in your publication/copies.

2. Suitable acknowledgment to the source must be made, either as a footnote or in a reference list at the end of your publication, as follows:

   "Reprinted from Publication title, Vol number, Author(s), Title of article, Pages No., Copyright (Year), with permission from Elsevier".

3. Reproduction of this material is confined to the purpose for which permission is hereby given.

4. This permission is granted for non-exclusive world **English** rights only. For other languages please reapply separately for each one required. Permission excludes use in an electronic form. Should you have a specific electronic project in mind please reapply for permission.

5. This includes permission for UMI to supply single copies, on demand, of the complete thesis. Should your thesis be published commercially, please reapply for permission.

Yours sincerely

Helen Gainford
Rights Manager

Sent by: "Moss, Marion (ELS-OXF)" <m.moss@elsevier.co.uk>
To: "'cmurph4@lsu.edu'" <cmurph4@lsu.edu>
cc:
Subject: RE: Obtain Permission

Dear Ms Murphy

We hereby grant you permission to reproduce the material detailed below at no charge in your thesis, in print and on the Louisiana State University website, subject to the following conditions:

1. If any part of the material to be used (for example, figures) has appeared in our publication with credit or acknowledgement to another source, permission must also be sought from that source. If such permission is not obtained then that material may not be included in your publication/copies.

2. Suitable acknowledgement to the source must be made, either as a footnote or in a reference list at the end of your publication, as follows:

"Reprinted from Publication title, Vol number, Author(s), Title of article, Pages No., Copyright (Year), with permission from Elsevier".

3. Reproduction of this material is confined to the purpose for which permission is hereby given.

4. This permission is granted for non-exclusive English rights only. For other languages please reapply separately for each one required.

5.This includes permission for UMI to supply single copies, on demand, of the complete thesis. Should your thesis be published commercially, please reapply for permission.

Yours sincerely

Marion Moss
Senior Rights Assistant - Copyright

Elsevier
Global Rights
The Boulevard
Langford Lane
Kidlington
Oxford OX5 1GB

Tel : +44 1865 843280
Fax: +44 1865 853333
E-mail : m.moss@elsevier.com

VITA

Cheryl Anne Murphy was born in Edmonton, Alberta, Canada, on June 8, 1971, to Peter Patrick and Janet Marion Murphy. She attended Dalhousie University in Halifax, Nova Scotia, for her bachelor's degree where she majored in marine biology and minored in oceanography. She received her Bachelor of Science with first class honors in 1993. In May, 1998, she received a Master of Science degree in physiology and cell biology from the University of Alberta in Edmonton, Alberta, under the direction of Dr. Norm E. Stacey. She entered the Department of Oceanography and Coastal Sciences at Louisiana State University in August, 2000, as a graduate research assistant under the direction of Dr. Kenneth A. Rose and as a candidate for the degree of Doctor of Philosophy. Cheryl will receive a Doctor of Philosophy degree in oceanography and coastal sciences with a minor in experimental statistics in May, 2006.